INTERNATIONAL STUDIES AND EVALUATIONS IN THE FIELD OF

# SCIENCES AND MATHEMATICS

***December 2024***


EDITORS

PROF. DR. HASAN AKGÜL

PROF. DR. GÜNAY ÖZTÜRK

PROF. DR. ALPASLAN DAYANGAÇ



SERÜVEN YAYINEVİ

**Genel Yayın Yönetmeni / Editor in Chief** • C. Cansın Selin Temana

**Kapak & İç Tasarım / Cover & Interior Design** • Serüven Yayınevi

**Birinci Basım / First Edition** • © Aralık 2024

**ISBN** • 978-625-5955-77-7



**Serüven Yayınevi / Serüven Publishing**
**Türkiye Adres / Turkey Address:** Kızılay Mah. Fevzi Çakmak 1. Sokak
Ümit Apt No: 22/A Çankaya/ANKARA
**Telefon / Phone:** 05437675765
**web:** www.seruvenyayinevi.com
**e-mail:** seruvenyayinevi@gmail.com

**Baskı & Cilt / Printing & Volume**
Sertifika / Certificate No: 47083

INTERNATIONAL STUDIES AND EVALUATIONS IN THE FIELD OF

# SCIENCES AND MATHEMATICS

DECEMBER 2024

EDITORS

PROF. DR. HASAN AKGÜL
PROF. DR. GÜNAY ÖZTÜRK
PROF. DR. ALPASLAN DAYANGAÇ

# CONTENTS

# CHAPTER 1

## SUSTAINABILITY IN UNIVERSITIES AND GREEN UNIVERSITY INDICATORS

*Sezen COSKUN*[1,2]

1 (Assoc Prof Dr), Isparta University of Applied Sciences, Vocational School, Isparta, Türkiye
2 The Coordinatorship of Social Contributions in Isparta University of Applied Sciences, Isparta, Türkiye.
e-mail: sezencoskun@isparta.edu.tr Orcid: 0000-0001-7011-9187

## 1. INTRODUCTION

The rapid depletion of natural resources due to population growth and the decrease in livable areas for next generations increases the importance of sustainability. Sustainability essentially refers to protecting natural resources and their safe transfer from generation to generation (Koyuncuoglu, 2022). Humanity must choose between irresponsibly continuing the destruction of the past and the present or working for a sustainable world (Bozoğlu and Ciğerim, 2022). Developing a sustainable development model has become an obligation nationally and internationally and should be adopted by the world. In order to eliminate or minimize regional and global risks that threaten sustainable development, it is necessary to build a habitable planet without destroying resources to meet the needs of future generations (Mishelsen and Fischer, 2017). In this regard, the success of world economies depends on the viability of society, and the success of society will necessarily ensure the viability of the environment and the protection of natural resources (Amaeshi et al., 2019). The realization of this goal will be achieved by changing the learning processes in education, which is an integral part of sustainable development (Vare and Scott, 2007).

There are different approaches to assessing sustainability internationally, nationally, regionally and institutionally. It is of great importance that the approaches are measurable. Measurable approaches prepared based on indicators related to sustainability also increase transparency and durability. The declarations that set the conditions for sustainability can be listed as follows according to years; The Talloires Declaration (France - 1990), The Halifax Declaration (Canada - 1991), The Kyoto Declaration (Japan – 1993), The Swansea Declaration (Wales – 1993) – The Lüneburg Declaration (Germany – 2004), The Barselona Declaration (Spain– 2005), The Graz Declaration (Austria – 2009), The Abuja Declaration (Nigeria – 2009), The Torino Declaration (Italy) (Lozano et al., 2013; Günerhan and Günerhan, 2016).

One of the best examples of sustainability of organizations is the concept of a 'green university.' Education and training are among the key factors that promote sustainable development, enabling people to develop skills to cope with environmental and development challenges (Günay, 2011, Koyuncuoglu, 2022; Günerhan and Günerhan, 2016). On a pilot basis, university campuses can act as a laboratory and serve as a model (Kaldırım et al., 2023). The main objective of educational institutions committed to sustainable development should raise awareness among students about sustainable development issues and to make them feel responsible enough to deal with economic, ecological and social problems in their working life. It is important to include courses such as ecological responsibility, environmental management and social responsibility in the curriculum (Koyuncuoglu, 2022). A sustainable university can be defined as a institution that works to minimise the environmental

pollution, economic and social impacts of its activities and leads the effectively in a sustainable lifestyle (Günerhan and Günerhan, 2016; Velaquez et al., 2006).

It has been determined that educational research in the context of the idea of sustainability in Turkey has been intensively addressed since 2010, the studies have been carried out to determine the situation, concepts such as sustainable development, sustainable environment, sustainability education come to the fore in terms of concept, and the issue of sustainability has been examined especially in relation to science and social studies education (Yıldırım, 2020; Koyuncuoglu, 2022).

In this study, information about sustainable green evaluation criteria in international and national literature is presented. The scope of certain criteria used to become a green university, the perspective of universities in Turkey on the subject and examples of good studies are shown. The study aims to provide a guideline for universities that want to complete the green university criteria.

## 2. SUSTAINABILITY STUDIES AT UNIVERSITIES

Academics have a major role in the transition to a sustainable society and in managing sustainable activities. Higher education institutions can build a fairer and more sustainable society. Today, many academic studies emphasize the importance of sustainability in universities (Çardak et al., 2022; Kaldırım et al., 2023). According to Labanauskis (2017), the idea of sustainable development enables universities to remain resilient in the face of scarce resource management and other challenges and to respond to the needs and expectations of internal and external stakeholders. The idea of sustainable development provides universities with a competitive advantage and helps them to define and position themselves (Labanauskis, 2017). The importance of education for sustainable development was underlined in the 'UN Agenda 2030' and UNESCO, under the title 'Education for Sustainable Development', drew attention to the important role of universities in building a more sustainable society and achieving sustainable development goals (Fissi ve diğerleri, 2021; Filho ve diğerleri, 2019; Kaldırım et al., 2023).

In a study conducted in Canada, the extent to which sustainability is included in university policies and the best practices in creating plans were analyzed. It was found that the concepts in the plans were divided into three main headings: environmental, economic and social. It has been observed that these topics are conceptualized to include research, education, operations and outreach. Especially in the sustainable policies and plans of higher education institutions, the environmental aspects of campus and facility areas are emphasized (Lidstone, 2014). Chawla (2015) analyzed the curricula of 33 public universities in the United Kingdom in terms of sustainability education and stated that sustainability is mostly included in the hospitality curriculum. He concluded that the curriculum is still fragmented in this regard and

that the main agendas and curricula in universities need to be updated. Labanauskis (2017) stated that in addition to the research, development and commercialization missions of the university, the functions of contribution to society are also important.

Today, university success rankings are made by many international ranking organisations according to various categories. Times Higher Education (THE), Quacquarelli Syndoms World University Rankings (QS), Akacedemic Ranking of World Universities (ARWU), University Ranking By Academic Performance (URAP), Webometrics (World Universities' Ranking to the Web), National Taiwan University Ranking (NTU), HEEACT (Performance Ranking of Scienticific Papers for World Universities) are some of them. Different from the research of these organisations, GreenMetric is an organisation that evaluates and ranks sustainability efforts on university campuses (Kaldırım et al., 2023).

## 3. GREEN UNIVERSITY INDICATORS

Universities have a very crowded population with their academic staff, administrative staff and students, as well as a large number of buildings, roads and car parks. When the people receiving services from various units are included in the number, universities contain factors that can have a direct impact on the environment and social environment. Therefore, universities need to be sustainable both in terms of reducing their pollutants and in terms of leading and setting an example for society (Günerhan and Günarhan, 2016). The innovative structure of a country's industry and the competitiveness of its economy depend on the sustainable university-industry co-operation of that country (Günay, 2011; Günay and Çalık, 2019). Universities should make socio-economic contributions to society in addition to education training and research-development studies on ecological sustainability. In this sense, a sustainable university can be defined as "education institution that takes measures to minimize the negative environmental effects, economic and social impacts of its activities and contributes to society in terms of a sustainablity" (Günerhan and Günerhan, 2016).

Signed in 1990, the Tallories Declaration, which is the first official commitment to sustainability studies at universities, is an important document (Khan, 2013). This declaration has been accepted and signed by many universities and has taken its place among the rating programmes that are indicators of sustainable development today. While many universities have established environmental management plans and environmental audit systems, some universities have taken a step further by publishing sustainability reports (Michelsen and Fischer, 2017).

The evaluation of the work of universities on environmental issues is a relatively new issue. The specific metrics used for a green university are

as follows (Günerhan and Günerhan, 2016; Zeybek, 2023; Özdoğan and Civelekoğlu, 2019):

- UI GreenMetric
- GASU (Graphical Assessment of Sustainability in Universities)
- People&Planet

### 3.1. UI GREENMETRIC

UI GreenMetric is the most widely used metric in the world, providing international recognition of sustainable universities (Muñoz-Suárez, Guadalajara and Osca, 2020; Özdoğan and Civelekoğlu, 2019). It is an international university ranking developed by the University of Indonesia in 2010. In this ranking, which is based on the evaluation of universities on their own criteria, six main criteria have a percentage distribution The percentage distribution of the criteria is as follows (GreenMetric 2024; Zeybek, 2023):

- Installation and Infrastructure (15%)
- Energy and Climate Change (21%)
- Waste (18%)
- Water (10%)
- Transport (18%)
- Education and Research (18%)

The purpose of this ranking is to provide conclusions about the status of universities in green and sustainable campus policies. Therefore, such policies need to change universities towards more sustainable behavior and consider equity for all (staff, faculty and students) (Günerhan and Günerhan, 2016; GreenMetric 2024).

### 3.2. GASU (Graphical Assessment of Sustainability in Universities)

GASU automatically draws nine charts, ranking each indicator on a scale from zero (no information) to four (excellent performance). These graphs are used to analyze the current situation of the university to identify the dimensions in which it excels and the dimensions that need further attention. The comparison of the charts from each year is the basis for the university managers' efforts towards sustainability (Lozano, 2006; Tanç et al., 2022). The indicators are defined below (Lozano, 2006; Günerhan and Günerhan, 2016; Zeybek, 2023):

- Economic Indicators: Customers, suppliers, employees, capital providers, public sector.
- Environmental Indicators: Materials, energy, water, biodiversity,

emissions, fluids and waste, suppliers, products and services, compliance, transport.

- Social Indicators:

o Labour practices and decent work: Employment, labour/management relations, health and safety, education and training, diversity and opportunity.

o Human rights: Strategy and management, non-discrimination, freedom of association and collective bargaining, child labour, disciplinary practices, natural rights.

o Society: Society, bribery and corruption, political contributions.

o Product liability: Customer health and safety, products and services, advertising, respect for privacy.

- Indicators of Training Performance

o Curriculum: Existing courses on sustainability, administrative support

o Research: Grants, extension and products, programmes and centres

o Service: Community activity and service, service learning.

**3.3. People&Planet**

People&Planet (P&P), a student network in the UK, was founded in 2007 and aims to achieve social and environmental justice to achieve an equal world in the future. The aim is to build a generation of competent, skilled and motivated people who will change the world in a fairer and more sustainable way. P&P maintains an annual ranking of UK universities based on their environmental and ethical performance (People&Planet, 2024). The results of this ranking are published annually in a national journal to increase the level of environmental management in higher education. It should be noted that the P&P model modifies its factors every year according to new environmental changes. In 2012, the number of main indicators of the model reached 13, and then a new indicator was added in 2015. The current indicators of the model with a large number are as follows (Godemann et al., 2014, People&Planet, 2024; Günerhan and Günerhan, 2016):

- Environmental staff (8%)
- Environmental monitoring and systems (10%)
- Ethical investment and banking (7%)
- Carbon management (7%)
- Labour rights (6%)
- Sustainable food (4%)

- Staff and student engagement (5%)
- Sustainable development in curriculum and training (10%)
- Energy sources (8%)
- Waste and recycling (8%)
- Reduction in carbon emissions (15%)
- Reduction in water use (8%)

When the factors of this model are analyzed, it can be said that the model covers all sustainable university factors such as the long-term plans of universities, the number of research on the environment and green transportation. Nevertheless, it is claimed that the factors do not have a direct impact on reducing the carbon footprint of the university. However, this model and alliance is an important factor in terms of sustainability as it has an important role in educating new generations (Zeybek, 2023).

## 4. GREEN UNIVERSITY STUDIES

On an international scale, 2015 data ranked the top three universities in the general ranking of the green university measurement as the University of Nottingham, University of Connecticut, University of California (Günerhan and Günerhan, 2016; University of Nottingham, 2024). In the 2023 initial rankings, Wageningen University & Research (Netherlands), Nottingham Trent University (United Kingdom), University of Groningen (Netherlands) are the top three universities (GreenMetric, 2024). It is noteworthy that these universities similarly include courses such as sustainability, environment and climate change in their curricula. Their preference for environmentally friendly technologies and organizing environmental activities to raise awareness are also among their similar policies (Günerhan and Günerhan, 2016).

The University of Nottingham is a leading university in environmental sustainability. At undergraduate and postgraduate level, the curriculum includes courses that cover the economic, environmental and social dimensions of sustainability. In terms of recycling at the University of Nottingham, while 3000 tonnes of waste are produced annually and 95% of it is sent to landfill, the recycling rate success has been increased to 85% with sustainability efforts. Food waste and garden waste are composted and used to improve gardens. Students are encouraged to donate items they no longer wish to use to local charities when vacating their rooms. There is public transport to the campuses, car-sharing options for staff, cycle paths and secure cycle parks on campus. A Carbon Management Plan covering the period 2010-2020 has been prepared to reduce energy consumption, increase energy efficiency, use more renewable energy and thus reduce the carbon footprint. Events for the local community are also organized on the campus at certain times (University of Nottingham, 2024).

At the University of Connecticut, the Environmental Policy Office was established in 2002 to carry out similar studies, a council of advisors was formed, and a Climate Action Plan was established in 2009. To reduce greenhouse gas emissions from fossil fuels, using green technologies, increasing the use of renewable energy, expanding the use of biofuel, solar energy, hydrogen-fuelled vehicles, and making pedestrian and bicycle priority arrangements are among the priorities. Campus development plans have been prepared for waste reduction and recycling, solid waste disposal, compost production from garden and food waste, water conservation and reuse, and the use of biodegradable cleaners. The inclusion of environment, climate change and sustainability courses in undergraduate and graduate education, organizing environmental activities and competitions to encourage students and raise their awareness are among the important activities. (UCONN, 2024).

In the studies conducted on green universities in Turkey in 2017, Razman et al. (2017) found that the common activities that are frequently implemented are 'placing marked signs on garbage bins to increase recycling' and 'generating electricity on campus by establishing electricity generation facilities' with 87% and 83%, respectively. When the theses on sustainable universities are analyzed, it is noteworthy that mostly in-university research has been conducted. In the first place, it is seen that research topics related to course contents, curriculum and the effect of education in general on students sustainable thinking and awareness levels are addressed. In the second place, it is observed that intra-university research has been conducted under the theme of 'green campus (Koyuncuoğlu, 2022).

In the studies conducted on green universities in Turkey in 2017, Razman, Abdullah, Wahid & Muslim (2017) found that the common activities that are frequently implemented are 'placing marked signs on garbage bins to increase recycling' and 'generating electricity on campus by establishing electricity generation facilities' with 87% and 83%, respectively. When the theses on sustainable universities are analyzed, it is noteworthy that mostly in-university research has been conducted. In the first place, it is seen that research topics related to course contents, curriculum and the effect of education in general on students sustainable thinking and awareness levels are addressed. In the second place, it is observed that intra-university research has been conducted under the theme of 'green campus (Koyuncuoğlu, 2022).

In the dimension of the framework conditions of the university, it can be said that the issues of 'green campus' and 'sustainability thinking' and 'sustainability culture' are mainly investigated. Ayten (2016) stated that thesis studies mostly focus on graduates who support sustainable lifestyles, focus more on education and research, and the widespread social impact and benefit has not yet emerged clearly.

Bülent Ecevit University, which ranks first among Turkish universities, participated in the green measurement study for the first time in 2014. Examples of the studies carried out by the university with the aim of green university: The forested area is larger than the total area of the university located in Zonguldak province, the sheathing process has been completed in terms of building thermal insulation, LED (Light Emitting Diode) lighting has been made widespread for energy saving, the use of natural gas is emphasized, recycling bins are located in the campus buildings, and projects have been developed in the field of renewable energy use. Studies are being carried out on solar-powered cars. Thanks to the public transport and private car usage policies, the number of vehicles entering the campus daily has been reduced. The percentage of bicycle transport to the campus is high. There are projects and courses on environment and sustainability, training on separate collection of packaging wastes given to kindergartens in the province through the 'Environmental Problems Research and Application Centre,' and club activities on the environment also carry out important studies for the green university award (Zonguldak Bülent Ecevit University, 2016).

Sabancı University and Özyeğin University also rank among the top green universities in Turkey. The International Climate and Energy Centre at Sabancı University brings together important stakeholders in the fields of energy and climate and encourages the development and exchange of ideas, while Özyeğin University has been conducting similar studies on energy saving with the Energy, Environment and Economy Centre established in 2009. Özyeğin University has an energy distribution center, building automation applications, solar panels and seven buildings with green roofs. Sabancı University organizes the International Energy Forum every year to contribute to the discussion of sustainable future solutions for the region and the world in the field of energy. In both universities, course curricula related to sustainability and the environment are important for green university criteria. Another important criterion is the large number of green areas on campus (Özyeğin University, 2016; Sabancı University, 2016).

## 5. RESULTS and DISCUSSION

The keywords that stand out in scientific research conducted in Turkey are "sustainable university", "sustainable development and higher education", "green campus", "green university", "eco-campus", "ecological university", "environmental campus", "sustainable education" (Koynuncuoğlu, 2022). When the reports, conferences, summits and environmental education conducted by public institutions in Turkey in 2015 are examined, it is stated that Turkey's national strategy cannot be clearly stated, educational materials are insufficient to inform the society about sustainable development, and quality education cannot be provided in primary, secondary and higher education (Kaya et al., 2015).

After examining the studies conducted by universities on sustainability and the declarations they signed, it was seen that the studies conducted by universities in Turkey were limited (Günerhan and Günarhan, 2016). In the examined theses, it was seen that surveys were used more than scales. Scale studies can be conducted on the sub-topics of sustainable universities. In addition, in future studies, comparative sample events or case studies can be conducted in developed and developing countries, considering macroeconomic indicators (Ayten, 2016).

A model definition for sustainable universities was introduced to the literature by Günerhan and Günarhan (2016). Accordingly, a university that decides to become a sustainable university must first determine its sustainability vision and minimize the negative environmental, social and economic impacts that may arise in every initiative it will take, as per the definition of sustainability. The second stage is the definition of the university mission. In terms of sustainability, the current situation must first be determined and the university must well define its internal and external stakeholders. The third stage is the establishment of a sustainability office or coordination office where all sustainability-related studies will be carried out. Studies should be directed and recorded by a control mechanism. Studies carried out in terms of transparency should be shared with the society and stakeholders through social media and a website. The fourth stage should be the establishment of a committee/board consisting of experts on the subject. The committee/board should determine the sustainability goals, objectives and policies of the university and ensure that these are included in the daily operation. Another important issue is the provision of financial resources for sustainability studies. The fifth stage is to determine the university strategy and record it in writing. The strategy can be organized in four stages: teaching, research, social access and collaborations, sustainability on campus. Course content, research and collaborations related to sustainability should be provided (Günerhan and Günarhan, 2016). For these four strategies to be successfully implemented, raising awareness about sustainability and using technology to reduce the damage to the environment are two important points (Valequez et al., 2006; Günerhan and Günerhan, 2016).

## 6. CONCLUSION

In conclusion, it is of great importance to increase research on sustainability and green universities. In these studies, good practice examples can be developed with all stakeholders, starting from the management dimension and these practices can be spread throughout the process, contributing to the society's internalization of sustainability efforts. Student communities should be involved in sustainability activities so that good practice habits can be passed on to future generations. Universities should include sustainability in their vision, mission, strategic plan and annual activity reports, and should be able to objectively demonstrate that they have achieved their plans and goals through the events and projects they organize. Since environmental protection plays an important role in achieving goals and in feeling the social equality and social responsibility of universities, increasing the widespread impact on these issues will also improve the position of our universities in international standards. Reaching the top ranks in green university rankings depends on adding environmental protection, climate change, and sustainability courses to the curriculum, increasing R&D studies on these topics, expanding social responsibility course practices on environmental protection and climate change, utilizing renewable energy types in campus areas, reducing vehicle traffic, reducing fossil fuel use, utilizing reusable water obtained through water harvesting, saving water, and increasing green areas.

## ACKNOWLEDGEMENTS

I would like to thank Social Contribution Coordinator of Isparta University of Applied Sciences Prof Dr Nilgün BUDAK for their support to the study.

## RESOURCES

Amaeshi K, Muthuri JN, Ogbechie C 2019. Incorporating sustainability in management education: An interdisciplinary approach. Springer. Available at: https://books.google.com.tr/books/about/Incorporating_Sustainability_in_Manageme.html?id=qt-GDwAAQBAJ&redir_esc=y [28.05.16]

Ayten AM 2016. Yükseköğretim kurumlarında stratejik sürdürülebilir alan yönetimi. Yükseköğretim Dergisi, 6(3): 142–154. https://doi.org/10.2399/yod.16.010

Bozoğlu O, Ciğerim E 2022. Sürdürülebilirlik, sürdürülebilir kalkınma ve sürdürülebilir üniversiteler. Socrates Journal of Interdisciplinary Social Studies, 18: 146-158.

Chawla G 2015. Sustainability in hospitality education: A content analysis of the curriculum of British universities. In: Proceedings of the European Conference on Research Methodology for Business and Management Studies. Malta, June 11-12. pp. 135-139

Çardak D, Tanç GŞ, Tanç A, Yağlı İ 2022. Türkiye'deki üniversitelerin sürdürülebilirlik çalışmalarının incelenmesi. Muhasebe ve Denetime Bakış Dergisi, 66: 83-100. https://doi.org/10.55322/mdbakis.1063261

Filho LW, Shiel C, Pacho A, Misfud M, Avilla LV, Brandling LL, Hill PM, Pace P, Azeiteiro UM, Vargas, VR, Caeiro JS 2019. Sustainable development goals and sustainability teaching at universities: Falling behind or getting ahead of the pack. Journal of Cleaner Production, 232: 285-294.

Fissi S, Romolini A, Gori E, Contri M 2021. The path toward a sustainable green university: The case of the University of Florence. Journal of Cleaner Production, 279: 1-9. https://doi.org/10.1016/j.jclepro.2020.123655

Godemann J, Bebbington J, Herzig C, Moon J 2014. Higher education and sustainable development: Exploring possibilities for organizational change. Accounting, Auditing & Accountability Journal, 27(2): 218-223. https://doi.org/10.1108/AAAJ-12-2013-1553

GreenMetric 2024. GreenMetric universities. Available at: https://greenmetric.ui.ac.id/rankings/overall-rankings-2024 [20.12.2024].

Grindsted TS 2011. Sustainable universities from declarations on sustainability in higher education to national law. Environmental Economics, 2(2): 29-36.

Günay D 2011. Türk yükseköğretiminin yeniden yapılandırılması bağlamında sorunlar, eğilimler, ilkeler ve öneriler – I. Yükseköğretim Dergisi, 1(3): 113-121.

Günay D, Çalık A 2019. İnovasyon, icat, teknoloji ve bilim kavramları üzerine. Üniversiteler Araştırmaları Dergisi, 2(1): 1-11. https://doi.org/10.26701/uad.549654

Günerhan S, Günerhan H 2016. Türkiye İçin Sürdürülebilir Üniversite Modeli. Mühendis ve Makina, 57(682): 54-62.

Kaldırım Z, Özcan İ, Ergün İ 2023. Çevresel Sürdürülebilirlik ve Akademik Başarı

İlişkisi: UI Greenmetric ile Urap ve The Üniversite Sıralamalarının Karşılaştırılmalı Analizi. Muhasebe Bilim Dünyası Dergisi, Özel Sayı, 187-206.

Kaya N, Çobanoğlu MT, Artvinli E 2015. Sürdürülebilir kalkınma için Türkiye'de ve dünyada çevre eğitimi çalışmaları. In Türkiye Coğrafyası Araştırma ve Uygulama Merkezi (TÜCAUM) VI. Coğrafya Sempozyumu (pp. 407-418). Ankara: Ankara Üniversitesi Dil ve Tarih-Coğrafya Fakültesi.

Khan T 2013. Sustainability accounting courses, Talloires Declaration and academic research. International Journal of Sustainability in Higher Education, 14(1): 42-55. https://doi.org/10.1108/14676371311288949

Koyuncuoglu Ö 2022. A Review of Graduate Theses on the Sustainable University in Turkey. Journal of University Research, 5(1): 84-100.

Labanauskis R 2017. Key features of sustainable universities: A literature review. Journal of Business Management, 13: 56-69.

Lidstone L 2014. A content analysis of sustainability policies and plans from stars-rated Canadian higher education institutions (Unpublished master's thesis). Dalhousie University, Nova Scotia, Canada.

Lozano R 2006. A tool for a Graphical Assessment of Sustainability in Universities (GASU). Journal of Cleaner Production, 14 (9-11): 963-972.

Lozano R, Lukman R, Lozano FJ, Huisingh D, Lambrechts W 2013. Declarations for Sustainability in Higher Education: Becoming Better Leaders, Through Addressing the University System. Journal of Cleaner Production, 48: 10-19.

Michelsen G, Fischer D 2017. Sustainability and Education. In M. v. Hauff & C. Kuhnke (Eds.), Sustainable Development Policy: A European Perspective. London: Routledge.

Muñoz-Suárez M, Guadalajara N, Osca JM 2020. A comparative analysis between global university rankings and environmental sustainability of universities. Sustainability, 12(14): 5759. https://doi.org/10.3390/su12145759

Özdoğan B, Civelekoğlu G 2019. Üniversite Yerleşkeleri İçin Ulusal Çevresel Sürdürülebilirlik Endeksinin Geliştirilmesi. Mühendislik Bilimleri ve Tasarım Dergisi, 7(1): 65-80.

Özyeğin University 2016. GreenMetric. Available at: http://www.ozyegin.edu.tr/RESEARCH/ [05.02.2016].

People & Planet 2024. University-League. Available at: https://peopleandplanet.org/university-league [20.12.2024].

Razman R, Abdullah AH, Wahid AZA, Muslim R 2017. Web content analysis on sustainable campus operation (SCO) initiatives. MATEC Web of Conferences, 87: 1-6. doi:10.1051/matecconf/20178701020.

Sabancı University 2016. Campus Life. Available at: https://www.sabanciuniv.edu/tr/kampus-hayati/gol [05.02.2016].

Suwartha N, Sari RF 2013. Evaluating UI Green Metric as a Tool to Support Green

Universities Development: Assessment of the Year 2011 Ranking. Journal of Cleaner Production, 61: 46-53.

Tanç GŞ, Tanç A, Çardak D, Yağlı İ 2022. Türkiye'deki üniversitelerin sürdürülebilirlik çalışmalarının incelenmesi. Muhasebe ve Denetime Bakış Dergisi, 2022(66), 83-100. https://doi.org/10.55322/mdbakis.1063261

UConn 2024. UConn Earns Top 10 Spot for UI GreenMetric Sustainability Ratings. Available at: https://sustainability.uconn.edu/2024/12/19/uconn-earns-top-10-spot-for-ui-greenmetric-sustainability-ratings/ [20.12.24].

University of Nottingham 2024. Available at: http://www.nottingham.ac.uk [20.12.24].

Vare P, Scott WR 2007. Learning for a change: Exploring the relationship between education and sustainable development. Journal of Education for Sustainable Development, 1(2): 191-198. https://doi.org/10.1177/097340820700100209.

Velaquez L, Munguia N, Platt A, Taddei J 2006. Sustainable University: What Can Be Matter. Journal of Cleaner Production, 14(8): 810-819.

Yıldırım G 2020. Sürdürülebilirlik konusunda eğitim araştırmalarının tematik olarak incelenmesi. Akdeniz Eğitim Araştırmaları Dergisi, 14(33): 70-106. doi:10.29329/mjer.2020.272.4.

Yücel Işıldar Y 2015. Sürdürülebilir Kentler İçin Üniversitesi Yerleşkelerinin Rolü. Yerel Politikalar, 1.

Zeybek B 2023. Sektörel Sürdürülebilirlik, Yeşil bir üniversite için uluslararası değerlendirme ölçütleri. Available at: https://yesilbuyume.org/yesil-bir-universite-icin-uluslararasi-degerlendirme-olcutleri/ [20.12.2024].

Zonguldak Bülent Ecevit University 2016. Greenmetrics. Available at: http://web.beun.edu.tr/greenmetrics/ [21.02.2016].

# CHAPTER 2

# USE OF MEDICINAL PLANTS IN DIETHYLNITROSAMINE-INDUCED LIVER CANCER MODELS

*Neşe Eray Vuran*[1]
*İsmail Çelik*[2]

1 Dr. Neşe Eray Vuran Van YuzuncuYil University Faculty of Science- Orcid ID: 0000-0001-6387-1493
2 Prof. Dr. İsmail Çelik Van YuzuncuYil University Faculty of Science - Orcid ID: 0000-0003-2199-6348
* It was produced from the doctoral thesis with thesis number 690326.

Cancer is a pathological condition characterized by the uncontrolled proliferation and growth of cells in any organ or tissue in the body. The term "cancer" encompasses more than 277 distinct types of cancer diseases (Hassanpour and Dehghani, 2017). Despite the diversity of cancer types, they all originate from the uncontrolled proliferation of abnormal cells. However, uncontrolled proliferation alone is insufficient for cancer progression. The cell must also acquire other malignant properties, such as invasion (spreading into other healthy tissues) and metastasis (spreading to distant tissues through the circulation) (Aliustaoğlu, 2009).

Cancer is a disease group with a long historical background. Evidence of bone tumors has been found in dinosaur fossils dating back approximately 50 million years BCE. Records of tumors have also been discovered in the Ebers Papyrus from around 500 BCE, and osteosarcoma has been observed in skeletal remains in Egyptian pyramid tombs. The Greek physician Hippocrates (460–370 BCE) introduced the terms carcinos and carcinoma to describe ulcer-forming and non-ulcer-forming tumors (Bayık, 1989).

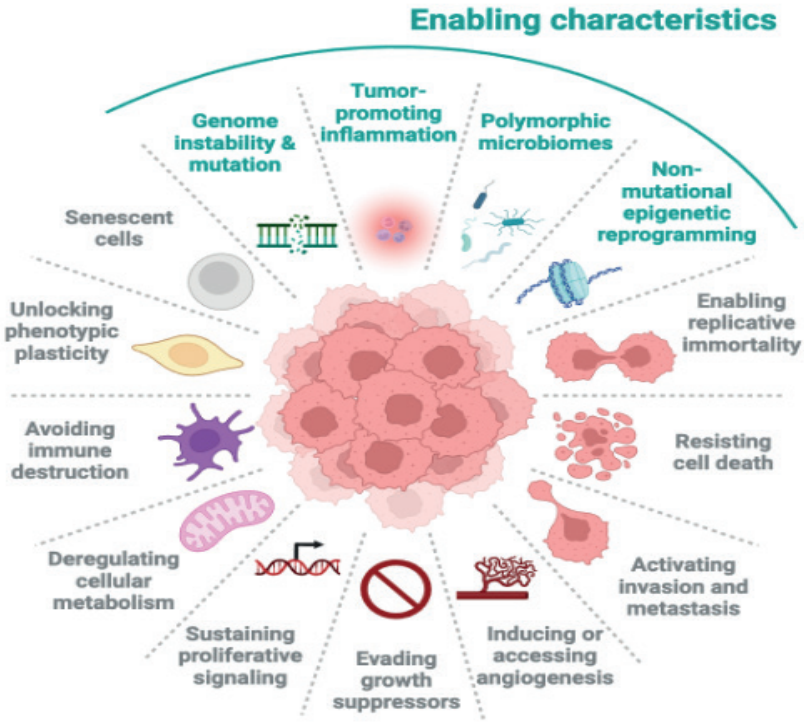


*Figure 1. Characteristics of cancer (Hanahan, 2022).*

Cancer poses a serious problem affecting the health of all human societies. Unfortunately, it is a disease at the tissue level, and this diversity complicates diagnosis. In men, cancer is most commonly found in the prostate, lung, colon, rectum, and bladder. In women, the highest prevalence of cancer is in the breast, lung, colon, uterine corpus, and thyroid. For children, the most common types of cancer are blood cancers and cancers related to the brain and lymph nodes (Hassanpour and Dehghani, 2017). Cancer-causing factors can be grouped into internal and external factors. Internal factors are inherent and unchangeable, including age, gender, heredity, race, hormonal system, endocrine system, and immunity. External factors include smoking and alcohol use, radiation exposure, certain viruses, poor eating habits, food additives, prolonged sunlight exposure, excessive x-ray exposure, various chemicals (such as tar, gasoline, dyes, and asbestos), and air pollution (Hassanpour and Dehghani, 2017).

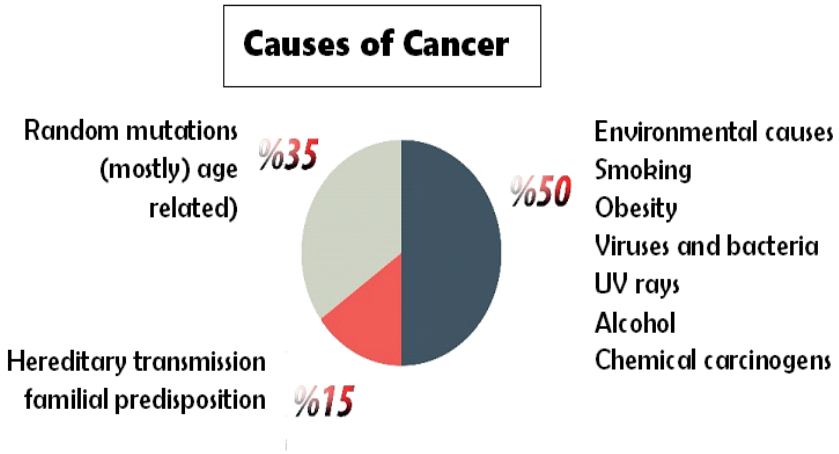


*Figure 2. Causes of cancer (Anonymous Prof. Dr. Mustafa Özdoğan)*

According to 2020 data, there are 50.6 million cancer patients worldwide. One in five people is diagnosed with cancer at least once in their lifetime, and one in eight men and one in eleven women die from cancer. The projected increase in cancer cases by 2040 is 47%. In 2020, 19.3 million new cases and 10 million new deaths were reported worldwide. In Turkey, the annual number of new cancer cases in 2020 was reported as 233,834, with 126,335 cancer-related deaths. The five most common types of cancer in Turkey in 2020 were lung, breast, colorectal, prostate, and thyroid cancer (Sung et al., 2021).

### Liver Cancer

Primary liver cancer is the seventh most common cancer in the world and the second most common cause of cancer deaths. Globally, hepatocellular carcinoma (HCC) is the predominant type of liver cancer, accounting for approximately 75% of all liver cancers and is three times more common in men than in women (Bray et al., 2018).

Approximately 70–90% of patients with HCC have a history of chronic liver disease and cirrhosis, including chronic infection with hepatitis B virus (HBV), hepatitis C virus (HCV), and alcoholic liver disease (El-Serag and Rudolph, 2007). The rate of liver cancer development varies depending on the cause of cirrhosis. In Turkey, the most common cause is hepatitis B infection, followed by cirrhosis due to alcohol, hepatitis C, and fatty liver. However, in the coming years, due to the increasing prevalence of obesity and improved control of viral infections, liver cancers due to cirrhosis caused by fatty liver are expected to be the leading cause (Vatansever and Karasu, 2019). Additional risk factors for the development of HCC include aflatoxin-contaminated food intake, diabetes, obesity, certain hereditary conditions such as hemochromatosis, and some metabolic disorders (Montalto et al., 2002; Gomaa et al., 2008).

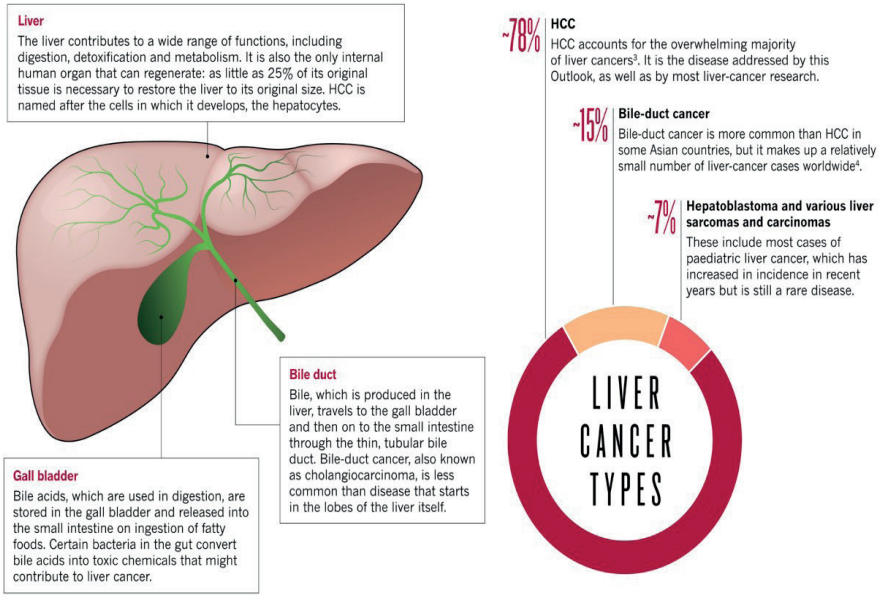


*Figure 3. Liver cancer types (Laursen, 2014).*

**Diethylnitrosamine (DEN) and Hepatocellular Carcinoma (HCC)**

The liver is the primary target site for hundreds of chemicals including pesticides, food additives, pharmaceuticals and industrial intermediates. Identifying hepatocarcinogenic compounds and understanding the cellular and molecular processes during carcinogenic transformation of hepatocytes is an ongoing challenge (Bakiri and Wagner, 2013).

Creating animal models for HCC is very important for the diagnosis and treatment of the disease. Rodent models have been used for years to study the pathogenesis of HCC. Rats are one of the best experimental systems due to their physiological, molecular and genetic similarities to humans, their reproductive capacity, short lifespan and the unlimited options offered by genetic engineering (Bakiri and Wagner, 2013).

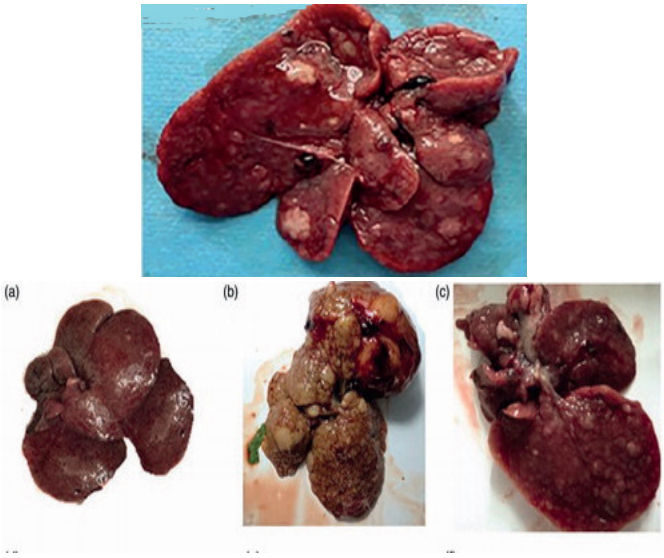


*Figure 4. DEN induced liver cancer in rats (Yang et al., 2018, Hu et al., 2020).*

Some chemical reagents induce tumor formation when applied in sufficient doses and for the appropriate time interval. There are two types of carcinogenic compounds: (i) genotoxic compounds, characterized by their ability to induce structural DNA changes, and (ii) compounds that are not directly genotoxic but that enhance tumor formation after being initiated by a hepatotoxic compound. The advantage of chemically induced models is that they mimic the injury-fibrosis-malignancy cycle seen in humans. This makes them favorite models for HCC research (Heindryckx et al., 2009). Nitrosamines began to be studied after 1956, and of the approximately 300 nitrosamines and N-nitroso compounds, 90% have been identified as carcinogenic. Most are organ specific. For example, dimethylnitrosamine

causes liver cancer in experimental animals, while some tobacco-specific nitrosamines cause lung cancer. Since nitrosamines are metabolized in the same way in human and animal tissues, it seems likely that humans are sensitive to the carcinogenic properties of nitrosamines (Scanlan, 2000). N-nitrosamines have been found in air, water, foods, cosmetics, tobacco, and packaging materials. N-nitrosamines have been a problem in processed meats because of nitrite added to prevent the growth of *Clostridium botulinum*. Thus, high concentrations of nitrosamines have been reported in bacon, sausage, and ham, while low levels have been detected in unprocessed meats. Nitrosamines have also been reported in salted fish, beer, and water (Scanlan, 1975).

Diethylnitrosamine (DEN), a genotoxic drug, has been used to induce HCC in rodents since the 60s (Rajewsky et al., 1966) and is the most commonly used chemical to induce liver cancer in mice. DEN is a DNA alkylating agent that leads to the formation of mutagenic DNA adducts. In addition, DEN bioactivation by cytochrome P450 can generate reactive oxygen species (ROS) (Qi et al., 2008), which damage DNA, proteins, and lipids and lead to hepatocyte death. The target organ to which DEN induces malignant tumors is species-specific and varies. A single low starting dose does not lead to neoplasm formation, while high-dose administration induces Hepatocellular Carcinoma (HCC) after the latent stage. Several DNA repair mechanisms, such as nonhomologous end joining, recombinational repair, base excision repair, and others, prevent the mutagenicity of DNA insertions when DEN is administered in a single low dose (Pegg 1990; Teoh et al., 2008). The time required to develop HCC after a single DEN injection depends not only on the administered dose but also on the sex, age, and strain of mice (Rao and Vesselinovitch, 1973). The younger the mice, the faster HCC occur due to the high hepatocyte proliferation rates of young animals (Vesselinovitch and Mihailovich, 1983). After a long-term repeated DEN administration, HCC develops in 100% of male mice and 30% of female mice. The gender-related difference in HCC incidence is due to the inhibitory effect of estrogens and the stimulatory effect of androgens on hepatocarcinogenesis (Nakatani et al., 2001).

DEN, which acts as a full carcinogen if applied at an early stage, requires tumor stimulants in later applications and for this purpose, thioacetamide (TAA), phenobarbital (PB), carbon tetrachloride, partial hepatectomy or recent high-fat diet feeding methods can be used as stimulants (Park et al., 2010).

A two-stage model is usually used to create an HCC model, in which a genotoxic compound is administered followed by a stimulant. DEN can be used as an initiator and thioacetamide (TAA) as a promoter (Heindryckx, 2009).

Thioacetamide (TAA) is a hepatotoxin that can be administered in drinking water (0.02-0.05%) or by intraperitoneal injections. Repeated administration leads to the development of liver fibrosis in mice over a period of 10–15 weeks (Palacios et al., 2008). The hepatotoxic effect is a result of the oxidation properties of the compound, leading to hepatic oxidative stress and liver damage (Heindryckx et al., 2009). DEN is mainly used as an initiating agent of rodent hepatocarcinogenesis, while TAA is frequently applied to create a supportive environment for DEN-induced lesions (Ito et al., 2000; Wallace et al., 2015). Hepatic bioactivation of DEN produces reactive metabolites and reactive oxygen species (ROS), which lead to the formation of mutagenic DNA adducts (Qi et al., 2008). In addition, bioactivation of TAA produces reactive metabolites that bind to proteins and lipids, thereby causing oxidative stress, centripetal necrosis and ultimately collagen deposition (Wallace et al., 2015). The genome instability that occurs with this oxidative stress-altered microenvironment resembles hepatocarcinogenesis with cirrhosis in humans (Cichoż-Lach and Michalak, 2014).

The following are compiled studies examining medicinal plants and plant derived chemicals that have been explored for their therapeutic or protective effects in hepatocellular carcinoma models:

Oxidative damage of cellular components by free radicals and other reactive oxygen molecules is believed to be associated with the development of degenerative diseases. A study aimed to evaluate the antioxidant capacity and free radical scavenging activity of the golden strawberry plant in a DEN and carbon tetrachloride (CCl4) (3 mL/kg b.w.)-induced Hepatocellular Carcinoma (HCC) rat model. The rats were divided into 4 groups: Group 1 (control): The rats of this group did not receive any treatment; Group 2 (CGJ): The rats were given golden strawberry juice at a daily dose of 1 ml/kg; group 3 (HCC): treated with a single intraperitoneal dose DEN injection (200 mg/kg body weight) and a subcutaneous CCl4 injection (3 mL/kg/week); group 4: (HCC + CGJ): rats were treated with DEN (200 mg/kg) and CCl4 (3 mL/kg weight per week) along with daily golden strawberry juice administered at a dose of 1 ml/kg. DEN+CCl4 administration caused a significant increase in tumor marker level, alphafetoprotein level and liver function enzymes activity as well as malondialdehyde. This indicated oxidative stress with a significant decrease in antioxidant biomarkers including glutathione, total antioxidant capacity, superoxide dismutase and catalase in the examined tissues. However, it has been reported that GGJ administration can reduce these changes to control levels (Hassan et al., 2017).

In a study investigating the protective effects and possible mechanisms of garlic oil (GO) against N-nitrosodiethylamine (NDEA)-induced hepatocarcinoma in rats, morphology, histology, biochemical indices of serum, and changes in DNA oxidative damage of liver were examined to

evaluate the protective effects. Lipid peroxidation (LPO), antioxidant defense system, and apoptosis-related proteins were measured to investigate the potential mechanisms. At the end of the study (21 weeks), it was revealed that GO administration inhibited the increase in nodule incidence and nodule number per liver and significantly reduced the NDEA-induced elevation of serum biochemical indices. The mRNA and protein levels of Bcl-2, Bcl-xl, and β-arrestin-2 decreased significantly, while the values of Bax and caspase-3 increased significantly. These data revealed that GO showed significant protection against NDEA-induced hepatocarcinogenesis, which may be related to the increase of antioxidant activity and induction of apoptosis (Zhang et al., 2012).

Amereh et al. (2012) aimed to investigate the chemopreventive effect of water extract of Elanus angustifolia fruit (AEA) in DEN-induced HCC model in rats. 200 mg/kg DEN was administered to rats as a single dose as a cancer initiator and acetylaminofluorene (AAF) was used as a stimulant. In the study, a significant decrease was observed in serum biomarkers of liver damage and cancer, including alpha-fetoprotein (AFP), gamma glutamyl transpeptidase (GGT), alanine transaminase (ALT), and aspartate transaminase (AST) compared to rats with HCC. In addition, the fruit extract exhibited in vivo antioxidant activity by increasing the content of reduced glutathione (GSH) as well as preventing lipid peroxidation in liver tissues of DEN-treated rats. The relative weight of the liver, a prognostic marker of HCC, was also reduced in rats treated with AEA. In conclusion, the fruit was shown to have a significant chemopreventive effect against DEN-induced primary liver cancer in rats.

Karakurt (2018) investigated the protective effects of silymarin on rats in the HCC model in terms of biochemical and histological aspects. In the study that lasted for 21 weeks, DEN was applied to rats at a concentration of 50 mg/kg every week. As a result, nodular structures of different sizes and numbers were detected macroscopically in the DEN group. According to biochemical parameters (ALT, AST, ALP and TOS), a statistically significant decrease was observed in the DEN+Silymarin group compared to the DEN group.

Sehrawat and Sultana (2006) investigated the inhibitory properties of the *Tamarix gallica* plant in the HCC rat model initiated with DEN and induced with 2-AAF. It was reported that liver tumor formation decreased with 25 and 50 mg/kg *T. gallica* methanol extracts. In this study, hepatocarcinogenesis was also tried to be stimulated by performing partial hepatectomy.

*Annona senegalensis* extracts were administered at 100 mg/kg and 200 mg/kg to rats which were first exposed to 100 mg/kg DEN and then to 0,5 mL/kg CCl4 i.p. once a week for 3 weeks. Antioxidant enzyme and liver function parameters were determined spectrophotometrically. BCL-2, P53, P21, IL-6, FNTA, VEGF, HIF, AFP, XIAP and EGFR mRNA expressions were examined

by RT-PCR technique. ALT and AST activities caused a significant decrease ($p < 0.05$) in the DEN-administered group. At the same time, a decrease in MDA level and a significant increase in SOD and GSH activities occurred. After the application, IL-6, BCL-2, VEGF, EGFR, XIAP, FNTA and P21 mRNA expressions decreased significantly ($p < 0.05$). Histopathological examinations showed that the extract improved liver appearance (Yakubu et al., 2020).

Velid (2013) designed an experiment consisting of 64 animals, 8 female rats in each group. DEN and 2-AAF were used to create the HCC model. The experiment was planned for five weeks. As a result of the experiment, a significant increase was observed in the MDA levels of the animals given only DEN and 2-AAF, while a decrease was observed in the MDA levels in the group given both DEN and 2-AAF and the chemotherapeutic agent octreotide. While SOD activity increased in the DEN and 2-AAF group animals, it decreased in the group given both DEN and 2-AAF and the chemotherapeutic agent octreotide. While CAT activity decreased in the DEN and 2-AAF group animals, it increased in the group given both DEN and 2-AAF and the chemotherapeutic agent octreotide.

In a study investigating the effects of *Medemia argun* extract in a HCC rat model, HCC initiated with a single dose of 200 mg/kg i.p. DEN and stimulated with 3 ml/kg CCl4 per week. As a result, an increase in AFP levels, liver size and weight, collagen fibril amount, and cellular proliferation was observed in the cancer group. In the group where the extract was started before carcinogens, the plant extract protected the liver against the cancer process. There was an increase in caspase-3 expression in the extract-applied groups compared to the HCC group. In the HCC groups, DEN and CCl4 caused a decrease in antioxidant defense enzymes and BAX/Bcl-2 ratio (Abdel-Hamid et al., 2021).

Keleş (2020) conducted a study investigating the antitumor effects of nettle seed in a rat HCC model. For this purpose, 40 rats were divided into 5 groups of 8 each. As a result of the experiment, DEN application increased AST, ALT and LDH activities and TOS and MDA levels, while decreasing TAS, GSH, CAT, SOD and GSH-Px levels. However, it was observed that the use of nettle seed extract together with DEN increased antioxidant capacity, suppressed oxidative stress and prevented liver damage. On the other hand, it was determined that DEN application significantly increased the activities of tumor markers, especially CA 15-3, CA 19-9 and CA 125-II, and apoptotic factors, especially caspase-3 levels, and the use of the extract together with DEN reduced these increases. Pathologically, a fine granular appearance was observed in the liver in the DEN group; histopathologically, dysplasia characterized by widespread large and small cell changes in hepatocytes and degeneration, bile duct hyperplasia, inflammatory cell infiltrations, fibrosis and cholestasis were observed. Immunohistochemically, significant reactions were observed in Hep par-1, AFP, caspase-3 and iNOS staining in the DEN

group, while a significant decrease in the expression of these antibodies was detected in the groups that were given extract together with DEN.

In a study investigating the anticancer effects of dates, DEN was administered to rats as a cancer stimulant at a dose of 180 mg/kg in 2 doses, 15 days apart. The extracts were administered to rats together with DEN at doses of 0.5 and 1 g/kg every day for 10 weeks. In the groups that were administered DEN together with the extract, SOD, GR, GPx, KAT activities increased compared to the group that was administered only DEN, while ALT, AST, ALP and lipid peroxidation levels decreased significantly. Again, while AFP and IL-6 gene expressions decreased in the groups that were administered DEN together with the extract, they increased in the group that was administered DEN (Khan et al., 2017).

You et al. (2021) investigated the effects of phylanthin, one of the lignans with anticancer properties, on a rat HCC model and HepG2 (liver cancer cell line). DEN administration caused an increase in liver weight, 8-OHdG, hepatic tissue damage marker, lipid peroxidation and tumor marker levels in rats. Phylanthin improved all liver function enzymes, oxidative DNA damage and tumor-specific markers. MTT test showed that phylanthin inhibited HepG2 cell growth in a dose-dependent manner. Surprisingly, phylanthin did not show a significant effect on the normal cell line HL7702.

In the study conducted by Özeren (2018), rats were given Diethylnitrosamine (DEN) and phenobarbital (FB) and the protective effect of Oleuropein was investigated. The animals was divided into 5 groups as Control Group, Diethylnitrosamine (DEN) group, Diethylnitrosamine (DEN) and Phenobarbital (FB) Group, DEN+FB+Oleuropein (OLE) group and Oleuropein (OLE) group. At the end of the 8-week experimental period, an increase was observed in liver MDA levels in all groups compared to the control group. A significant decrease was found in the DEN+FB+OLE group compared to the DEN+FB group. In liver CAT levels, the OLE group showed a significant decrease compared to the DEN, DEN+FB and DEN+FB+OLE groups. While liver GSH levels among all groups showed a significant decrease in the DEN and DEN+FB groups compared to the control group, the OLE and DEN+FB+OLE groups were consistent with the control group. No difference was found between the groups in liver SOD levels.

Dai et al. (2013) aimed to determine the protective effects of *Scutellaria barbata* extract, a traditional Chinese medicinal plant, against diethylnitrosamine (DEN)-induced rat liver tumor formation. The results obtained from histological examination showed that the number of liver nodules in the extract groups decreased compared to the model group ($p < 0.05$). The MDA content determined in the liver decreased significantly and the SOD level increased with the extract application. It was concluded that the

extract could inhibit experimental liver tumor formation and alleviate liver damage in rats.

In the study evaluating the effects of Naringenin on N-nitrosodiethylamine (NDEA)-induced hepatocarcinogenesis in rats, the administration of NDEA-induced Hepatocellular Carcinoma (HCC) could be established as evidenced by changes in histopathological architecture, increased cytochrome P450 activity, decreased glutathione S-transferase (GST) activity, decreased antioxidant status, increased lipid peroxidation and increased liver marker enzymes. Naringenin effectively suppressed NDEA-induced hepatocarcinoma and associated preneoplastic lesions by modulating xenobiotic metabolizing enzymes, alleviating lipid peroxidation (both through free radical scavenging and increased antioxidant status). These results indicate that Naringenin prevents lipid peroxidation and hepatic cell damage and also protects the antioxidant system in N-nitrosdiethylamine-induced hepatocarcinogenesis (Arul and Subramanian, 2013).

Fahmi et al. (2019) investigated the effects of ginger essential oil against DEN toxicity in rats. Serum HDL increased in rats given ginger, while LDL, ALT, and ALP decreased. Serum GSH-Px activity increased by 75.06%. Ginger essential oil also showed anticancer effects in HepG2 lines and the IC50 value was calculated as 40 mg/mL.

In a study investigating the curative effect of methanol extracts of *Rubia cordifolia* plant on Diethylnitrosamine-induced experimental hepatocellular carcinogenesis in rats, high AST, ALT levels and low SOD, CAT, and GPx activities were determined in DEN groups. It was reported that antioxidant enzyme activities increased in the extract groups. It was concluded that Rubia cordifolia may be a powerful antioxidant source for the treatment of diseases such as cancer (Shilpa et al., 2012).

Salimi et al. (2020) aimed to investigate the effects of alone or in combination of ellagic acid (EA) and sorafenib (SOR) on HCC hepatocyte viability and apoptosis signaling in vitro and in vivo. The results showed that SOR and EA administered alone or in combination increased reactive oxygen species (ROS), mitochondrial membrane potential (MMP), and cytochrome c release from HCC hepatocyte group to mitochondria. In addition, SOR and EA administered alone or in combination increased caspase-3 activity and decreased hepatocyte viability only in HCC group. EA and SOR were shown to be effective in HCC rat model via targeting mitochondria and hepatocyte.

In the study investigating the protective effect of olive water extract on rat HCC model, a significant decrease was detected in serum liver damage and cancer markers (AFP, GGT, ALT, AST) of rats in the extract group. The extract reduced lipid peroxidation and prevented liver weight gain, which is a prognostic marker. Histopathological experiments on liver sections confirmed

the preventive effect of olive extract against DEN-induced HCC (Shirazi et al., 2018).

In the study aiming to evaluate the chemo-prophylactic adequacy and other possible activities of *Moringa oleifera* leaf ethanol extract (MOLEE) against diethylnitrosamine (DEN)-induced HCC, an increase in serum biochemical parameters and a 29% increase in hepatic 8-hydroxy-2-deoxyguanosine (8-OHdG) levels due to DEN were reported. The expression of Bcl-2, Bcl-xl and β-arrestin-2 was reported to be decreased ($p < 0.05$); however, the expression of Bax and caspase-3 was reported to be increased ($p < 0.05$). The results indicated that MOLEE may have critical defensive effects against DEN-induced hepatocarcinogenesis, which can be defined by the application of antioxidant activity and the induction of apoptosis (Sadek et al., 2017).

Al-Attar and Shawush (2015) conducted a study to evaluate the protective activity of olive and rosemary leaf extracts on thioacetamide (TAA)-induced experimental liver cirrhosis in Wistar male rats. A highly significant decrease in body weight gain values and a statistical increase in liver/body weight ratio were recorded in TAA-administered rats. In addition, serum alanine aminotransferase, aspartate aminotransferase, gamma glutamyl transferase, alkaline phosphatase and total bilirubin levels were statistically increased. In addition, light microscopic examination of liver sections of rats treated with TAA showed a significant increase in the extracellular matrix collagen content. Collagen bundles were formed surrounding the lobules, resulting in large fibrous septa and distorted tissue architecture. The findings of this experimental study showed that olive and rosemary leaf extracts and their combinations have hepatoprotective properties against TAA-induced liver cirrhosis by inhibiting physiological and histopathological changes. Furthermore, these results suggest that the hepatoprotective effects of these extracts can be attributed to their antioxidant activity.

## REFERENCES


Abdel-Hamid, N. M., Abd Allah, S. G., Hassan, M. K., Ahmed, A. A., Anber, N. H., Adel Faried, I., 2021. Possible Protective Potency of Argun Nut (*Medemia argun*–An Ancient Egyptian Palm) against Hepatocellular Carcinoma in Rats. ***Nutrition and Cancer***, 1-12.

Al-Attar, A. M., Shawush, N. A., 2015. Influence of olive and rosemary leaves extracts on chemically induced liver cirrhosis in male rats. ***Saudi journal of biological sciences*, 22**(2): 157-163.

Aliustaoğlu, M., 2009. Temel Kanser Fizyopatolojisi. Klinik Gelişim, 22(3), 46-49.

Amereh, Z., Hatami, N., Shirazi, F. H., Gholami, S., Hosseini, S. H., Noubarani, M., ..., Eskandari, M. R., 2017. Cancer chemoprevention by oleaster (*Elaeagnus angustifoli* L.) fruit extract in a model of hepatocellular carcinoma induced by diethylnitrosamine in rats. ***EXCLI journal,* 16**: 1046.

Anonymous, 2021. https://www.drozdogan.com/kanserin-sebepleri-kisaca-nelerdir/. Access Date: 15.03.2021.

Arul, D., Subramanian, P., 2013. Inhibitory effect of naringenin (citrus flavonone) on Nnitrosodiethylamine induced hepatocarcinogenesis in rats. ***Biochem Biophys Res Commun.,* 434** (2): 203-209, doi: 10.1016/j.bbrc.2013.03.039.

Bakiri, L., Wagner, E. F., 2013. Mouse models for liver cancer. Molecular oncology, 7(2): 206-223.

Bayık, A., 1989. Kanser Epidemiyolojisi. Journal of Ege University Nursing Faculty, 5(3): 58-71.

Bray, F., Ferlay, J., Soerjomataram, I, Siegel, R. L., Torre, L. A., Jemal, A., 2018. Global cancer statistics 2018: GLOBOCAN estimates of incidence and mortality worldwide for 36 cancers in 185 countries. CA Cancer J Clin, 68: 394-424.

Cichoż-Lach, H., Michalak, A., 2014. Oxidative stress as a crucial factor in liver diseases. ***World J. Gastroenterol.,* 20:** 8082.

Dai, Z. J., Wu, W. Y., Kang, H. F., Ma, X. B., Zhang, S. Q., Min, W. L., Kang, W. F., Ma, X. B., Zhang, S. Q., Min, W. L., Lu, W. F., Lin, S., Wang, X. J., 2013. Protective effects of *Scutellaria barbata* against rat liver tumorigenesis. ***Asian Pac J Cancer Prev.,* 14** (1): 261-265.

El-Serag, H. B., Rudolph, K. L., 2007. Hepatocellular carcinoma: epidemiology and molecular carcinogenesis. Gastroenterology, 132: 2557-2576.

Fahmi, A., Hassanen, N., Abdur-Rahman, M., Shams-Eldin, E., 2019. Phytochemicals, antioxidant activity and hepatoprotective effect of ginger (*Zingiber officinale*) on diethylnitrosamine toxicity in rats. ***Biomarkers,* 24**(5): 436-447.

Gomaa, A. I., Khan, S. A., Toledano, M. B., Waked, I., Taylor-Robinson, S. D., 2008. Hepatocellular carcinoma: epidemiology, risk factors and pathogenesis. World journal of gastroenterology. WJG, 14(27): 4300.

Hanahan D. Hallmarks of Cancer: New Dimensions. Cancer Discov. 2022 Jan;12(1):31-46. doi: 10.1158/2159-8290.CD-21-1059. PMID: 35022204.

Hassan, H. A., Ghareb, N. E., Azhari, G. F., 2017. Antioxidant activity and free radical-scavenging of cape gooseberry (*Physalis peruviana* L.) in hepatocellular carcinoma rats model. ***Hepatoma Research, 3***: 27-33.

Hassan, H. A., Ghareb, N. E., Azhari, G. F., 2017. Antioxidant activity and free radical-scavenging of cape gooseberry (*Physalis peruviana* L.) in hepatocellular carcinoma rats model. ***Hepatoma Research, 3***: 27-33.

Hassanpour, S. H., Dehghani, M., 2017. Review of cancer from perspective of molecular. Journal of Cancer Research and Practice, 4(4): 127-129.

Heindryckx, F., Colle, I., Van Vlierberghe, H., 2009. Experimental mouse models for hepatocellular carcinoma research. International journal of experimental pathology, 90(4): 367-386.

Hu, J. W., Chen, B., Zhang, J., Qi, Y. P., Liang, J. H., Zhong, J. H., & Xiang, B. D. (2020). Novel combination of celecoxib and metformin improves the antitumor effect by inhibiting the growth of Hepatocellular Carcinoma. Journal of Cancer, 11(21), 6437.

Ito, N., Imaida, K., Asamoto, M., Shirai, T., 2000. Early detection of carcinogenic substances and modifiers in rats. ***Mut. Res.* 462**: 209–217.

Karakurt E., 2018. ***Ratlarda Deneysel Karaciğer Kanser Modelinde Silymarin'in Koruyucu Etkisinin Histopatolojik ve Biyokimyasal Yöntemlerle Araştırılması.*** (PhD Thesis), Institute of Health Sciences, Kars.

Keleş, Ö. F., 2020. Ratlarda Deneysel Olarak Dietilnitrozamin ile İndüklenen Hepatosellüler Karsinogenezis Sürecinde Urtica Dioica'nin Antitümör Etkinliğinin Araştırılması. (PhD Thesis), Institute of Health Sciences, Van.

Khan, F., Khan, T. J., Kalamegam, G., Pushparaj, P. N., Chaudhary, A., Abuzenadah, A., Al-Qahtani, M., 2017. Anti-cancer effects of Ajwa dates (Phoenix dactylifera L.) in diethylnitrosamine induced hepatocellular carcinoma in Wistar rats. BMC complementary and alternative medicine, 17(1): 1-10.

Laursen, L. (2014). A preventable cancer. Nature, 516.

Montalto, G., Cervello, M., Giannitrapani, L., Dantona, F., Terranova, A., Castagnetta, L. A., 2002. Epidemiology, risk factors, and natural history of hepatocellular carcinoma. Annals of the New York Academy of Sciences, 963(1): 13-20.

Nakatani T., Roy G., Fujimoto N., Asahara T., Ito A., 2001. Sex hormone dependency of diethylnitrosamineinduced liver tumors in mice and chemoprevention by leuprorelin. ***Jpn. J. Cancer Res.* 92**: 249–256.

Özeren, N. N., 2018. ***Ratlara Dietilnitrozamin ve Fenobarbital Verilerek Oluşturulan Deneysel Karaciğer Hasarına Karşı Oleuropein'in Koruyucu Etkisi***. (PhD Thesis), Institute of Health Sciences, Elâzığ.

Palacios, R. S., Roderfeld, M., Hemmann, S., Rath, T., Atanasova, S., Tschuschner, A., ..., Roeb, E., 2008. Activation of hepatic stellate cells is associated with cytokine

expression in thioacetamide-induced hepatic fibrosis in mice. ***Laboratory investigation,*** **88**(11): 1192-1203.

Park, E. J., Lee, J. H., Yu, G. Y., He, G., Ali, S. R., Holzer, R. G., ..., Karin, M., 2010. Dietary and genetic obesity promote liver inflammation and tumorigenesis by enhancing IL-6 and TNF expression. ***Cell,*** **140**(2): 197-208.

Pegg, A. E., 1990. Mammalian O6-alkylguanine-DNA alkyltransferase: regulation and importance in response to alkylating carcinogenic and therapeutic agents. ***Cancer Res.*** **50**(19): 6119–6129.

Qi, Y., Chen, X., Chan, C. Y., Li, D., Yuan, C., Yu, F., ..., Lai, L., 2008. Two-dimensional differential gel electrophoresis/analysis of diethylnitrosamine induced rat hepatocellular carcinoma. ***International journal of cancer,*** **122**(12): 2682-2688.

Rajewsky, M. F., Dauber, W., Frankenberg, H., 1966. Liver carcinogenesis by diethylnitrosamine in the rat. Science, 152(3718): 83-85.

Rao, K. V. N., Vesselinovitch, S. D., 1973. Age-and sex-associated diethylnitrosamine dealkylation activity of the mouse liver and hepatocarcinogenesis. ***Cancer research,*** **33**(7): 1625-1627.

Sadek, K. M., Abouzed, T. K., Abouelkhair, R., Nasr, S., 2017. The chemo-prophylactic efficacy of an ethanol *Moringa oleifera* leaf extract against hepatocellular carcinoma in rats. ***Pharmaceutical biology,*** **55**(1): 1458-1466.

Salimi, A., Saboji, M., Seydi, E., 2020. Synergistic effects of Ellagic acid and Sorafenib on hepatocytes and mitochondria isolated from a hepatocellular carcinoma rat model. ***Nutrition and Cancer***, 1-9.

Scanlan, R. A., 2000. Nitrosamines and cancer. The Linus Pauling Institute Newsletter.

Scanlan, R. A., Issenberg, P., 1975. N-nitrosamines in foods. Critical Reviews in Food Science & Nutrition, 5(4): 357-402.

Sehrawat, A., Sultana, S., 2006. Evaluation of possible mechanisms of protective role of *Tamarix gallica* against DEN initiated and 2-AAF promoted hepatocarcinogenesis in male Wistar rats. ***Life sciences,*** **79**(15): 1456-1465.

Shilpa, P. N., Venkatabalasubramanian, S., Devaraj, S. N., 2012. Ameliorative effect of methanol extract of *Rubia cordifolia* in N-nitrosodiethylamine-induced hepatocellular carcinoma. ***Pharmaceutical biology,*** **50**(3): 376-383.

Shirazi, F. H., Piri, M., Keshavarz, S., Gholami, S., Hosseini, S. H., Noubarani, M., ..., Eskandari, M. R., 2018. Olive fruit (*Olea europaea* L.): Chemopreventive effect in the rat model of hepatocellular carcinoma. ***PharmaNutrition,*** **6**(4): 207-214.

Sung, H., Ferlay, J., Siegel, R. L., Laversanne, M., Soerjomataram, I., Jemal, A., Bray, F., 2021. Global cancer statistics 2020: GLOBOCAN estimates of incidence and mortality worldwide for 36 cancers in 185 countries. CA: a cancer journal for clinicians, 71(3): 209-249.

Teoh, N. C., Dan, Y. Y., Swisshelm, K., Lehman, S., Wright, J. H., Haque, J., …, Fausto, N., 2008. Defective DNA strand break repair causes chromosomal instability and accelerates liver carcinogenesis in mice. ***Hepatology,*** **47**(6): 2078-2088.

Vatansever, S., & Karasu, Z. (2019). Karaciğer Kanseri.

Velid, U., 2013. ***Ratlarda Oluşturulan Karaciğer Tümor Modelinde Octreotid Kemoterapötik Ajanının, Isı Şok Proteinleri, 8- Hidroksi Deoksiguanozin ve Oksidaitf Stres Parametreleri Düzeylerine Etkilerinin Araştırılması.*** (PhD Thesis), Institute of Health Sciences, Kahramanmaraş.

Vesselinovitch, S. D., Mihailovich, N., 1983. Kinetics of diethylnitrosamine hepatocarcinogenesis in the infant mouse. ***Cancer research,*** **43**(9): 4253-4259.

Wallace, M. C., Hamesch, K., Lunova, M., Kim, Y., Weiskirchen, R., Strnad, P., Friedman, S. L., 2015. Standard operating procedures in experimental liver research: thioacetamide model in mice and rats. ***Laboratory animals,*** **49**(1): 21-29.

Yakubu, O. F., Metibemu, D. S., Adelani, I. B., Adesina, G. O., Edokwe, C. B., Oseha, O. E., Adebayo, A. H., 2020. Annona senegalensis extract demonstrates anticancer properties in N-diethylnitrosamine-induced hepatocellular carcinoma in male Wistar rats. ***Biomedicine & Pharmacotherapy,*** **131**: 110786.

Yang, W., Zhou, G., Zou, S., Yang, W., Liu, A., Sun, S., & Xie, B. (2018). Metabonomics of d-glucaro-1, 4-lactone in preventing diethylnitrosamine-induced liver cancer in rats. Pharmaceutical biology, 56(1), 643-648.

You, Y., Zhu, F., Li, Z., Zhang, L., Xie, Y., Chinnathambi, A., ..., Lu, B., 2021. Phyllanthin prevents diethylnitrosamine (DEN) induced liver carcinogenesis in rats and induces apoptotic cell death in HepG2 cells. ***Biomedicine & Pharmacotherapy,*** **137**: 111335.

Zhang, C. L., Zeng, T., Zhao, X. L., Yu, L. H., Zhu, Z. P., Xie, K. Q., 2012. Protective effects of garlic oil on hepatocarcinoma induced by N-nitrosodiethylamine in rats. ***International journal of biological sciences,*** **8**(3): 363.

# CHAPTER 3

## METHODS OF STERILIZATION

*Meryem Doymuş*[1]
*Tuğba Nafızoğlu*[2]

1 Öğr. Gör. Dr., Atatürk Üniversitesi Hınıs Meslek Yüksekokulu
0000-0002-3184-1422
2 Arş. Gör. Dr., Atatürk Üniversitesi Fen Fakültesi
0000-0002-9573-7448

## 1. INTRODUCTION

The process of killing or removing all microorganisms in an environment is called sterilization. In a broader definition, the process of killing or removing all the vegetative forms or resistant spores of all microorganisms with the use of either physical or chemical agents is called sterilization. The material on which the sterilization process is applied is called sterile (Madigan et al. 1997).

Although the sterilization process kills all microorganisms, it may not eliminate all harmful microbial activities. For example; endotoxins produced by microorganisms can remain in the environment even as a result of the sterilization process and can enter the body of other living things and damage them (Madigan et al. 1997).

Sterilization processes are used for various purposes in medicine. In surgery, instruments which will touch the tissues must be sterilized to avoid infections. Medicines to be injected into the body must also be sterile. Sterilization is one of the most important processes in microbiology. It is impossible to carry out microbiological studies unless the working environment, tools and equipment used, and medium are free of microorganisms. The food industry is also one of the main areas where sterilization is used. Food products offered to consumers should be sterile (Govindaraj and Muthuraman, 2015).

There are many sterilization methods such as physical and chemical methods. Physical methods including filters, use of heat, radiation and chemical methods are performed by using chemical agents. Some chemicals when used at appropriate concentration for appropriate duration can be used for sterilization and are called sterilant liquids. Those chemicals which can be safely applied over skin and mucus membranes are called antiseptics.

A disinfection is a process eliminating many or all pathogenic microorganisms except bacterial spores, on inanimate objects. With the disinfection process, there is a great decrease in the number of microorganisms in the working area, but not all of them are killed. Agents used for disinfection are called disinfectants (Gorman and Scott, 2004).

## 2. METHODS OF STERILIZATION

Sterilization process can be carried out by physical and chemical methods. These methods have advantages and disadvantages in terms of cost and applicability. Hot, cold, dryness, rays, electric current, sonic-ultrasonic vibrations, high pressure, osmotic changes and filtration methods can be listed as physical methods. Chemical sterilization can be done by chemical agents (liquid or gas). The methods of sterilization are shown in figure 1.

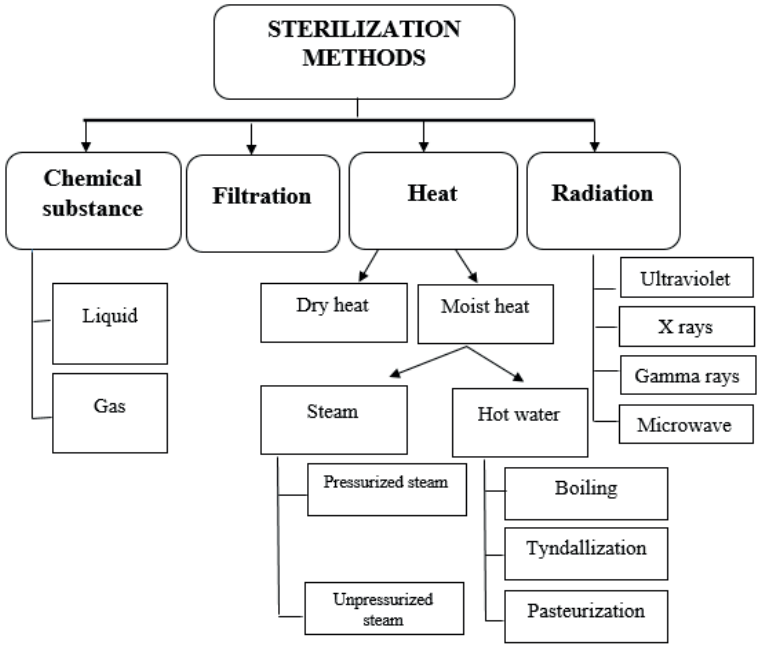


**Figure 1**. *Physical and chemical sterilization methods*

### 2.1. Heat Sterilization

In general, temperature causes deterioration of the protein, nucleic acid and fat structure of microorganisms. Protein and other substances coagulated by temperature causes cell death. Temperature is a very commonly used sterilization method (McDonnell, 2020). Glass materials used in the laboratory are heat resistant, but plastic materials differ in their heat resistance (Özyılmaz, 2015). In sterilization with heat, factors such as temperature, duration of heat, amount of humidity in the environment, pH of the environment, osmotic pressure are effective on sterilization.

Sterilization with heat is divided into two groups: dry heat sterilization and moist heat sterilization.

#### 2.1.1. Dry heat sterilization

Dry heat is used for the sterilization of materials which cannot be sterilized by humid air or damaged by moisture (McDonnell, 2020). Before the heat sterilization process, the materials should be placed in aluminum foil, glass / plastic carriers or gelatin bags which can resist sterilization. Thus, after the sterilization process, the sterility is preserved during the transportation of the materials or waiting until they are used. For example, before sterilization,

the mouths of the mortars and the tips of the pestle hands should be covered with aluminum foil (Klement et al. 1990). For a good sterilization, there should be spaces between the materials where air can easily circulate. It is very important for air circulation not to overfill the oven. Dry heat; denaturing protein, fat and nucleic acids besides, it causes oxidation (removal of electron from the cell) and loses its function (McDonnell, 2020).

Methods of dry heat sterilization are listed below:

- Flaming
- Hot air oven

#### 2.1.1.1. Flaming

Flaming is one of the most frequently used methods in the laboratory is to make the material incandescent or to lick its surface to the flame and then cool it and use it over and over again. Bunzen (Jensen, 2005), which was first described in 1857 for this purpose, is one of the most used tools today. Bunzen flame should not be yellow in color and should not burn sooty. The gas valve and air duct under the bunze should be brought into proper position and a blue flame, which is not too tall and does not produce soot, should be obtained (Morgan 1941). The temperature in the Bunzen flame varies between about 1000-2000 °C experimentally, depending on the type of bunzen, gas / air mixture and the point where the flame is measured (Chen et al. 1996). Under normal operating conditions, its temperature is around 1500 C. When looking at the bunzen flame with a suitable gas-air ratio, 3 conical colored parts with common intertwined bases catch the eye. The hottest part of the flame is the peak of the second conical flame in the interior (Özyılmaz, 2015). This temperature can kill microorganisms in a short time.

#### 2.1.1.2. Hot air oven

Since the moisture factor disappears in the dry hot air sterilization process, it requires both higher temperatures and longer application times. Pasteur ovens are used for this purpose. With this method, tools made of glass and metal materials (tube, petri dish, balloon, pipette, scissors, scalpel, etc.), oils which cannot be sterilized in autoclave and filter papers are sterilized due to the inability of moisture to reach them. Medium and liquids cannot be sterilized by this method. In this method, materials are kept at 175 °C (170 °C for one hour), 165 °C for two hours and 150 °C for three hours for complete sterilization (Chen et al. 1996).

### 2.1.2. Moist Heat Sterilization

Water and saturated water vapor are very effective in transmitting heat. Therefore, they are used as one of the sterilization methods (McDonnell, 2020).

#### 2.1.2.1. Boiling

In this method, it is necessary to keep the materials at 100 °C for at least 30 minutes. Syringes, rubber goods and surgical instruments may be sterilized by this method. Almost all bacteria and certain spores are killed in this method (Kumar et al. 2018).

#### 2.1.2.2. Tyndallization

Another form of moist heat sterilization is gradual heating or tyndallization. It is to sterilize liquid substances, which are based on bacteria, at a certain temperature for three consecutive days, each time. It is made in a sterilization device called a water bath. Depending on the temperature resistance of the sterilized liquid, it is kept at 60 °C for one hour and at 80-100 °C for half an hour, then it is removed and kept overnight at room temperature. In addition, substances such as blood serum and vaccines are tindalized at 56 °C. With the first heating, the vegetative forms of the microbes die, the spores do not die. The same process is applied on the second and third days, allowing the spores to die (Harrigan and McCance, 2014).

#### 2.1.2.3. Autoclaving

It is the most widely used method, except in cases where penetration is limited or where heat or moisture damage would be a problem. Autoclaving is performed by steam under pressure. The materials to be sterilized in the autoclave should be wrapped in packages that are resistant to high temperatures and where steam can enter. If the packages are placed in an upright position, contact with steam will be easier. When water is heated indoors, its boiling point rises and the temperature of the steam rises. Instruments are sterilized by keeping them at 121 °C, under 1.5 atmospheres (atm) pressure, for 15 minutes (min) (Thomas et al. 2008; Gordon et al. 2001).

#### 2.1.2.4. Unpressurized steam (Koch boiler) sterilization

It is a method of sterilization by applying unpressurized steam with the Koch boiler method. It is used in the sterilization of materials that will deteriorate at temperatures over 100 °C and under pressure. For example, surgary solutions which cannot withstand high temperatures are also sterilized in the koch boiler (Özyılmaz, 2015).

#### 2.1.2.5. Pasteurization

This method works below 100°C heat. This process is used in heating of milk and other liquid food. The product is held at temperature and for a period of time to kill pathogenic bacteria that may be present in the product. This process does not destroy complete organism including spores (Kumar et al. 2018).

### 2.2. Filtration

Filtration used as the oldest and most common method; It is an application that physically cleans liquids and gases from contaminating materials. It is not a true biocidal, as it is a method that separates microorganisms rather than neutralizing them. Liquids and gases are attached to the filters according to their weight and molecular structure. Filters can be made of organic materials such as paper, fiber, cotton, as well as glass, ceramics, and can be produced. It is used to disinfect or sterilize heat sensitive materials. With the micro filtration method, particles up to 0.05 μm can be filtered. However, general purpose filtration in laboratories is performed with economical 0.2 μm hole diameter disposable filters. Filtration is also used to clean air in the laboratory. For this, filters called HEPA (High-Efficiency Particulate Air) are often used. They aim to create a clean working environment by filtering the sterile working cabinets or the air in the laboratory environment and they can hold parts larger than 0.3 μm (McDonnell, 2020).

### 2.3. Centrifugation

Centrifuge is a laboratory instrument that is given an extraordinary rotational motion with a motor and enables solid particles (cells, red blood cells, bacteria) in suspension or even emulsion form to separate them by applying centrifugal force. The device turns the rotational movement up to 10000 cycles per minute for the desired time and allows the substance with high density to collect at the bottom. Centrifugation is based on the principle of sedimentation of microorganisms in solution by rotating for a certain period of time in centrifuges. Microorganisms gather at the bottom. The liquid in the upper part generally does not contain microorganisms. This method is not widely used for sterilization purposes (Graham, 2020).

### 2.4. Sterilization by ultrasonic vibration

Ultrasonic (high sound) waves have a lethal effect on bacteria. When ultrasonic waves are applied to microorganisms in the liquid, the cells are ruptured and their contents are exposed. This method does not kill microorganisms, but rather the cells. It is used for the extraction of walls and intracellular structures, enzymes. This method is not widely used for sterilization.

Ultrasonic vibration is also used for cleaning. In normal cleaning, brushes sometimes cannot reach all surfaces. The vibration created by sound waves is almost reminiscent of high speed brushing. Ultrasonic cleaning is especially used for cleaning instruments made of stainless steel.

It is also suitable for mechanically sensitive instruments (microsurgery, dental instruments). Ultrasonic vibration is used both as a mechanical support in manual cleaning processes and before washing with a machine. It can be used as a supportive method in the removal (Harrigan and McCance, 2014).

### 2.5. Chemical sterilization

Many chemical substances can be used to disinfect laboratory materials, living / non-living tissues, hands, surfaces, places and air. These; acids and their derivatives, bases, aldehydes, anilides, antimicrobial dyes, biguanides, diamidines, phenolic compounds, surface surfactants, essential oils, plant extracts, metals, peroxygen and other oxygens, halogens and halogen donating chemicals and alcohols (McDonnell, 2020).

#### 2.5.1. Gaseous Sterilization

Reactive gases such as formaldehyde, ethylene oxide, chemicals show a biocidal effect. The antimicrobial effect of both of the mentioned reactive gases is thought to be through the alkylation of the amino group of nucleic acids and sulfhydryl, amino and hydroxyl and carboxyl groups of proteins. Generally, the concentration ranges (gas weight per unit room volume) for ethylene oxide and formaldehyde at operating temperatures of 45-63 °C and 70-75 °C are in the range of 800-1200 mg / L and 15-100 mg / L, respectively. These substances, which are alkylating gases, have mutagenic and carcinogenic potential. In addition to this, it causes acute toxicity such as irritation of the skin, conjunctiva and nasal mucosa.

#### 2.5.2. Liquid Sterilization

##### 2.5.2.1. Hydrogen Peroxide Sterilization

This liquid chemical agent stabilizes the basic cellular components by oxidizing and this leads to the inactivation of microorganisms. In this sterilization method, the temperature is kept at 40-50 °C. This is particularly suitable for the sterilization of heat and moisture sensitive medical devices. Hydrogen peroxide (both vaporized and gas plasma) is a known method used for sterilization of medical devices. There are many studies on the inactivation of viruses and bacterial spores when hydrogen peroxide is used as a sterilant (Heckert et al. 1997; Bar et al. 2001). The instruments are wrapped before sterilization. It can be used or stored after sterilization.

##### 2.5.2.2. Peracetic acid liquid sterilization

Low concentrations of peracetic acid have been determined to be sporocidal. This substance is also soluble in water and no residue remains after rinsing. It has also been shown to have no harmful effects on health and the environment. The mechanism of action takes place in the following ways: It destroys the bonds in enzymes and proteins, destroying the cell wall, interfering with the transport function of the spring, and its enzymes can oxidize and even disrupt vital biochemical pathways.

#### 2.5.2.3. Aqueous glutaraldehyde solution

This technique is used when the product is sensitive to heat. FDA should be immersed in 2.4% glutaraldehyde solution at 25 °C for 45 minutes to ensure high level of disinfection. It has been determined that 2% glutaraldehyde is an effective method for sterilization of endoscopes (Balsamo et al. 2012).

#### 2.5.2.4. Ozone ($O_3$)

$O_3$ is formed when $O_1$ molecules collide with high energy $O_2$ molecules. The third oxygen intermediate is loosely bound and easily oxidizes and stabilizes by binding to other molecules. $O_3$ causes the cell membranes of microbes to break down. The sterilization cycle takes 4 hours and 15 minutes at 30-35 (Rutala and Weber, 1999).

#### 2.5.2.5. Chlorine Dioxide ($ClO_2$)

Sodium chlorite and dilute $Cl_2$ gas are converted to $ClO_2$ by reacting. It is then exposed to the equipment to be sterilized (Patel, 2012).

#### 2.5.2.6. Ethyl alcohol (EtOH)

Alcohols, especially ethyl alcohol, are the most common, broad-spectrum and fast results disinfectants used in all laboratories is one. When alcohols do not contain water, they are less effective. Especially those with an alcohol content of more than 80% cause the proteins in the cell wall to become crowded very quickly and prevent the entry of alcohol into the cell. Therefore, when they are used in disinfection, they are used at a rate of 50-80% and optimum 60-70% (Klement et al. 1990; McDonnell, 2020).

It causes protein denaturation and coagulation in cells, followed by impairment of structure and functions. Effectiveness varies according to the evaporation rate and residence time.

Ethyl alcohol (70%) has a bactericidal effect in as little as 30 seconds. The effect on viruses and fungi lasts a little longer (> 2 minutes). It has little or no effect on bacterial spores. In high concentrations there is a risk of ignition and burns. It is used as an antiseptic for hands. However, using too much can cause drying and cracking of the skin (Klement et al. 1990).

#### 2.5.2.7. Hypochlorites

Hypochlorites, especially liquid sodium hypochlorite (bleach) solutions, are widely used in the disinfection of hard surfaces. In some cases, especially metals with this chemical In disinfection, the surface should be washed in a sterile manner at the end of the process. Because sodium hypochlorite causes corrosion in metals and causes deterioration of materials. Chlorine is recognized as a safe broad spectrum antimicrobial agent. It is an inexpensive, effective, easy-to-use method. The ones sold in the supermarkets, commonly available for home use, contain approximately 5% sodium hypochlorite.

Bacteria can withstand 0.1-0.3 m g / l of chlorine to 3 0 hours. But the rest is the other microorganisms are more durable. In high concentrations, it causes skin irritation and burns. Its effect is through the oxidation of proteins, fats and carbohydrates. This also causes function and structure deterioration. Effects on nucleic acids have also been reported. It is reported that about 3 ppm active chlorine stops the growth of *Escherichia coli* bacteria within 5 minutes by inhibiting DNA synthesis (McDonnell, 2020).

### 2.6. Radiation sterilization

Particle radiation such as electrons accelerated by electromagnetic radiation such as gamma rays and UV light are used for sterilization. The main target of radiation is the DNA of the microorganism. Gamma rays and electrons create free radicals. In contrast, UV light causes stimulation. Radiation sterilization is one of the most widespread and successful applications of radiation (Jinia et al. 2020). It is used for the sterilization of items which are damaged by heat or cannot be sterilized by other methods. The effects of radiation on cells and microorganisms depend on the effects of the radiation's wavelength, dose rate and exposure time (Silindir and Özer, 2009).

#### 2.6.1. Gamma radiation sterilization

Gamma rays are formed by self-degradation of cobalt 60 (60Co) or cesium -137 (137C). Gamma rays have high penetration and are one of the commonly used sterilization methods; It is used in the sterilization of disposable medical equipment such as syringes, needles, cannulas, cosmetics and i.v sets. It can be used for the sterilization of many materials. However, it is not suitable for the sterilization of materials containing polyvinyl chloride (PVC), acetal and polytetrafluoroethylene (PTFE). The exact penetration depends on the thickness of the material. Sterilization with gamma rays saves energy and is not dependent on chemicals or heat. There is no residue after the sterilization process (Al-Assaf et al. 2016; Ling et al. 2018). Although high-energy gamma-ray sterilization is a useful method in industrial applications, there are substances such as water that radiolyze when exposed to light.

There are two ways of gamma ray inactivation of bacteria, fungi viruses and cell damage due to the direct and indirect effect of gamma ray. The first of these mechanisms occurs directly by excitation of critical macromolecules by ionizing radiation. Ionizing radiation or high-energy photons of the active free radical can damage the DNA chain (Yusof, 2001). It causes single and double strand breaks in DNA. Although ionizing radiation causes structural defects that prevent DNA synthesis, it causes errors in protein synthesis. In this case, it results in cell death. Another mechanism of action of radiation is the formation of free radicals by hydrolysis of water in microorganisms. This situation is known as indirect effect. Free radicals interact with biological molecules, damaging DNA and killing the microorganism. Wire and double

strand fractures, intra-helix cross-linking, and base and sugar changes occur due to the indirect effects of ionizing Radiation (Singh et al. 2016).

### 2.6.2. X- rays Sterilization

Large packages and many medical devices can be sterilized by high energy X-rays, a form of ionizing energy called Bremsstrahlung. X-rays are an effective way to sterilize low density packages and have very good dose uniformity. In addition to being electrically based, it does not require chemical or radioactive material. It is not among the official sterilization methods for the sterilization of drugs and medical devices (Silindir and Özer, 2009).

### 2.6.3. UV Sterilization

Electromagnetic radiation with wavelengths between 100-400 nm is called Ultraviolet (UV) light (Mills and Andersen, 1981). UV has direct and indirect lethal effects on microorganisms. Direct effect occurs with UV rays and indirect effect occurs with the formation of hydrogen peroxide ($H_2O_2$) and ozone ($O_3$) in the environment (microwave). UV radiation causes single and double strand breaks in DNA. This situation is life threatening. If significant double strand breaks occur in DNA, it may cause loss of genetic material (Rastogi et al. 2010). The wavelength of UV light is important in the success of sterilization. DNA and RNA give maximum absorbance at 260 nm (Rastogi et al. 2010). UV absorption by bacteria is mainly due to purines and pyrimidines in nucleic acids (at maximum 260 nm). In addition, they absorb aromatic chains of tryptophan, tyrosine and phenylalanine in proteins more moderately (at max 280 nm). The sterilization spectrum is parallel to the absorption spectrum of bacteria. This means that the absorption by both nucleic acids and proteins has a lethal effect. Lethal mutations have little contribution in UV-related death. The main cause of death is changes in DNA that block replication and transcription. Since most of the changes in DNA can be repaired, the effect of UV sterilization is generally quite low (Davis et al. 1989).

Most of the UV rays do not penetrate through glass, opaque solids and liquids, and due to this feature, it can be used for the sterilization of the air in work areas, rooms or surgical environments (Boylan et al. 1987).

## 3. CONCLUSION

Adhering to aseptic working conditions in the laboratory and selecting the appropriate sterilization and disinfection methods are of paramount importance for safeguarding the health of laboratory personnel as well as ensuring the accurate conduct of the study. The disinfection of hospital environments, along with the sterilization of medical instruments, equipment, and operating theaters, is crucial. It is essential to choose the correct sterilization and disinfection techniques, carefully considering the environment in which these processes are carried out and the nature of the materials being treated.

For this reason, conditions such as time and temperature must be determined carefully. It is not possible to get results if sterilization performed under wrong or inadequate conditions.

## REFERENCES

Al-Assaf, S., Coqueret, X., Zaman, H. M. D. K., Sen, M., & Ulański, P. (Eds.). (2016). The radiation chemistry of polysaccharides (p. 486). Vienna, Austria: International Atomic Energy Agency.

Balsamo, A. C., Graziano, K. U., Schneider, R. P., Antunes Junior, M., & Lacerda, R. A. (2012). Removing biofilm from a endoscopic: evaluation of disinfection methods currently used. Revista da Escola de Enfermagem da USP, 46, 91-98.

Bär, W., de Bär, G. M., Naumann, A., & Rüsch-Gerdes, S. (2001). Contamination of bronchoscopes with Mycobacterium tuberculosis and successful sterilization by low-temperature hydrogen peroxide plasma sterilization. American journal of infection control, 29(5), 306-311.

Boylan, R. J., Goldstein, G. R., & Schulman, A. (1987). Evaluation of an ultraviolet disinfection unit. The Journal of Prosthetic Dentistry, 58(5), 650-654.

Chen, Y. C., Peters, N., Schneemann, G. A., Wruck, N., Renz, U., & Mansour, M. S. (1996). The detailed flame structure of highly stretched turbulent premixed methane-air flames. Combustion and flame, 107(3), 223-IN2.

Davis, D. R., Curtis, D. A., & White, J. M. (1989). Microwave irradiation of contaminated dental casts. Quintessence Int, 20(8), 583-5.

Gordon, B. L., Burke, F. J. T., Bagg, J., Marlborough, H. S., & McHugh, E. S. (2001). Systematic review of adherence to infection control guidelines in dentistry. Journal of dentistry, 29(8), 509-516.

Gorman, S., & Scott, E. (2004). Chemical disinfectants, antiseptics and preservatives. Hugo and Russell's Pharmaceutical Microbiology, 285-305.

Govindaraj, S., & Muthuraman, M. S. (2015). Systematic review on sterilization methods of implants and medical devices. Int J ChemTech Res, 8(2), 897-911.

Graham, J. (2020). Biological centrifugation. Garland Science.

Harrigan, W. F., & McCance, M. E. (2014). Laboratory methods in microbiology. Academic press.

Heckert, R. A., Best, M., Jordan, L. T., Dulac, G. C., Eddington, D. L., & Sterritt, W. G. (1997). Efficacy of vaporized hydrogen peroxide against exotic animal viruses. Applied and environmental microbiology, 63(10), 3916-3918.

Jensen, W. B. (2005). The origin of the Bunsen burner. Journal of Chemical Education, 82(4), 518.

Jinia, A. J., Sunbul, N. B., Meert, C. A., Miller, C. A., Clarke, S. D., Kearfott, K. J., ... & Pozzi, S. A. (2020). Review of sterilization techniques for medical and personal protective equipment contaminated with SARS-CoV-2. Ieee Access, 8, 111347-111354.

Klement, Z. (1990). Methods in Phytobacteriology. Akademiai Kiadó, Budapest, Hungary.

Kumar, A., Murthy, L. N., & Jeyakumari, A. (2018). Sterilization technique used in microbiology.

Ling, M. L., Ching, P., Widitaputra, A., Stewart, A., Sirijindadirat, N., & Thu, L. T. A. (2018). APSIC guidelines for disinfection and sterilization of instruments in health care facilities. Antimicrobial Resistance & Infection Control, 7, 1-11.

Madigan, M. T., Martinko, J. M., & Parker, J. (1997). Brock biology of microorganisms (Vol. 11). Upper Saddle River, NJ: Prentice hall.

McDonnell, G. E. (2020). Antisepsis, disinfection, and sterilization: types, action, and resistance. John Wiley & Sons.

Mills, L. F., & Andersen, F. A. (1981). Ultraviolet and microwave radiation in dentistry. General Dentistry, 29(6), 481-486.

Morgan, A. P. (1941). Simple chemical experiments. D. Appleton-Century.

Özyılmaz, Ü. (2015). Fitopatoloji Laboratuvarında Sterilizasyon Ve Dezenfeksiyon Yöntemleri. Adnan Menderes Üniversitesi Ziraat Fakültesi Dergisi, 12(1), 129-138.

Patel, M., Ebonwu, J., & Cutler, E. (2012). Comparison of chlorine dioxide and dichloroisocyanurate disinfectants for use in the dental setting. South African Dental Journal, 67(7), 364-369.

Rastogi, R. P., Richa, N., Kumar, A., Tyagi, M. B., & Sinha, R. P. (2010). Molecular mechanisms of ultraviolet radiation-induced DNA damage and repair. Journal of nucleic acids, 2010(1), 592980.

Rutala, W. A., & Weber, D. J. (1999). Infection control: the role of disinfection and sterilization. Journal of Hospital Infection, 43, S43-S55.

Silindir, M., & Özer, A. Y. (2009). Sterilization methods and the comparison of E-beam sterilization with gamma radiation sterilization. Fabad Journal of Pharmaceutical Sciences, 34(1), 43.

Singh, R., Singh, D., & Singh, A. (2016). Radiation sterilization of tissue allografts: A review. World journal of radiology, 8(4), 355.

Thomas, M. V., Jarboe, G., & Frazer, R. Q. (2008). Infection control in the dental office. Dental Clinics of North America, 52(3), 609-628.

Yusof, N. (2001). 19 Effect Of Radıatıon On Mıcroorganısms—Mechanısm Of Radıatıon Sterılısatıon. The Scientific Basis of Tissue Transplantation, 5, 342.

# CHAPTER 4

# ELECTROCHEMICAL APPROACHES TO THE ANALYSIS OF ANTIOXIDANTS

*Kuddusi Karaboduk*[1]

1 Assoc. Prof. Dr., Gazi University, Vocational School Of Health Services, Department of Health Care Services
Orcid: 0000-0003-0078-723X

## 1. FREE RADICALS AND ANTIOXIDANTS

Free radicals and antioxidants, which have become key research subjects in recent years, are gaining increasing significance in scientific discussions and studies. Free radicals such as hydroxyl, superoxide, and hydrogen peroxide are molecules released during routine cellular activities and are part of the natural physiological process in all living organisms (Hatice Karaboduk, Adiguzel, Apaydin, Kalender, & Kalender, 2024; Simioni et al., 2018). Oxidative stress occurs when the balance between antioxidants and pro-oxidants is disrupted in favor of oxidants, resulting from either an increase in reactive oxygen species (ROS) or a decrease in antioxidant levels, as the body maintains a balance between ROS and antioxidants under normal conditions (Adiguzel, Karaboduk, Apaydin, Kalender, & Kalender, 2023; Mahlooji, Beni, Mehraban, & Seyedarabi, 2025). Antioxidants are molecules that inhibit the formation of free radicals, thereby decelerating the process of autoxidation, and cells naturally contain both enzymatic and non-enzymatic antioxidants that safeguard against oxidative stress (HATİCE Karaboduk & Kalender, 2021; Uçak & Zahid, 2020). Enzymatic antioxidants consist of crucial enzymes such as Glutathione Peroxidase (GPx), Glutathione Reductase (GR), Glutathione S-transferase (GST), Superoxide Dismutase (SOD), and Catalase (CAT) (Baş, Kalender, Karaboduk, & Apaydın, 2015; Jomova et al., 2023; Hatice Karaboduk, Adıgüzel, et al., 2024; Kunter, Zabib, & Kosar, 2020). Non-enzymatic antioxidants are further divided into exogenous and endogenous types based on their origin. Exogenous antioxidants, including selenium, vitamins C and E, polyphenols, and carotenoids, are taken in by consuming fresh fruits and vegetables, which are essential sources. In contrast, endogenous antioxidants, such as melatonin, urate, glutathione, and coenzyme Q10, are synthesized internally as byproducts of the body's metabolic processes (Moussa, Judeh, & Ahmed, 2019). These enzymes are illustrated in Figure 1.

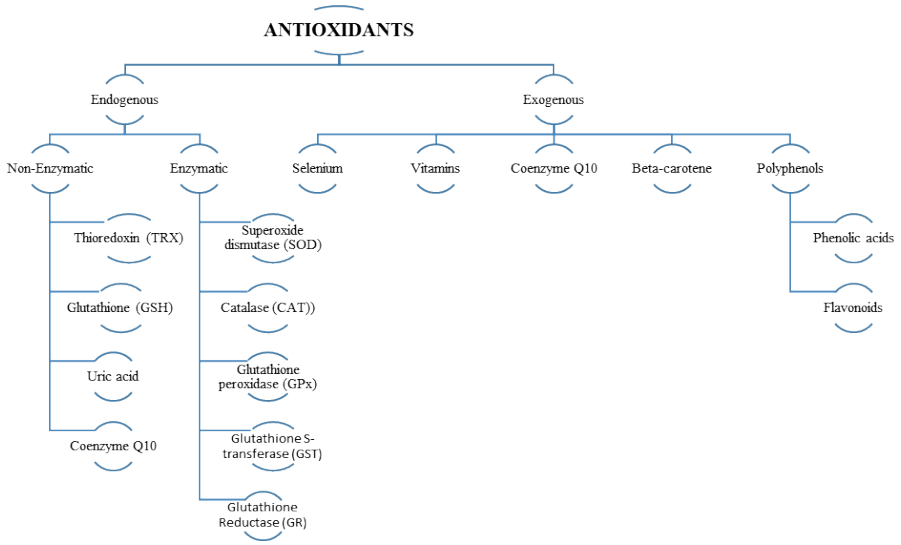


*Figure 1. The classification of antioxidants*

Non-enzymatic, and Enzymatic antioxidants protect the body against oxidative stress (Adiguzel & Kalender, 2020; Hatice Karaboduk, Uzunhisarcikli, & Kalender, 2015). Antioxidants can effectively suppress oxidation processes, even in minimal concentrations, by reducing or delaying the oxidation of various substrates within the body (Rasheed & Azeez, 2019). Antioxidants function through various mechanisms, including scavenging free radicals, converting them into less toxic compounds, delaying or inhibiting their production, chelating metal ions to reduce their catalytic activity, interrupting chain propagation reactions (as chain-breaking antioxidants), preventing the formation of secondary toxic reactive species, and enhancing the endogenous antioxidant protect system by synergistically interacting with other antioxidants (Losada-Barreiro, Sezgin-Bayindir, Paiva-Martins, & Bravo-Díaz, 2022).

The effectiveness of antioxidants has been widely investigated in biological systems such as animal models and cell cultures (Adiguzel, Karaboduk, & Uzunhisarcikli, 2024; Apaydın, Baş, Kalender, Adıgüzel, & Kalender, 2019; Hatice Karaboduk, Adiguzel, Apaydin, Uzunhisarcikli, et al., 2024; Mallamaci, Barbarossa, Carocci, & Meleleo, 2024).

In previous studies, the scavenging effect of antioxidants on free radicals has been reported with various parameters (DPPH radical scavenging and metal chelating activity, e.g.) (K. Karaboduk, Karabacak, Dogan, et al., 2014; K. Karaboduk, Karabacak, Karaboduk, & Tekinay, 2014).

Oxidative stress is widely acknowledged as a key factor in the development of various health issues, including diabetes mellitus, cancers, autoimmune diseases, cardiovascular dysfunction, and its strong association with the aging process (Hussain & Kayani, 2020; Toydemir et al., 2022).

Accurate analysis of antioxidant compounds (qualitative and quantitative) is crucial for effectively assessing oxidative stress and its impact on health.

## 2. ELECTROCHEMISTRY and VOLTAMMETRY

Electrochemistry is a branch of chemistry that investigates reactions involving electron transfers, integrating studies from electrical engineering and chemistry to examine the electrical behavior of substances. Electrochemistry links the flow of electrons to chemical transformations. The field of electrochemistry focuses on electron transfer processes occurring at the solution/electrode interface (Kalvoda & Parsons, 1985). Electrochemistry is a method that allows the analysis of many analytes at low concentrations (Doyle & Forster, 2024). Electrochemical techniques provide an environmentally friendly alternative to conventional chemical processes, utilizing electricity to drive molecular transformations that typically require high temperatures or harmful reagents (Pence, Hazen, & Rodríguez-López, 2024). Electrochemical sensors offer significant potential for highly sensitive detection of analytes, as well as for advancing miniaturization, large-scale manufacturing, and the integration of sensor components (Ab Mutalib & Suzuki, 2024). Many electrochemical sensors have been produced recently, and many species have been analyzed with high sensitivity (Bouali, Erk, Genc, Salamat, & Soylak, 2024; El-Zahry, 2024; Han, Zhang, Ding, Pan, & Wang, 2024; K. Karaboduk, 2019, 2021; Ma, Wu, Xu, & Fan, 2022; Vazan, Tashkhourian, & Haghighi, 2023; Wang et al., 2024).

Voltammetric measurements involve the determination of current as a function of the applied potential using a working electrode. Voltammetry is a key dynamic technique widely employed in electrochemistry and related fields to study interface charge transfer processes (Mirceski & Lovric, 2024). Voltammetry serves as a method for determining the concentration of substances by utilizing their redox properties. Chemically speaking, oxidation involves the loss of electrons from a molecule, whereas reduction represents the gain of electrons. Voltammetry involves the transfer of electrons to or from chemical species, a process initiated by applying an electrical potential at the boundary between an electrode and the solution. (Stamford, 1991). The plot of current against applied voltage, known as a voltammogram, provides quantitative and qualitative data about the species involved in the reaction (Figure 2). The peak potential (*Ep*) and peak current (*ip*) shown in Figure 2 are used for qualitative and quantitative analysis, respectively. While the potential is specific to the substance under certain experimental conditions, the current

is proportional to the concentration of the substance (Choudhary, Jothi, & Nageswaran, 2017).

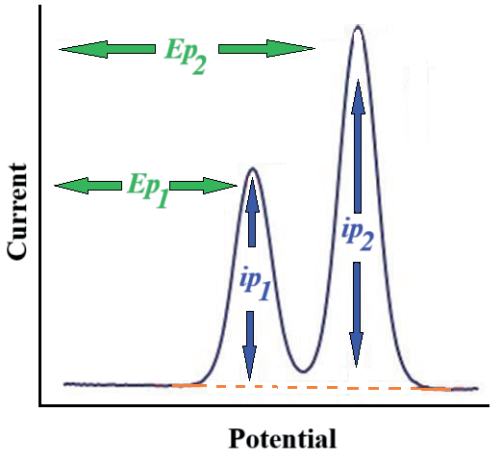


*Figure 2. A typical voltammogram*

A modern voltammetric setup typically includes three-electrodes: a counter (auxiliary) electrode, a reference electrode, and a working electrode (Figure 3) (Scholz, 2010). When a potential is applied between the working electrode and the reference electrode, voltammetric measurements can be taken by measuring the current between the counter electrode and the working electrode.

Working electrodes can take various forms, such as small mercury drops or wires, plates, and disks made from platinum, carbon, or gold. This diversity in geometry and material allows for the analysis of specific species. In general, a working electrode should:

- Be conductive,
- Remain inert within the potential range being used,
- Have a high negative potential limit,
- Be easily shaped into the desired geometry and processed efficiently.

The potential of the reference electrode remains stable throughout the experiment. In aqueous systems, saturated calomel and Ag/AgCl electrodes are commonly used, while Ag/AgNO3 electrodes are preferred in non-aqueous environments. An ideal reference electrode should:

- Be reversible and comply with the Nernst equation,
- Maintain a stable potential over time,

- Show no significant potential shift even with minimal current flow,
- Exhibit minimal sensitivity to temperature variations.

The counter electrode facilitates the flow of electric current from the signal source through the solution and toward the working electrode. While materials like gold or graphite are occasionally used, platinum wire is commonly chosen as the counter electrode.

Voltammetry involves the application of variable potential excitation signals to electrochemical cells containing an electrode. These excitation signals generate characteristic current responses, which form the basis of the method. The most commonly used excitation signals in voltammetry include linear sweep, differential pulse, square wave, and triangular wave signals. The type of excitation signal used often defines the specific voltammetric technique, such as square wave voltammetry or differential pulse voltammetry. These techniques are primarily employed in quantitative analysis. Additionally, cyclic voltammetry is used to investigate the electrochemical behavior of electroactive species (Skoog, West, Holler, & Crouch, 1996).

The modified electrode approach in electrochemistry stems from the need to control the electrode surface. The process of covering the electrode surface to create a new electrode with distinct properties is called modification. The resulting electrode is referred to as a modified electrode. After modification, the electrode surface undergoes a complete transformation, adopting the properties of the species used in the coating. Modified electrodes allow for controlling reaction rates and selectivity in electrochemical processes. Additionally, unwanted adsorption can be prevented, and desirable optical properties can be introduced in some cases. This approach helps lower the detection and quantification limits while preventing fouling of the electrode surface (Pimpilova, 2024).

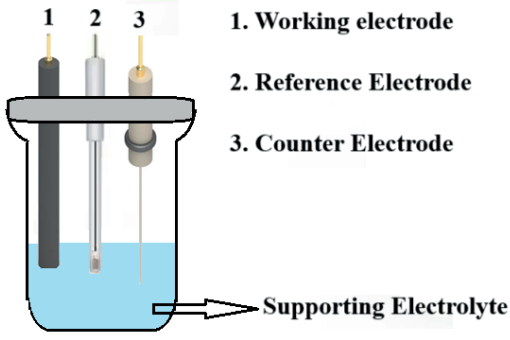


*Figure 3. Electrochemical cell and its components (three-electrode system)*

The advantages of voltammetric methods over other analytical techniques include the ability to analyze small amounts of substance, their low cost, ease of implementation, minimal need for pre-purification of analytes, reduced solvent requirements, and greater sensitivity(Arabkhani, Javadian, Asfaram, Sadeghfar, & Sadegh, 2021; K. Karaboduk & Hasdemır, 2018; Yu, Shi, Yue, & Qu, 2016).

Antioxidants are defense substances that are vital in preventing degenerative diseases. For a healthier life, it is important to obtain antioxidants from natural sources such as fruits, vegetables, and aromatic plants (Rajkumar et al., 2024). For this reason, the analysis of antioxidants is critical. The voltammetry technique is a highly sensitive method frequently preferred in antioxidant analyses. Several studies in which antioxidant analysis was performed using the voltammetric method are provided below:

Tomášková et al. (2013) developed a voltammetric method for determining N-phenyl-1-naphthylamine and butylated hydroxytoluene. N-phenyl-1-naphthylamine is an amine-type antioxidant, while butylated hydroxytoluene is a phenol-type antioxidant. They employed a gold electrode as the working electrode and analyzed these compounds in mineral oils (Tomášková, Chýlková, Machalický, Šelešovská, & Navrátil, 2013).

Petković et al. (2015) developed a voltammetric technique for determining gallic acid. Gallic acid is a widely recognized antioxidant compound. This method utilizes an electrochemical sensor, incorporating $[Cu_2tpmc](ClO_4)_4$ immobilized in a PVC matrix and coated onto graphite or glassy carbon rod. A graphite electrode was effectively utilized to determine the antioxidant capacity of GA equivalents for real samples. White, rosé, and red wine have been used as real samples (Petković, Stanković, Milčić, Sovilj, & Manojlović, 2015).

Karaboduk K. (2019) modified the glassy carbon electrode surface with silver nanoparticles/polyvinylpyrrolidone. After characterizing the electrode, ascorbic acid, an antioxidant, was analyzed in banana, kiwi, mango, and pineapple. The results were consistent with chromatographic data (K. Karaboduk, 2019)vit.

Raja et al. (2020) modified a glassy carbon electrode using graphite nanopowder and bismuth (III) oxide ($Bi_2O_3$) and characterized the modified electrode through Scanning Electron Microscopy-Energy Dispersive X-ray, Electrochemical Impedance, Fourier Transform Infrared, and X-Ray Diffraction techniques. Using the sensor, they successfully determined ellagic acid in walnut and pomegranate extracts (Raja, Singh, & Jain, 2020).

Prasad et al. (2020) utilized the prepared electrode (NiO/TiO2 NWA electrode) as an electrochemical sensor to study the electrochemical behavior of

the flavonoid naringenin. Additionally, naringenin in vegetable samples, such as tomato and ginger, was determined using differential pulse voltammetry under optimized conditions. The modified electrode was used to analyze the very low concentrations of naringenin (Prasad, Chen, Ni, & Kumar, 2020).

Ulbrich et al. (2020) modified a carbon paste electrode with $NiTe_2$, then characterized the electrode using X-ray powder diffraction analysis and transmission electron microscopy and analyzed the antioxidant properties of morin in various wine samples. They reported that the modified electrode was successfully used for the determination of morin in samples with high, medium, and low polyphenol content (de Fatima Ulbrich, Winiarski, Jost, & de Campos, 2020).

Ali et al. (2022) developed a method for the voltammetric analysis of selenite ($Se^{4+}$). For this purpose, they modified the surface of a carbon paste electrode (CPE) with multiwall carbon nanotubes (MWCNTs) and poly(1-aminoanthraquinone) (p-AAQ). The resulting electrode provided highly successful analytical results (Ali, Altahan, Beltagi, Hathoot, & Abdel-Azzem, 2022).

Yadav et al. (2022) developed a protein nanodots-conjugated gold nanoparticle and poly-lysine biointerface for the voltammetric estimation of Melatonin. The results demonstrated that the modified electrode exhibited improved electro-catalytic activity and facilitated charge transfer, contributing to enhanced sensitivity for Melatonin detection. The sensor displayed minimal interference from common substances such as uric acid, ascorbic acid, and hypoxanthine. Furthermore, the biointerface was successfully applied to determine melatonin in commercial pharmaceutical products and food samples, highlighting its potential for practical applications (Yadav, Garg, Singh, Singh, & Parmar, 2022).

Blandon-Naranjo et al. (2023) present a simple and reliable voltammetric method for determining butyl hydroxyanisole, butylhydroxytoluene, and propyl gallate in edible olive oils. In their study, square wave voltammetry was employed using platinum and carbon fiber disk ultra-microelectrodes combined with chemometric techniques to carry out the analysis (Blandon-Naranjo et al., 2023).

Mahmoud et al. (2023) developed a novel electrochemical electrode for the detection of glutathione (GSH). The electrode, composed of polyethylene glycol, chitosan, silver nanoparticles, and porous magnesium metasilicate enhanced electrocatalytic activity and GSH adsorption. Cu(II) ions released from Cu(II)-PMMS were used for precise detection without external Cu(II) addition. The sensor demonstrated a characteristic GSH-Cu(II) peak at 0.43 V, with a linear response to GSH concentration (Mahmoud et al., 2023).

Sordon and Jakubowska developed a voltammetric method for the determination of caffeic, ferulic, syringic, and vanillic acids, which are polyphenols with antioxidant properties. In their study, they utilized a boron-doped diamond electrode. After investigating the electrochemical characteristics of these four compounds, they successfully determined their presence in real samples (Sordoń & Jakubowska, 2023).

Shih and Chen aimed to analyze chlorogenic acid using voltammetry. Chlorogenic acid is a type of antioxidant. To achieve this, they coated the surface of a glassy carbon electrode with a film of poly(3,4-ethylenedioxythiophene). Using the modified electrode, they successfully determined chlorogenic acid in coffee samples (Shih & Chen, 2024).

Yang et al. (2024) modified the surface of a glassy carbon electrode by coating it with Pt NA-$Ti_3C_2$. After completing the characterization process, they performed a highly sensitive analysis of quercetin. They measured the quercetin levels in fresh apples and sweet peppers. The study reported the electrode's suitability for quercetin determination (Yang et al., 2024).

## References

Ab Mutalib, N. A., & Suzuki, H. (2024). Evolution in the development of next generation electrochemical microdevices via bipolar electrochemistry. *Current Opinion in Electrochemistry, 43*, 101424.

Adiguzel, C., & Kalender, Y. (2020). Bendiocarb-induced nephrotoxicity in rats and the protective role of vitamins C and E. *Environmental Science and Pollution Research, 27*, 6449-6458.

Adiguzel, C., Karaboduk, H., Apaydin, F. G., Kalender, S., & Kalender, Y. (2023). Comparison of nickel oxide nano and microparticles toxicity in rat liver: molecular, biochemical, and histopathological study. *Toxicology Research, 12*(5), 741-750.

Adiguzel, C., Karaboduk, H., & Uzunhisarcikli, M. (2024). Protective Role of Melatonin Against Abamectin-Induced Biochemical, Immunohistochemical, and Ultrastructural Alterations in the Testicular Tissues of Rats. *Microscopy and Microanalysis, 30*(5), 962-977.

Ali, A. G., Altahan, M. F., Beltagi, A. M., Hathoot, A. A., & Abdel-Azzem, M. (2022). Voltammetric and impedimetric determinations of selenium (iv) by an innovative gold-free poly (1-aminoanthraquinone)/multiwall carbon nanotube-modified carbon paste electrode. *Rsc Advances, 12*(8), 4988-5000.

Apaydın, F. G., Baş, H., Kalender, S., Adıgüzel, C., & Kalender, Y. (2019). Histopathological effect of bendiocarb on small intestine tissues of rats: Role of vitamins C and E. *Gazi University Journal of Science, 32*(2), 402-407.

Arabkhani, P., Javadian, H., Asfaram, A., Sadeghfar, F., & Sadegh, F. (2021). Synthesis of magnetic tungsten disulfide/carbon nanotubes nanocomposite (WS2/Fe3O4/CNTs-NC) for highly efficient ultrasound-assisted rapid removal of amaranth and brilliant blue FCF hazardous dyes. *Journal of hazardous materials, 420*, 126644.

Baş, H., Kalender, S., Karaboduk, H., & Apaydın, F. (2015). The effects on antioxidant enzyme systems in rat brain tissues of lead nitrate and mercury chloride. *Gazi University Journal of Science, 28*(2), 169-174.

Blandon-Naranjo, L., Alaniz, R. D., Zon, M. A., Fernández, H., Granero, A. M., Robledo, S. N., & Pierini, G. D. (2023). Development of a voltammetric electronic tongue for the simultaneous determination of synthetic antioxidants in edible olive oils. *Talanta, 261*, 124123.

Bouali, W., Erk, N., Genc, A. A., Salamat, Q., & Soylak, M. (2024). Green electrochemical sensor for selective determination of anticancer drug Ribociclib based on banana peel activated carbon/CuCoFe-MOF/CoFe2O4 modified carbon paste electrode in pharmaceutical and biological samples. *Microchemical Journal, 207*, 112058.

Choudhary, Y. S., Jothi, L., & Nageswaran, G. (2017). Electrochemical characterization. In *Spectroscopic Methods for Nanomaterials Characterization* (pp. 19-54): Elsevier.

de Fatima Ulbrich, K., Winiarski, J. P., Jost, C. L., & de Campos, C. E. M. (2020). Green and facile solvent-free synthesis of NiTe2 nanocrystalline material applied to voltammetric determination of antioxidant morin. *Materials Today Communications, 25*, 101251.

Doyle, O. F., & Forster, R. J. (2024). Wirefree electrochemistry for enhanced detection and treatment of disease. *Electrochemistry Communications*, 107832.

El-Zahry, M. R. (2024). Electrochemical sensor based on molybdenum-doped graphene oxide nanorods anchored carbon spheres/vanadium pentoxide nanocomposites for simultaneous determination of diclofenac sodium and posaconazole. *Microchemical Journal, 206*, 111593.

Han, H., Zhang, S., Ding, S., Pan, D., & Wang, N. (2024). An electrochemical sensor based on black phosphorus/covalent organic framework nanoflowers for determination of p-nitrophenol in seawater. *Sensors and Actuators B: Chemical*, 136998.

Hussain, F., & Kayani, H. U. R. (2020). Aging-Oxidative stress, antioxidants and computational modeling. *Heliyon, 6*(5).

Jomova, K., Raptova, R., Alomar, S. Y., Alwasel, S. H., Nepovimova, E., Kuca, K., & Valko, M. (2023). Reactive oxygen species, toxicity, oxidative stress, and antioxidants: Chronic diseases and aging. *Archives of toxicology, 97*(10), 2499-2574.

Kalvoda, R., & Parsons, R. (1985). *Electrochemistry in research and development*: Springer.

Karaboduk, H., Adiguzel, C., Apaydin, F. G., Kalender, S., & Kalender, Y. (2024). Investigating the impact of different routes of nano and micro nickel oxide administration on rat kidney architecture, apoptosis markers, oxidative stress, and histopathology. *Journal of Molecular Histology*, 1-12.

Karaboduk, H., Adiguzel, C., Apaydin, F. G., Uzunhisarcikli, M., Kalender, S., & Kalender, Y. (2024). The ameliorative effect of Naringenin on fenamiphos induced hepatotoxicity and nephrotoxicity in a rat model: Oxidative stress, inflammatory markers, biochemical, histopathological, immunohistochemical and electron microscopy study. *Food and Chemical Toxicology, 192*, 114911.

Karaboduk, H., Adıgüzel, Ç., Apaydın, F. G., Kalender, S., Uzunhisarcikli, M., & Kalender, Y. (2024). Fenamifos' un Sıçan Kan ve Dalak Dokusunda Sebep Olduğu Oksidatif Stres Üzerine Naringenin'in Koruyucu Rolü. *Journal of the Institute of Science and Technology, 14*(2), 625-635.

Karaboduk, H., & Kalender, Y. (2021). The effects of lead nitrate and mercury chloride on rat liver tissue. *Fresenius Environmental Bulletin, 30*(3).

Karaboduk, H., Uzunhisarcikli, M., & Kalender, Y. (2015). Protective effects of sodium selenite and vitamin E on mercuric chloride-induced cardiotoxicity in male rats. *Brazilian Archives of Biology and Technology, 58*(2), 229-238.

Karaboduk, K. (2019). Electrochemical Determination of Ascorbic Acid Based on AgNPs/PVP-Modified Glassy Carbon Electrode. *ChemistrySelect, 4*(20), 6361-6369.

Karaboduk, K. (2021). Modification of screen-printed gold electrode with 1, 4-dithiothreitol: application to sensitive voltammetric determination of Sudan II. *Food Quality and Safety, 5*, fyaa039.

Karaboduk, K., & Hasdemır, E. (2018). Voltammetric determination of sudan 1 in food samples using its Cu (II) Compound. *Food technology and biotechnology, 56*(4), 573-580.

Karaboduk, K., Karabacak, O., Dogan, S. Y., Karaboduk, H., Gunduzer, E., & Tekinay, T. (2014). Comparison of antimicrobial, antioxidant capacities and HPLC analysis of three Stachys species in Turkey. *J Environ Prot Ecol, 15*(3A), 1293-1302.

Karaboduk, K., Karabacak, O., Karaboduk, H., & Tekinay, T. (2014). Chemical analysis and antimicrobial activities of the Origanum vulgare subsp. hirtum. *Journal of environmental protection and ecology, 15*(3A), 1283-1292.

Kunter, I., Zabib, N., & Kosar, M. (2020). A review of oxidants and antioxidants in biological systems. *Journal of Pharmaceutical Sciences, 3*(1), 64-72.

Losada-Barreiro, S., Sezgin-Bayindir, Z., Paiva-Martins, F., & Bravo-Díaz, C. (2022). Biochemistry of antioxidants: Mechanisms and pharmaceutical applications. *Biomedicines, 10*(12), 3051.

Ma, C., Wu, D., Xu, E., & Fan, Y. (2022). Molecularly imprinted electrochemical sensor based on g-C3N4 for determination of endosulfan insecticide in Agricultural Food. *International Journal of Electrochemical Science, 17*(12), 221232.

Mahlooji, M., Beni, R. N., Mehraban, F., & Seyedarabi, A. (2025). The molecular effects of ozone on human hemoglobin oligomerisation pre-and post-COVID-19 infection accompanied by favoured antioxidant roles of cinnamaldehyde and phenyl ethyl alcohol. *Journal of Molecular Structure, 1321*, 140131.

Mahmoud, A. M., Alyami, B. A., Mahnashi, M. H., Alshareef, F., Alqahtan, Y. S., & El-Wekil, M. M. (2023). Facile fabrication of a superior electrochemical sensor with anti-fouling properties for sensitive and selective determination of glutathione. *Microchemical Journal, 187*, 108419.

Mallamaci, R., Barbarossa, A., Carocci, A., & Meleleo, D. (2024). Evaluation of the Potential Protective Effect of Ellagic Acid against Heavy Metal (Cadmium, Mercury, and Lead) Toxicity in SH-SY5Y Neuroblastoma Cells. *Foods, 13*(3), 419.

Mirceski, V., & Lovric, M. (2024). Genuine differential voltammetry. *Talanta, 279*, 126560.

Moussa, Z., Judeh, Z., & Ahmed, S. A. (2019). Nonenzymatic exogenous and endogenous antioxidants. *Free radical medicine and biology, 1*, 11-22.

Pence, M. A., Hazen, G., & Rodríguez-López, J. (2024). An automated electrochemistry platform for studying pH-dependent molecular electrocatalysis. *Digital Discovery, 3*(9), 1812-1821.

Petković, B. B., Stanković, D., Milčić, M., Sovilj, S. P., & Manojlović, D. (2015). Dinuclear copper (II) octaazamacrocyclic complex in a PVC coated GCE and grap-

hite as a voltammetric sensor for determination of gallic acid and antioxidant capacity of wine samples. *Talanta, 132*, 513-519.

Pimpilova, M. (2024). A brief review on methods and materials for electrode modification: electroanalytical applications towards biologically relevant compounds. *Discover Electrochemistry, 1*(1), 1-20.

Prasad, M. S., Chen, R., Ni, H., & Kumar, K. K. (2020). Directly grown of 3D-nickel oxide nano flowers on TiO2 nanowire arrays by hydrothermal route for electrochemical determination of naringenin flavonoid in vegetable samples. *Arabian Journal of Chemistry, 13*(1), 1520-1531.

Raja, A. N., Singh, K., & Jain, R. (2020). Ultrasensitive quantification of ellagic acid using Gr/Bi2O3/GCE as voltammetric sensor. *International Journal of Electrochemical Science, 15*(10), 10040-10057.

Rajkumar, C., Veerakumar, P., Nkenyereye, L., Tamtam, M. R., Chung, W.-Y., & Shim, J. (2024). Carbon spheres anchored on sulfur-doped nanosheet/nanowire g-C3N4 isotype heterojunctions as a metal-free hybrid electrode for voltammetric determination of antioxidant. *Microchemical Journal*, 110961.

Rasheed, A., & Azeez, R. F. A. (2019). A review on natural antioxidants. *Traditional and complementary medicine*, 1-24.

Scholz, F. (2010). *Electroanalytical methods* (Vol. 1): Springer.

Shih, W.-L., & Chen, L.-C. (2024). Voltammetric detection of chlorogenic acid by Poly (3, 4-ethylene-dioxythiophene) electrodes. *Journal of Electroanalytical Chemistry, 974*, 118736.

Simioni, C., Zauli, G., Martelli, A. M., Vitale, M., Sacchetti, G., Gonelli, A., & Neri, L. M. (2018). Oxidative stress: role of physical exercise and antioxidant nutraceuticals in adulthood and aging. *Oncotarget, 9*(24), 17181.

Skoog, D. A., West, D. M., Holler, F. J., & Crouch, S. R. (1996). *Fundamentals of analytical chemistry* (Vol. 33): Saunders College Pub. Fort Worth.

Sordoń, W., & Jakubowska, M. (2023). Electrochemical evaluation and voltammetric determination of some phenolic acids on the boron-doped diamond electrode. *Diamond and Related Materials, 138*, 110236.

Stamford, J. A. (1991). In vivo voltammetry. In *Methods in Neurosciences* (Vol. 4, pp. 127-142): Elsevier.

Tomášková, M., Chýlková, J., Machalický, O., Šelešovská, R., & Navrátil, T. (2013). Voltammetric determination of different antioxidants in petroleum products by working gold electrode. *International Journal of Electrochemical Science, 8*(2), 1664-1677.

Toydemir, G., Subasi, B. G., Hall, R. D., Beekwilder, J., Boyacioglu, D., & Capanoglu, E. (2022). Effect of food processing on antioxidants, their bioavailability and potential relevance to human health. *Food Chemistry: X, 14*, 100334.

Uçak, İ., & Zahid, M. (2020). Natural antioxidants and therapeutic effects. *Eurasian Journal of Food Science and Technology, 4*(1), 24-33.

Vazan, M., Tashkhourian, J., & Haghighi, B. (2023). A novel electrochemical sensor based on MoO3 nanobelt-graphene oxide composite for the simultaneous determination of paracetamol and 4-aminophenol. *Diamond and Related Materials, 140*, 110549.

Wang, L., Hu, J., Wei, W., Song, Y., Li, Y., Shen, Y., . . . Qin, L. (2024). Electrochemical paper-based sensor based on molecular imprinted polymer and nitrogen-doped graphene for tetracycline determination. *Microchemical Journal, 207*, 111809.

Yadav, K., Garg, S., Singh, A. K., Singh, S., & Parmar, A. S. (2022). Protein nano Dots conjugated AuNP, poly-Lysine biointerface for the selective voltammetric estimation of Melatonin in pharmaceutical and food samples. *Microchemical Journal, 179*, 107563.

Yang, T., Li, J., Qiao, C., Xiao, X., Wan, J., Hong, W., . . . Gao, F. (2024). Electrochemical detection of quercetin at a Pt nanoaggregate-decorated Ti3C2-modified electrode. *Microchemical Journal, 206*, 111575.

Yu, L., Shi, M., Yue, X., & Qu, L. (2016). Detection of allura red based on the composite of poly (diallyldimethylammonium chloride) functionalized graphene and nickel nanoparticles modified electrode. *Sensors and Actuators B: Chemical, 225*, 398-404.

# CHAPTER 5

# AN INTRODUCTION TO INVESTIGATING COSMIC MICROWAVE BACKGROUND AND ITS IMPLICATIONS FOR THE FORMATION OF THE UNIVERSE

*E. Nihal Ercan*[1]

1 Prof. Dr., Boğaziçi University, Physics Department

## 1. Introduction

The universe and its formation have always been a mystery investigated by many philosophers. Physicists eventually continued this investigation. Philosophical observations of the universe gave us many qualitative benefits, for example, defining periods like months, days and even hours. All these were achieved by observing the motions of the Moon and the Sun. These observations were strictly made using the naked human eye in the historical periods of old philosophers. Without sufficient equipment, deducing scientific facts from observations is almost impossible. Observing these motions, many people concluded that the Earth was in the centre of the Universe, and all the stars and other celestial bodies revolved around it…

This idea of the Earth being placed at the centre of the universe was not formed coincidentally. The authorial body at those times was the Church. And for the Church, keeping the Earth at the centre of the universe seemed beneficial. The teaching of the Church suggested that everything was created for the sake of humans, and if so, they should be placed at the centre, right? This concept of putting the Earth at the centre of the universe is called "Geocentricism". Geocentricism was considered inaccurate when Nicolaus Copernicus tried to use it to predict planetary motion. Using his observations and calculations, Copernicus hypothesized that the Earth was not the centre of the Universe; it was revolving around the Sun just like all the other planets. This concept of planets revolving around the Sun is called "Heliocentrism". However, Copernicus, knowing the values of people at his time and the Church's strong teachings for Geocentricism, delayed publishing his work until near his death. He published his work in 1543 and died very soon after. His ideas did not initially get strong reactions from the Church, yet later, heliocentrism was classified as "unorthodox, " prohibiting anyone from supporting it. After his work was published, it mostly got mixed views from the intellectuals of the time; some believed in it while others thought it lacked proof. One of the supporters of heliocentrism, Giordano Bruno, went above and beyond with the idea. He strongly supported the heliocentric universe and added the concepts of infinity of the universe and all the stars, just like the Sun, potentially having planets that revolve around them. His contributions were not rooted much in scientific observations or data but in his religious beliefs. He believed that an infinite universe would suggest an infinite God. He was somewhat of a spiritual person, yet his views contradicted the Church's. Being the outspoken person that he is, he faced strong opposition from the Church. Eventually, this contradiction between him and the Church ended in 1600 when he faced prosecution under the Roman Empire, which resulted in Giordano being burned.

This intense backlash towards the scientists who try to examine the Universe, even though frightening, was not enough to silence reality much

longer. In 1632, a revolutionary scientist who was also one of the founding fathers of scientific astronomy published a work that supported heliocentrism and was backed by strong scientific data. This scientist is none other than Galileo Galilei. Galilei is known as the first person to use the telescope to observe celestial bodies like planets and moons of planets. However, he was not even the inventor of the telescope! The telescope was invented in 1608 by a Dutch optician, and Galileo, hearing about this invention, engineered his version of it. The spectacular part about this is that the version developed by the Dutch optician was able to achieve 3x magnification, but Galilei's version achieved a staggering 20x magnification! This allowed him to observe the moon's surface, Jupiter's moons and many others. His observations of the moons of Jupiter directly opposed the concept of "all celestial bodies revolving around the Earth". Therefore, when he published all these findings, he was opposed by the Church just like his historical colleagues. He was able to avoid execution, yet he was sentenced to house arrest for the rest of his life...

Even in this brief exploration of the history of investigations regarding the universe, we may see that scientific developments are usually faced with pressure not only by insufficient equipment but also by figures of power. The universe is our home, though there are many rooms we have yet to discover. While we try to do so, we start to question it. What is the Universe? What is its composition? How did the Universe come to existence? Has it always been there? Has it always been infinite?

All these questions regarding the nature of the universe lead one to try to reach the source or the beginning point of the Universe. When we think about how the universe came into existence, we think directly about the Big Bang theory today. Recent observations and theories agree with this concept of the Big Bang, making it the mainstream answer to that question.

We needed to know about the geocentrism to understand the importance of heliocentrism. Learning about the old, misleading concept makes us appreciate the up-to-date one. Therefore, to enjoy the Big Bang, we need to know the theory it was chosen over; now, before discussing that "other" theory, one needs to keep in mind that scientific developments most of the time destroy what came before it. Therefore, just because the Big Bang is generally accepted today does not mean it is the accurate theory explaining the universe and its formation…

In the coming years, observations made via stronger telescopes will commonly show us that most neighbouring galaxies are moving away from us. This observation made it obvious that the universe was expanding. Two main theories explained the idea of an expanding universe: one suggesting a constant density for the universe and the other suggesting an ever-decreasing density.

The first theory suggested that new matter was formed in free space as the universe expanded. This formation resulted in a constant density over time. This idea of creating new matter in free space may seem weird and not so instinctual, but if we want to investigate the rate of formation of matter, it becomes more logical. One may say that if new matter were formed in free space, we should be able to observe it around us. But when we calculate the needed creation of matter rate to keep the density constant, we see that even a rate of 1 Hydrogen atom per cubic meter per billion years is enough to keep the density constant! Keeping in mind that the existence of humanity is way longer than a billion years, it makes sense that we have not observed any formation of new matter around us. This theory is called the Steady State Theory.

The latter theory, being widely known today, suggests that as the universe is expanding, there has been a moment back in time when the whole universe and everything in it was found at an infinitely dense point. This theory is the Big Bang Theory and is one of the main concerns of this research. The data supporting this theory came from observations that suggested a "background radiation" that can be observed anywhere, anytime and coming from many different directions.

Before discussing the first observations made regarding this background radiation, investigating the reason for it and its relationship with the Big Bang theory is beneficial. Using the Big Bang theory, we conclude that the universe was a dense point back in time. At this infinite density state, the only things that existed were gaseous particles and photons. The particles could not form matter because the high density and energetic universe made them unstable. As the universe expanded, it also cooled down and at some point, these particles formed matter as we know it today. Yet the photons continued flying around. The only thing that changed about the photons, as a result of the expansion of the universe, was that as the space they travelled in expanded, their wavelengths also stretched. These stretched photons are expected to fill the universe to form a "background radiation uniformly".

The first observation of such radiation was made in 1965 by Arno Penzias and Robert Wilson. They were not looking for the Cosmic Microwave Background Radiation (CMB Radiation) when they observed it. Instead, they tried to cancel out all noise detected by their radio signal receivers and observe the emissions of the Milky Way. While attempting to do so, they realised a consistent "hiss" noise at the wavelength of 7.35 cm came from no apparent source. It was coming from all directions! They contacted many other physicists to discuss the phenomena, including Robert Dicke at Princeton University, who was searching for evidence of the Cosmic Microwave Background Radiation (CMB Radiation). This unexpected discovery of CMB supported the Big Bang theory over the Steady State theory. The discovery also brought the Nobel Prize in Physics for Penzias and Wilson in 1978…

## 2. Observational Aspects of the Cosmic Microwave Background (CMB) Radiation

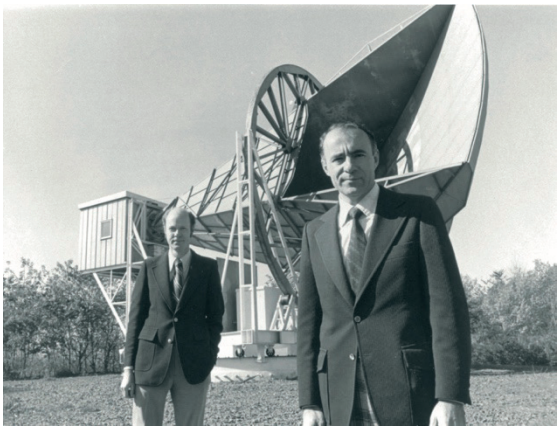

*Figure 1: Penzias and Wilson*

The first observation of the CMB Radiation came from the abovementioned experiment. It was not intended to check for CMB radiation; rather, it was focused on removing unwanted noise received by the radio wave receiver. The two scientists were trying to observe radio waves in the millimetre range to identify some specific molecules in the interstellar clouds that form stars and possibly galaxies. The pair worked in the telecommunications field at Bell Laboratories.

As they were trying to develop new techniques for better transfer of radio waves, physicists were trying to see how useful Echo balloon satellites would be. All other radiation coming from surrounding emitters needed to be removed to see their effect so that no interference occurred. After eliminating many sources, the pair realised a persistent noise at the wavelength of 7.35 cm. To ensure the radar's frequency didn't cause the noise, the radar was cooled down to -269 °C, only 4 degrees above absolute zero. Also, it was checked if the source of this noise was the Earth, The Sun or the Milky Way, yet none was the source.

At the same time, another group of physicists was theoretically working on CMB radiation and preparing to start looking for experimental data. This group, Robert Dicke, Jim Peebles, and David Wilkinson, believed that the Big Bang not only scattered matter that forms stars and galaxies today but also should have scattered tremendous amounts of radiation that can be observed in the radio wave region due to the high amount of redshift. This redshift was caused by the universe's expansion, stretching the space that these photons travel in.

When the scientist at the Bell Laboratories, Penzias, was explaining the unexpected observation he and his colleague made during the experiment,

Bernard Burke, another physicist from MIT, told him about a pre-paper he read on the possible residues of the Big Bang. Finding out more about this paper, Penzias and Wilson realised they might have found something significant. Doing so, Penzias directly contacted Robert Dicke, asking for a copy of the unpublished paper they had prepared. Reading the paper, Penzias saw that what they observed fits the expectations perfectly. Following this, he called Robert Dicke and his colleagues at Princeton to show the observations made at the Bell Laboratories. Academicians collectively concluded that this was the remnant of radiation of the Big Bang. **What they found was the Cosmic Microwave Background Radiation…**

After this initial discovery of CMB Radiation, further investigations were necessary, as the crew that gathered the data did not even intend to do so. NASA made one of the initial vigorous attempts to uncover this phenomenon. A 5000-pound observation device was developed to observe such silent radiation, called COBE (Cosmic Background Explorer). COBE consists of 3 sophisticated instruments to delve into the background radiation of our universe: Differential Microwave Radiometer (**DMR**), Far Infrared Absolute Spectrometer (**FIRAS**) and Diffuse Infrared Background (**DIRBE**).

DMR was going to focus specifically on the radiation's homogeneity. Why is this homogeneity essential? As we know, the most dominant force in the celestial body scale is the gravitational attraction force. This force depends on a couple of variables: the distance between the interacting particles. Let me explain what that means. Assume we have two identical particles fixed in position. If we place a third particle right in the middle of these particles, this third particle would not approach either of the fixed particles. This is because both would attract the third particle with equal force. Now, if the early universe were entirely homogeneous, that would bring the question of "How did particles approach each other to form structures like stars, galaxies, clusters of galaxies and even clusters of clusters of galaxies, while some regions of the space is left empty…" To answer this critical question, we needed the data that DMR collected.

FIRAS tried to see if the spectrum of emission matches theoretical expectations. FIRAS's observation range was between 0.1 to 10 millimetres. The Big Bang theory suggests that the so-called "Big Bang" explosion is the only source of energy and matter in our universe. The emission spectrum resulting from a single "Bang" can be easily found. Therefore, the data from FIRAS was supposed to tell us if a single explosion formed the universe or if there were other energy sources in the early universe apart from the Big Bang. These different sources of energy may be anti-matter annihilation, explosions of supermassive bodies or other large explosions.

DIRBE was going to focus on emissions of radiation outside of our galaxy, in the range of 1 to 300 micrometres. As the visible region starts at 400 micrometres, DIRBE will focus on the Infrared region of the EM Spectrum. This data is expected to provide information about the early universe.

As discussed, the COBE satellite's equipment tries to gather data to investigate the Big Bang Theory. All three equipment's data align with the theory to a great extent, so recent findings agree with it. After the COBE findings, scientists at NASA developed an even more sophisticated device. This new device was called the Wilkinson Microwave Anisotropy Probe (**WMAP**) and was designed specifically to gather data to reveal some properties of the early universe.

WMAP, like COBE, observed the CMB Radiation coming from the universe. There is some need for a more detailed theoretical exploration of the nature of the early universe before we start discussing the findings of WMAP. The oldest photons we can observe come from 375,000 years after the universe's birth. The reason for that is the heat distribution of the early universe. In the years before that, the universe had an average temperature of over 3000 K. At this temperature, only the elementary particles and photons existed; no bound state could be found. Bound state refers to what we call "atom" today. For an atom to exist, at least one proton and one electron must form a "bound state". But these particles are too energetic at such high temperatures to come together and create a bound state; therefore, they travel freely through space. In such an environment, any photon can interact with any electron and excite it. Here, we need to recall some basic knowledge; when an electron is in a bound state, it can only absorb photons with the correct amount of energy to transition from its initial state to a higher state. It cannot absorb any photon; there is a set of photons it can absorb. But if it is not in a bound state, the photon can interact with any electron. When photons could interact with any electron, they could not travel through any space before being absorbed. Therefore, this first 375,000 years of the universe is called the "opaque era", referring to the fact that photons could not travel through space. After 375,000 years, the universe's temperature was below 3000 K, and the very first bound states of electrons and protons started to form. This decreased the density of free electrons, allowing photons to travel for a longer time freely…

WMAP observed these early photons, looking towards different directions in the universe. WMAP was equipped with structures to block any emitted or reflected photons from the Sun, the Earth and the Moon. This was vital because WMAP tried to reveal whether there were any anisotropies in the CMB radiation. Therefore, if these unwanted sources of photons were not blocked, the data would show some strong anisotropy. With the proper equipment to gather accurate data, WMAP was able to show that there is anisotropy in the CMB radiation. This anisotropy is believed to be the reason

for forming large structures like galaxy clusters and clusters of galaxy clusters. To reveal this minute anisotropy, WMAP uncovered a temperature difference of 0.0002 K, which shows how technologically advanced mechanisms were involved in making such a device…

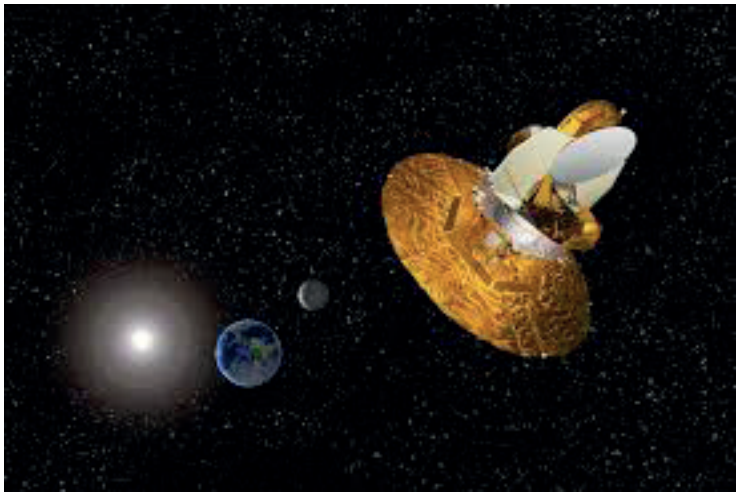

*Figure 2: WMAP Satellite*

## 3. Theoretical Aspects of the Cosmic Microwave Background (CMB) Radiation

Theoretical investigations that suggested the existence of CMB Radiation came from the research discussed by Robert Dicke et al. in the Princeton Physics Department. They did an unbelievably clear and straightforward examination of the behaviour of matter and radiation in our universe, which led them to reach the experimental value with great accuracy. Their approach was brilliant, and I will extensively discuss it. However, before that, I would like to theoretically explain why the earliest photons we can observe today, as the CMB radiation, come from 375,000 yearly after the universe's birth.

The earliest observable photons come from 375,000 years after the recombination and decoupling of photons caused the universe's birth. Before explaining those terms, let us understand the behaviour of the photons we observe from 375,000 years after the universe's birth. These photons are called the Cosmic Microwave **Background** Radiation for a reason. This is because they form the homogeneous background of radiation in our universe. By creating the background, it means that they are non-interacting and have been so for almost the last 13.8 billion years. These photons have not interacted with any particle for so long, so they allow us to look back in time and see the early universe.

During the first 375,000 years, the universe was a hot-dense energy sphere. When the temperature of this early universe was $10^{10}$ K, electrons were moving at relativistic rates. This high-energy state of electrons enabled them to interact continuously with the photons around them. Until the universe's temperature fell below $10^{9}$ K, the continuous interactions between photons, electrons and other elementary particles made it impossible for the photons to travel freely until they collided with another particle. This is why we call the first 375,000 years of the universe "the opaque era".

As Robert Dicke et al. stated in their groundbreaking research paper, the universe will follow one of three lifelines. Either it is continuously in a stable state, and new matter is generated as the universe expands, or it is in a dynamic state oscillating back and forth by repeated expansions and collapses, or it began from a singularity and has been expanding ever since. In the last two scenarios, it follows that the universe has been in a denser state than it is today. In the oscillating universe case, this denser state is needed for the burning of the residues of fusion reactions that take place at every moment; when the collapse occurs, and a new universe is about to come into existence, a high amount of Hydrogen is needed, which have been converted into heavier atoms by fusion reactions in the former universe. When faced with high temperatures, these heavier atoms will slowly become unstable. As temperature increases, the unstable heavy atoms decay into lighter stable atoms. At temperatures discussed above (around $10^{9}$ or $10^{10}$ Kelvin), atoms, molecules, and even electrons are so unstable that their behaviour becomes unpredictable. As the universe continues to collapse into itself, the density and temperature go to almost infinity. When the universe reaches a point-like state, it consists of a photon and elementary particle soup with no bound states. No molecules, atoms, or protons or neutrons: protons and neutrons consist of a bound state of 3 other elementary particles (new findings suggest that protons consist of a bound state of 5 quarks, up-up-down-strange-anti strange). This is when all the used-up particles have been reactivated and are ready to undergo many reactions to keep the universe warm and dynamic.

Theoretical calculations suggest that the least amount of matter density for a closed universe should be $2x10^{-29}$ gm/cm$^3$. Observational data roughly approximates $3x10^{-32}$ gm/cm$^3$ for the universe's density. However, this data does not directly represent the whole universe and, therefore, is insufficient to reject the possibility of a closed universe. Closed universe refers to the oscillating universe scenario: the amount of matter is enough to dominate so that, eventually, the universe will stop expanding and collapse into itself. Another connection between background radiation at 3 cm, just as found by Penzias and Wilson at the Bell Telephone Laboratories, and the density of the universe is the average temperature of the universe. From Penzias and Wilson's observations, the universe should have an average temperature of 3.5

Kelvin. Furthermore, this average temperature effectively suggests an average density below $3x10^{-32}$ gm/cm$^3$, aligning with observations.

## 4. Discussion and Conclusions

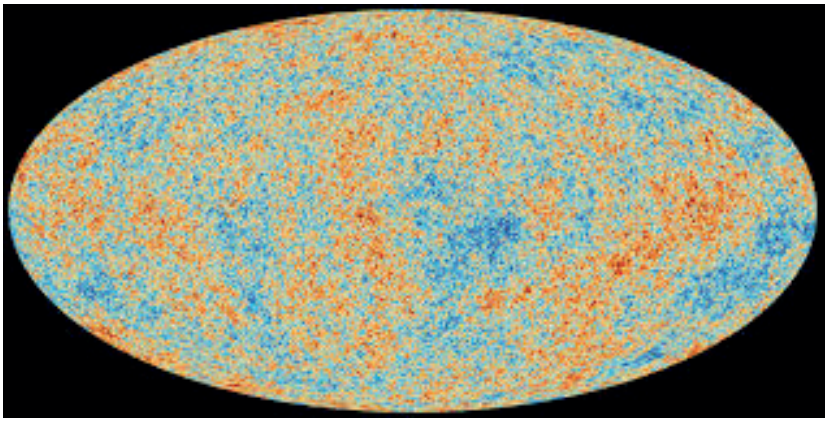

*Figure 3: Cosmic Microwave Background Radiation*

Initial findings of COBE, followed by WMAP, brilliantly and mesmerizingly uncover the nature of the early universe. The most puzzling mystery about the universe was how seemingly homogeneous it was. With such a homogeneity, no matter should tend to approach one another. However, we see that today, all matter is approaching under the influence of gravitational attraction. This mystery could only be solved by observing an anisotropy in the configuration of the early universe. And that's what was observed by these sophisticated devices. They showed us a precise picture of the universe in its earliest stages (Seen in the image). As can be seen, there are fluctuations in the temperature of the early universe. To explain the attractive nature of matter in our universe, an anisotropy like this was needed. However, this observation was made via such accurate equipment that the fluctuations shown are the deviation from the average temperature of CMB Radiation which is 2.725+-0.00057 K with uncertainty. Therefore, despite showing an anisotropy, such slight variations in the grand scheme of things signal an overwhelming isotropy among most regions of the universe…

Lastly, discussions need to be held to conclude this scientific article. The cooperation between the scientists at the Bell Laboratories and physicists at Princeton University is remarkable. Physicists have done a tremendous amount of research and put in a lot of effort to develop the theoretical concept of CMB. After seeing that Penzias and Wilson found some data that resembles CMB Radiation, they could've said we could easily follow a similar procedure to gather the same data to avoid giving credit to Penzias and Wilson. However, they wanted to include them in their research and use their data, as they were

the ones who used the proper method to pinpoint this radiation. This shows solidarity among the scientific community and needs to be appreciated. This cooperation eventually led to a Nobel Prize for both teams…

I would like to thank Necdet Yulaf, one of my undergraduate students, for his help during the preparation of the manuscript.

## References

National Aeronautics and Space Administration, **Cobe Press Kit** https://science.nasa.gov/mission/cobe/

Dicke, R. H., Peebles, P. J. E., Roll, P. G., & Wilkinson, D. T. (1965). **Cosmic black-body radiation**. *The Astrophysical Journal, 142*(1), 414–419. https://articles.adsabs.harvard.edu/pdf/1965ApJ...142..414D

Witze, A. (2024). **How scientists discovered the first evidence for the Big Bang**. *Nature*. https://doi.org/10.1038/d41586-024-00555-1

National Aeronautics and Space Administration. (n.d.). **WMAP mission**. *NASA* https://map.gsfc.nasa.gov/mission/

# CHAPTER 6

## FREQUENTIST AND BAYESIAN POLYTOMOUS LOGISTIC REGRESSION MODELS FOR SEVERAL RESPONSE LEVELS[1]

*Münire Tuğba Erdem Aladağ* [2]

*Zeynep Kalaylıoğlu*[3]

1 Bu çalışma Münire Tuğba Erdem Aladağ'ın 2011 yılında ODTÜ Fen Bilimleri Enstitüsüne sunduğu "Modeling Diseases with Multiple Disease Characteristics: Comparison Of Models And Estimation Methods" başlıklı yüksek linsas tezinden üretilmiştir.

2 Dr., Bağımsız araştırmacı, erdem.mt@gmail.com, ORCID No:0009-0000-0229-2359

3 Prof. Dr., ODTÜ İstatistik Bölümü, kzeynep@metu.edu.tr, ORCID No: 0000-0002-2216-188X

## 1. INTRODUCTION

In epidemiological studies, one of the main aims is to determine the association between disease risk factors and disease risk. This association is investigated by statistical modeling, and it has become common to have data that includes various specific characteristics of the disease, especially for complex diseases such as cancer. This type of disease data, with appropriate statistical modeling, makes it possible to understand the association of the disease with factors by going deep into the disease characteristic level.

One common approach to analyze this type of data is either i) by considering each tumor characteristic as a response variable in separate logistic regression models, or ii) creating disease subtypes by cross-classifying the disease characteristics and running a generalized logit regression on the resulting response variable. However, these approaches have serious problems. In the first case, disease characteristics are treated as independent when they may exhibit covariation. The second approach may lead to a large number of categories, resulting in dimension and estimation problems.

To overcome these issues, Chatterjee (2004) developed a two-stage polytomous logistic regression model. This model reduces the parameter space and provides an advantage in estimation for small or moderate sample-size studies. It also allows for examining the etiologic heterogeneity of the disease under investigation.

This study contributes to the field in three main areas. First, it compares the performance of three methods for estimating disease subtypes: the classical maximum likelihood estimation (MLE) approach, the Bayesian estimation approach, and the pseudo-conditional likelihood (PCL) estimation approach used in two-stage models. Second, it demonstrates the advantages of the two-stage polytomous logistic regression model over traditional methods using a dataset of Turkish breast cancer patients. Lastly, it investigates the relationship between known breast cancer risk factors and various breast cancer subtypes, providing a clearer picture of the disease's etiologic heterogeneity.

## 2. METHODOLOGY

This section outlines the models and methods used for analyzing diseases with multiple characteristics. Three estimation methods are considered: Maximum Likelihood Estimation (MLE), Bayesian Estimation, and Pseudo-Conditional Likelihood (PCL) Estimation in Two-Stage Polytomous Logistic Regression.

These methods are applied to model disease subtypes created by cross-classifying disease characteristics.

### 2.1. Maximum Likelihood Estimation For Polytomous Logistic Regression

Regression models are commonly used to explain the association between a response variable and predictor variables. When the response variable is categorical (nominal or ordinal), a proper link function, such as logit or probit, allows for the regression of a categorical response on numeric or categorical covariates. For binary responses, the binary logistic regression model is used. However, when the response has more than two levels, McFadden's (1974) polytomous (or multinomial) logistic regression model is employed.

For a categorical response Y with M+1 levels, and p covariates, the polytomous logistic regression model is defined as:

$$ln\frac{P(Y_i=m|X)}{P(Y_i=0|X)} = \alpha_m + X_i\beta_m \text{ , m=1,..., M}$$

We know that Y has a multinomial distribution with each level having the probability $P(Y=m)$, where $P(Y=m)=\frac{e^{\alpha_m+X_i\beta_m}}{1+\sum_{m=1}^{M}e^{\alpha_m+X_i\beta_m}}$ and $P(Y=0)=\frac{1}{1+\sum_{m=1}^{M}e^{\alpha_m+X_i\beta_m}}$

Then, the likelihood function for a sample of n independent observations is:

$$L(\alpha,\beta|X,Y)=\prod_{i=1}^{n}\prod_{m=0}^{M}[P(Y=m|X_i,\alpha,\beta)]^{y_{mi}}$$

where $y_{mi}$=1 if $Y_i$=m, and $y_{mi}$=0 otherwise; m=1,..., M. The maximum likelihood estimates (MLE) of model parameters are obtained by solving the score equations, which are derived by taking the derivatives of the log-likelihood function with respect to the unknown parameters. The asymptotic distribution of maximum likelihood estimators of logistic regression models are Normal (Agresti, 2002).

### 2.2. Bayesian Estimation for Polytomous Logistic Regression

Bayesian estimation offers a different approach by treating parameters as random variables with their own distributions, rather than fixed values. This approach allows for the incorporation of prior information about the parameters, which can be derived from previous studies or expert knowledge.

The Bayesian model is expressed as:

$P(\theta|X,Y) \propto P(Y|\theta,X)P(\theta)$

where θ=(α,β) represents the parameters to be estimated, $P(\theta|X,Y)$ is the posterior distribution, $P(X,Y|\theta)$ is the likelihood, and P(θ) is the prior distribution of the parameters.

In cases where there is little prior information about the parameters, non-informative priors are often used. In this study, a multivariate Normal prior distribution is assumed for α\alphaα and β\betaβ, reflecting the approximate normal distribution of logistic regression parameters.

To obtain samples from the posterior distribution, the Markov Chain Monte Carlo (MCMC) method is used, specifically the Gibbs sampling algorithm. This method generates a sequence of samples from the posterior distribution by iteratively updating each parameter conditional on the others. Gibbs sampling is particularly efficient because it avoids the need for a separate proposal distribution at each iteration.

In practice, software like WinBUGS is used to implement the Gibbs sampler, and the chain length and burn-in period are determined by monitoring convergence diagnostics, such as trace plots and the Brooks-Gelman-Rubin criterion.

### 2.3 Pseudo-Conditional Likelihood (PCL) Estimation in Two-Stage Polytomous Logistic Regression

When modeling diseases with multiple characteristics, traditional approaches—such as using separate logistic regression models for each characteristic or cross-classifying disease characteristics—often encounter problems of high dimensionality and estimation inefficiency. To address these issues, Chatterjee (2004) developed the two-stage polytomous logistic regression model, which incorporates the covariation between disease characteristics while reducing the complexity of the parameter space.

The two-stage model is particularly suited for cases where the disease subtypes are defined by multiple characteristics. These subtypes are obtained through the cross-classification of the characteristics' levels. For example, consider a case where we have K disease characteristics, and each characteristic k has $M_k$ levels. The total number of disease subtypes would be the product of the levels: $M= M_1 \times M_2 \times \ldots \times M_K$. If $Y_i$ represents the disease subtype for subject i, then $Y_i$

can take values from 0 (indicating disease-free) to M= $M_1 \times M_2 \times \ldots \times M_K$ (indicating one of the possible subtypes).

The first stage of the two-stage model involves fitting an unstructured polytomous logistic regression model, where the response variable is the disease subtype, and the goal is to estimate the association between the covariates and the disease subtypes. The first-stage model can be written as:

$$P(Y_i = m \mid X_i) = \frac{e^{\alpha_m + X_i^T \beta_m}}{1 + \sum_{m=1}^{M} e^{\alpha_m + X_i^T \beta_m}} \tag{2.2}$$

where $\alpha_m$ is the intercept, and $\beta_m$ is the regression parameter for the disease subtype m. Here, $e^{\beta_m}$ represents the odds ratio which expresses the association between the covariate and the $m^{th}$ disease subtype relative to the disease-free status. Dealing with p covariates, it is clear that the total number of regression coefficients $Q=M_1 \times M_2 \times \ldots \times M_K \times p$ can easily become too large. This can easily result in estimation problems as some of the disease subtype categories may include only very few or no subject. To overcome such problems that are caused by high dimensional parameter space, Chatterjee (2004) developed a novel approach in which the number of parameters are greatly reduced.

For effective illustration of the two staged method we will assume that there is only one covariate that effects the disease outcome. The same idea can then easily be extended to multi-covariate situations. With one covariate in the logistic regression model, the regression coefficients of the first stage model will be an Mx1 vector that is denoted by $\beta = (\beta_1, \beta_2, \ldots, \beta_M)$. We can also represent these parameters in the form of combinations of disease characteristics levels. For instance, $\{\beta_m\}_{m=1}^{M}$ can be represented as $\{\beta_{i_1 i_2 \ldots i_K}\}_{i_1=1, i_2=1, \ldots, i_K=1}^{M_1 M_2 \ldots M_K}$. By the help of this representation, the relationship between the first and second stage parameters can easily be shown as follows:

$$\beta_{i_1 i_2 \ldots i_K} = \theta^{(0)} + \sum_{k_1=1}^{K} \theta_{k_1(i_{k_1})}^{(1)} + \sum_{k_1=1}^{K} \sum_{k_2>k_1}^{K} \theta_{k_1 k_2 (i_{k_1} i_{k_2})}^{(2)} + \ldots + \theta_{12\ldots K(i_1 i_2 \ldots i_K)}^{(K)} \tag{2.3}$$

where $\theta^{(0)}$ is the regression coefficient for the reference disease subtype, and $\theta^{(1)}$'s represent the first order contrasts, and $\theta^{(2)}$'s represent the second order contrasts and so on.

To estimate the second-stage parameters $\theta$, the Pseudo-Conditional Likelihood (PCL) method is used. This method bypasses the need to estimate the nuisance intercept parameters $\alpha_m$, which can be numerous and are not of

scientific interest. The PCL method focuses on the covariate coefficients $\beta_m$, allowing for more efficient estimation.

The PCL method constructs a conditional likelihood by conditioning on the disease status and the covariates, effectively removing the intercept parameters from the likelihood function. This simplifies the estimation process and reduces the dimensionality of the parameter space. The PCL likelihood is given by:

$$L_{PCL} = \prod_{i \epsilon C_1} \frac{e^{X_i^T \beta_{m_i}}}{e^{X_i^T \beta_{m_i}} + \sum_{j \epsilon Co} e^{X_j^T \beta_{m_i}}}$$

where i,j=1,…,n; i≠j; $C_0$ is the set of nondiseased subjects, $C_1$ is the set of diseased subjects, $d_i$ is the observed disease subtype of the $i^{th}$ diseased subject. The PCL score equations are then solved to obtain the maximum likelihood estimates of the second-stage parameters $\theta$ (see: Chatterjee, 2004; Erdem, 2011).

By focusing on the second-stage parameters, the PCL method significantly reduces the number of parameters to be estimated, making it a more efficient and stable approach in situations with large numbers of disease subtypes. Additionally, the asymptotic properties of the PCL estimators are well understood, with the estimators being asymptotically normal under regular conditions.

## 3. SIMULATION STUDY

A simulation experiment was designed to compare the performances of three different approaches—Maximum Likelihood Estimation (MLE), Bayesian estimation, and Pseudo-Conditional Likelihood (PCL) estimation—used for polytomous logistic regression analysis of disease outcomes with subtype information. This section focuses on the results for the $M_1$=2, $M_2$=2, $M_3$=2 scenario, which represents a situation with three disease characteristics, each having two levels. This relatively simple case provides important insights into the methods' performance across different sample sizes.

### 3.1 Data Generation

In this scenario, the response variable Y consists of eight disease subtypes, created by cross-classifying three binary disease characteristics. As the first

step of the data generation process, we set the true values of the second stage model parameters, $\theta$'s at the same values in Chatterjee (2004) which provides that the percentage of diseased people in the population is about 10%. These are $\theta^{(0)}$=0.35, $\theta^{(1)}_{2(1)}$=0.15, $\theta^{(1)}_{2(2)}$=0, $\theta^{(1)}_{3(2)}$=0.5. Then, true values of first stage parameters are computed as $\beta_1$=0.35, $\beta_2$=0.85, $\beta_3$=0.35, $\beta_4$=0.85, $\beta_5$=0.5, $\beta_6$=1, $\beta_7$=0.5, $\beta_8$=1 by the relation shown in model 2.4. To obtain the true values of the intercept parameters, $\alpha_1$,…, $\alpha_M$, second order contrasts model is used, whereas the first order contrasts model is used to obtain the true values of the coefficients, $\beta_1$,…, $\beta_M$. Having the values of polytomous logistic regression parameters and a covariate of size $N'$x1, we got the probabilities of each of the M=2×2×2=8 disease subtypes and probability of being disease-free for the i$^{th}$ of the $N'$ subject by:

$$p_{mi} = P(Y_i = m \mid X_i) = \frac{e^{\alpha_m + X_i^T \beta_m}}{1 + \sum_{m=1}^{M} e^{\alpha_m + X_i^T \beta_m}}$$

and $p_{0i} = P(Y_i = 0 \mid X_i) = \frac{1}{1 + \sum_{m=1}^{M} e^{\alpha_m + X_i^T \beta_m}}$, m=1,…,8

Disease status has multinomial distribution with the probabilities as specified above. That is to say, i$^{th}$ subject has the disease subtype m with probability $p_{mi}$ and is disease-free with probability $p_{oi}$. Therefore, by using these probabilities we randomly generated disease subtype status for each of the $N'$ subjects from the multinomial distribution. Now, we have a sample of $N'$ =7000 subjects with response as disease status $Y_i$, where $Y_i$=0,…,8, and a continuous covariate generated from N(0,1) where i=1,…, $N'$. Suppose that $n_{case}$ is the number of diseased people (cases) in the whole sample. We selected disease-free people (controls) as many as the number of the cases, $n_{case}$, from the sample of size $N'$. At the end, we have a new sample of size n= $n_{case}$ + $n_{control}$ (where $n_{case}$ = $n_{control}$) with disease status and corresponding covariate information. $n_{case}$ was set as 250, 500 and 1000 to investigate the effect of sample size on estimation. Generating the $N'$ subjects in the first stage and then random selection of cases and controls in the second stage as described above has mainly two advantages: i) this process mimics the real life situation in which there are $N'$ subjects in the population of interest 10% of whom have the disease and n of them are selected for the study, ii) this process enables us to have a control over the percentage of the cases in the sample for the simulation study. The second point is especially important as it allows us to include sufficient number of cases in the study sample when the disease has a low prevelance.

### 3.2 Parameter Estimation Methods

The simulation study aimed to evaluate the performance of the three methods in estimating the first-stage parameters β. The following methods were applied:

1. Maximum Likelihood Estimation (MLE): The classical approach to polytomous logistic regression involves estimating the parameters by maximizing the likelihood function. For a categorical response with multiple levels, the MLE method constructs a log-likelihood function based on the multinomial distribution of the response variable. The parameters are estimated by solving the score equations obtained from the derivatives of the log-likelihood function with respect to the unknown parameters. In this study, MLE was implemented using the mnrfit function in MATLAB, which computes the maximum likelihood estimates for the regression coefficients based on the given covariates and response variable
2. Bayesian Estimation: Bayesian inference was conducted using Markov Chain Monte Carlo (MCMC) methods, implemented via Gibbs sampling in WinBUGS. A diffuse Normal prior was used for the regression parameters β. The chain size was set to 2500, with the first 500 iterations discarded as burn-in.
3. Pseudo-Conditional Likelihood (PCL) Estimation: The PCL method was applied to estimate second-stage parameters θ, which were then used to reconstruct the first-stage parameters β. This method avoids the high dimensionality of the full parameter space by focusing only on covariate effects, bypassing the need to estimate nuisance intercepts .

### 3.3 Results for Simulation Runs

The performance of the methods was assessed using Bias, Mean Squared Error (MSE), and Monte Carlo Standard Errors for the estimated parameters. The following tables summarizes the key findings from the M=2×2×2 scenario across different sample sizes:

**Bias and MSE Comparisons**

***Small Sample Size***

In this small sample size setting, the PCL method performed best in terms of both bias and MSE. The results showed that PCL had smaller bias and lower MSE compared to MLE and Bayesian methods, particularly for subtypes with fewer cases. The classical MLE approach had slightly higher bias and larger standard errors due to overfitting, while Bayesian estimation also showed slightly higher bias.

Table 3.1 : Simulation summary for 3 disease characteristics with levels $M_1$=2, $M_2$=2, $M_3$=2; $n_{case}$=$n_{control}$=250

| | | MLE | | | | Bayesian | | | | PCL | | | |
|---|---|---|---|---|---|---|---|---|---|---|---|---|---|
| j | true beta ($B_j$) | MC average | MC standard error | bias | MSE | MC average | MC standard error | bias | MSE | MC average | MC standard error | bias | MSE |
| 1 | 0.35 | 0.3509 | 0.0998 | 0.0807 | 0.0009 | 0.01 | 0.3489 | 0.1001 | 0.0801 | 0.0011 | 0.01 | 0.3511 | 0.0833 | 0.0683 | 0.0011 | 0.0069 |
| 2 | 0.85 | 0.8598 | 0.1203 | 0.1019 | 0.0098 | 0.0146 | 0.8681 | 0.1219 | 0.0983 | 0.0181 | 0.0152 | 0.8584 | 0.101 | 0.0882 | 0.0084 | 0.0103 |
| 3 | 0.35 | 0.3511 | 0.1333 | 0.1095 | 0.0011 | 0.0178 | 0.352 | 0.1326 | 0.1114 | 0.002 | 0.0176 | 0.3514 | 0.0955 | 0.0788 | 0.0014 | 0.0091 |
| 4 | 0.85 | 0.8668 | 0.1367 | 0.111 | 0.0168 | 0.019 | 0.8689 | 0.137 | 0.1069 | 0.0189 | 0.0191 | 0.8587 | 0.1049 | 0.0908 | 0.0087 | 0.0111 |
| 5 | 0.5 | 0.5066 | 0.1265 | 0.1083 | 0.0066 | 0.016 | 0.5034 | 0.1257 | 0.1097 | 0.0034 | 0.0158 | 0.5002 | 0.094 | 0.0805 | 0.0002 | 0.0088 |
| 6 | 1 | 1.0075 | 0.1265 | 0.1069 | 0.0075 | 0.0161 | 1.0084 | 0.1265 | 0.1026 | 0.0084 | 0.0161 | 1.0076 | 0.1053 | 0.0951 | 0.0076 | 0.0111 |
| 7 | 0.5 | 0.5024 | 0.1463 | 0.1182 | 0.0024 | 0.0214 | 0.5006 | 0.1468 | 0.1153 | 0.0006 | 0.0215 | 0.5006 | 0.0992 | 0.0832 | 0.0006 | 0.0098 |
| 8 | 1 | 1.0065 | 0.1082 | 0.0949 | 0.0065 | 0.0117 | 1.0122 | 0.1085 | 0.0925 | 0.0122 | 0.0119 | 1.0079 | 0.1035 | 0.0916 | 0.0079 | 0.0108 |

***Medium Sample Size***

As the sample size increased, MLE showed improved performance, particularly in terms of MSE. However, PCL continued to exhibit lower bias, especially for rare subtypes. Bayesian estimates also showed improvements, but they remained slightly less efficient than PCL. MLE became competitive with PCL in terms of MSE at this sample size.

Table 3.2: Simulation summary for 3 disease characteristics with levels $M_1$=2, $M_2$=2, $M_3$=2; $n_{case}$=$n_{control}$=500

| | | MLE | | | | | Bayesian | | | | | PCL | | | | |
|---|---|---|---|---|---|---|---|---|---|---|---|---|---|---|---|---|
| j | true beta ($B_j$) | MC average | est(se) | MC standard error | bias | MSE | MC average | est(se) | MC standard error | bias | MSE | MC average | est(se) | MC standard error | bias | MSE |
| 1 | 0.35 | 0.3563 | 0.115 | 0.147 | 0.0063 | 0.0216 | 0.3515 | 0.1153 | 0.1481 | 0.0015 | 0.0219 | 0.3542 | 0.0972 | 0.1201 | 0.0042 | 0.0145 |
| 2 | 0.85 | 0.8707 | 0.1454 | 0.1897 | 0.0207 | 0.0364 | 0.8857 | 0.1404 | 0.194 | 0.0357 | 0.0389 | 0.8586 | 0.1243 | 0.1435 | 0.0086 | 0.0207 |
| 3 | 0.35 | 0.362 | 0.1565 | 0.1991 | 0.012 | 0.0398 | 0.3654 | 0.1598 | 0.2008 | 0.0154 | 0.0406 | 0.3537 | 0.1122 | 0.1375 | 0.0037 | 0.0189 |
| 4 | 0.85 | 0.8574 | 0.1576 | 0.2008 | 0.0074 | 0.0404 | 0.8593 | 0.1522 | 0.2021 | 0.0093 | 0.0409 | 0.8582 | 0.1278 | 0.1492 | 0.0082 | 0.0223 |
| 5 | 0.5 | 0.5112 | 0.1547 | 0.1953 | 0.0112 | 0.0383 | 0.5079 | 0.1558 | 0.195 | 0.0079 | 0.0381 | 0.509 | 0.1147 | 0.1415 | 0.009 | 0.0201 |
| 6 | 1 | 1.0203 | 0.1536 | 0.1921 | 0.0203 | 0.0373 | 1.0244 | 0.1506 | 0.1936 | 0.0244 | 0.0381 | 1.0135 | 0.1341 | 0.1584 | 0.0135 | 0.0253 |
| 7 | 0.5 | 0.5151 | 0.1688 | 0.2189 | 0.0151 | 0.0481 | 0.516 | 0.1645 | 0.2214 | 0.016 | 0.0493 | 0.5086 | 0.1185 | 0.1482 | 0.0086 | 0.022 |
| 8 | 1 | 1.0182 | 0.136 | 0.1763 | 0.0182 | 0.0314 | 1.0304 | 0.1339 | 0.1793 | 0.0304 | 0.0331 | 1.013 | 0.1288 | 0.1557 | 0.013 | 0.0244 |

### *Large Sample Size*

For large sample sizes, MLE performed comparably to PCL in terms of MSE. However, PCL retained a slight advantage in terms of bias. The asymptotic properties of MLE became more apparent with larger sample sizes, as the standard errors decreased and the estimates approached their true values. Bayesian estimates improved as well but still lagged behind MLE and PCL.

Table 3.3: Simulation summary for 3 disease characteristics with levels $M_1$=2, $M_2$=2, $M_3$=2; $n_{case}$=$n_{control}$=1000

| | | MLE | | | | | Bayesian | | | | | PCL | | | | |
|---|---|---|---|---|---|---|---|---|---|---|---|---|---|---|---|---|
| j | true beta ($B_j$) | MC average | est(se) | MC standard error | bias | MSE | MC average | est(se) | MC standard error | bias | MSE | MC average | est(se) | MC standard error | bias | MSE |
| 1 | 0.35 | 0.3581 | 0.1639 | 0.1819 | 0.0081 | 0.0331 | 0.3539 | 0.1663 | 0.1851 | 0.0039 | 0.0343 | 0.3552 | 0.1383 | 0.1483 | 0.0052 | 0.022 |
| 2 | 0.85 | 0.8816 | 0.2083 | 0.2367 | 0.0316 | 0.057 | 0.9097 | 0.2053 | 0.2449 | 0.0597 | 0.0635 | 0.8631 | 0.1747 | 0.1902 | 0.0131 | 0.0363 |
| 3 | 0.35 | 0.36 | 0.2252 | 0.2616 | 0.01 | 0.0685 | 0.3653 | 0.228 | 0.2652 | 0.0153 | 0.0705 | 0.3537 | 0.1604 | 0.1753 | 0.0037 | 0.0308 |
| 4 | 0.85 | 0.8731 | 0.2268 | 0.2647 | 0.0231 | 0.0706 | 0.89 | 0.2184 | 0.2714 | 0.04 | 0.0753 | 0.8615 | 0.1799 | 0.1983 | 0.0115 | 0.0395 |
| 5 | 0.5 | 0.5205 | 0.2223 | 0.2642 | 0.0205 | 0.0702 | 0.5188 | 0.2254 | 0.2654 | 0.0188 | 0.0708 | 0.5148 | 0.1636 | 0.1881 | 0.0148 | 0.0356 |
| 6 | 1 | 1.039 | 0.2208 | 0.248 | 0.039 | 0.063 | 1.0528 | 0.2147 | 0.253 | 0.0528 | 0.0668 | 1.0226 | 0.1877 | 0.2161 | 0.0226 | 0.0472 |
| 7 | 0.5 | 0.5337 | 0.244 | 0.2826 | 0.0337 | 0.081 | 0.5377 | 0.2398 | 0.2885 | 0.0377 | 0.0847 | 0.5132 | 0.1691 | 0.1951 | 0.0132 | 0.0383 |
| 8 | 1 | 1.0244 | 0.1939 | 0.2294 | 0.0244 | 0.0532 | 1.0477 | 0.1915 | 0.2366 | 0.0477 | 0.0583 | 1.0211 | 0.1796 | 0.2093 | 0.0211 | 0.0443 |

### Efficiency and Asymptotic Behavior

The results show that PCL outperforms MLE in small-sample settings, especially when the number of disease subtypes is large relative to the sample size. As sample size increases, MLE becomes more efficient, with MSE and bias decreasing as the number of observations increases. The PCL method's

advantage lies in its faster convergence to asymptotic variance, particularly when sample sizes are limited. Bayesian estimation, while improving with larger sample sizes, remained computationally more demanding and less efficient than the other two methods in this scenario.

### 3.4 Discussion

In the M=2×2×2 scenario, the PCL method demonstrated clear advantages in small and moderate sample sizes, offering lower bias and MSE compared to MLE and Bayesian methods. MLE improved as sample size increased, becoming more competitive at larger sample sizes. Bayesian estimation was less efficient but provided an alternative when prior information was available. Overall, PCL is the preferred method for small sample sizes with a large number of subtypes, while MLE performs well with larger datasets.

## 4. DATA ANALYSIS

### 4.1. Study sample

The data are collected from 249 women with breast cancer and 251 women without breast cancer at Oncology Research and Education Hospital. The dataset includes various variables related to the presence of breast cancer and characteristics of the tumors in the cancer group. The primary variable is the binary outcome, indicating whether a woman has breast cancer (1 for presence, 0 for absence).

Several key variables describe the biological and clinical features of the breast cancer in the dataset. One such variable is the receptor status, which identifies whether the tumor cells are positive for estrogen receptor (ER), progesterone receptor (PR), or HER2/neu (C-erb B2) receptor. These receptors help classify the cancer into subtypes like Luminal A, Luminal B, HER2-positive, and triple negative. Each of these subtypes has different implications for prognosis and treatment strategies (Sotiriou & Pusztai, 2009).

The grade of the tumor is another important variable, determined by how much the cancer cells differ from normal cells. The tumors are classified as well-differentiated (low grade), moderately differentiated (intermediate grade), or poorly differentiated (high grade), with higher grades indicating more irregular cell behavior (Harris et al., 2010). Along with grade, tumor size is recorded, categorized as T1 (≤ 20 mm), T2 (20-50 mm), T3 (>50 mm), and

T4 (direct extension to chest wall or skin), reflecting the tumor's size and its spread to surrounding tissue. This classification is important for staging the cancer and determining the prognosis (Brooks & Harris, 2006).

The dataset also includes information on tumor type, which could be invasive ductal carcinoma (IDC), invasive lobular carcinoma (ILC), or tubular carcinoma. IDC is the most common type, starting in the ducts of the breast and spreading to the surrounding tissue, while ILC has poorly defined margins, making it harder to detect (Miller et al., 2002). Tubular carcinoma, one of the best-characterized types, has distinctive prognostic features (Brooks & Harris, 2006).

Finally, the number of axillary lymph nodes involved (N0, N1, N2, or N3) is another variable. This variable indicates whether the cancer has spread to the lymph nodes and, if so, to what extent. The more lymph nodes involved, the worse the prognosis. This is an important factor in determining the stage of the cancer and the potential for its spread to other parts of the body (Brooks & Harris, 2006).

Each of these variables provides information for understanding the nature of breast cancer, its progression, and the prognosis for affected individuals. The dataset captures biological and clinical data that can help shape treatment decisions and provide a clearer picture of how different factors influence the development of breast cancer.

A univariate analysis for the association between breast cancer and risk factors are conducted by using chi-square and t-tests (Table 4.1 and Table 4.2). Tables also show the distribution of the risk factors of interest and adjusting factors for cases and controls.

Table 4.1: Percentages for levels of categorical factors with respect to disease status (case, control), and chi-square test for indepence of disease and factors.

| Factor | Factor levels | Case | | Control | | | P-val. |
|---|---|---|---|---|---|---|---|
| | | ( %) | (N) | (%) | (N) | Total | |
| HRT | *Not taking* | 42 % | 210 | 39.4% | 197 | 407 | |
| | *Taking* | 7.8% | 39 | 10.8% | 54 | 93 | 0.092 |
| Family history | *Absent* | 38.4% | 192 | 39% | 195 | 387 | |
| | *1st order relative* | 8.4% | 42 | 9.2% | 46 | 88 | |
| | *2nd order relative* | 3% | 15 | 2% | 10 | 25 | 0.549 |
| Mammography | *Never* | 31.8% | 159 | 20.8% | 104 | 263 | |
| | *Semi-annually* | 18% | 90 | 29.4% | 147 | 237 | <.001 |

| | | | | | | | |
|---|---|---|---|---|---|---|---|
| Education | *No education* | 7.8% | 39 | 3% | 15 | 54 | |
| | *Primary school* | 22.4% | 112 | 22% | 110 | 222 | |
| | *Secondary sch.* | 6.2% | 31 | 5.4% | 27 | 58 | |
| | *High school* | 5.8% | 29 | 10.6% | 53 | 82 | |
| | *University* | 7.6% | 38 | 9.2% | 46 | 84 | |
| | *Post graduate* | 0% | 0 | 0% | 0 | 0 | <.001 |
| Region | *Central Anatolia* | 29.2% | 146 | 33% | 165 | 311 | |
| | *East /South-East Anatolia* | 6.8% | 34 | 5.2% | 26 | 60 | |
| | *Blacksea* | 8.6% | 43 | 7% | 35 | 78 | |
| | *Mediterrenean & Aegean&Marm.* | 5.2% | 26 | 5% | 25 | 51 | 0.383 |

Frequencies and percentages of the levels of categorical risk factors are given in Table 4.1. P-values correspond to the chi-square test for testing the association between breast cancer and factors. Results revealed that mammography screening status has association with breast cancer status ($p<0.001$). Also, one of the adjusting factors, education, is not independent of breast cancer, that means, having breast cancer differs for level of the education ($p<0.001$).

Table 4.2: Sample means and standard deviations (sd) for continuous risk factors with respect to disease status, and t-test for the difference of means

| Factor | Case | Control | |
|---|---|---|---|
| | Average *(sd)* | Average *(sd)* | P-value |
| Age | 51.752 *(10.94)* | 46.32 *(9.96)* | <.0001 |
| Age at first menstruation | 13.464 *(1.46)* | 13.552 *(1.36)* | 0.622 |
| Age at first birth | 21.946 *(5.17)* | 21.611 *(4.80)* | 0.614 |
| Age at last birth | 29.705 *(5.56)* | 27.531 *(5.41)* | 0.003 |
| Duration of breast feeding | 27.5 *(21.83)* | 23.143 *(20.32)* | 0.115 |
| Number of births | 2.624 *(1.58)* | 2.192 *(1.34)* | 0.021 |
| Age at menopause | 47.713 *(5.29)* | 45.711 *(5.20)* | 0.043 |
| BMI(pre-menopause) | 28.68 *(4.74)* | 26.59 *(5.18)* | 0.002 |
| BMI(post-menopause) | 29.27 *(5.06)* | 28.20 *(5.39)* | 0.122 |

Table 4.2 shows the t-test results for the difference of covariates of cases and controls. According to the results, number of births ($p=0.02$), age at

menopause (p=0.04) and BMI before the menopause (p=0.002) differs for diseased and nondiseased women. That is to say, these factors have statistically significant relationship with breast cancer status.

4.2. Two Stage Polytomous Logistic Regression

In order to investigate the association between the disease characteristics and the covariates in a multivariate way, when the data on subtypes is available, two stage logistic regression by Chatterjee (2004) is used to conveniently estimate these effects. The important risk factors by clinically important tumor characteristics based on a large scale study in Poland using the two stage approach is established (Garcia-Closas et al., 2006; Sherman et al., 2007). We established the risk factors and their effects by important tumor characteristics for Turkish female breast cancer patients.

In this approach, the association between a single tumor characteristic and the covariates is adjusted for the remaining tumor characteristics. This way the association between the specific tumor characteristic and the covariates are determined by holding the other tumor characteristics fixed. The results of this analysis is given in Table 4.3-4.7. Women who go through mammography seem less likely to develop grade-2 tumor than grade-1 or grade-3 tumor (OR=0.28, p=0.01; OR=0.21, p=0.006). Higher body mass index for women in post-menopausal term has lower association with having enlarged lymph nodes (OR=0.93, p=0.043). Small number of births is associated with PR positive. That is, the odds of PR positive is higher for woman with less number of births compared to a woman with more number of births (p=0.015). Note that, in this approach, the association between risk factor and a tumor characteristic is adjusted for all the remaining tumor characteristics.

Table 4.3: OR estimates, CIs, and p-values for two stage polyt. logistic regression for tumor size

| | Response: Tumor size | | | | | |
|---|---|---|---|---|---|---|
| | Tumor size: T2 (ref= Tumor size: T1) | | | Tumor size: T3,T4 (ref=T. size: T1) | | |
| | OR | 95% CI | p-val | OR | 95% CI | p-val |
| Age | 0.9657 | (0.918, 1) | 0.1713 | 1.0012 | (0.926,1.1) | 0.975 |
| Age at first menstruation | 1.0101 | (0.762,1.3) | 0.944 | 1.0586 | (0.6857,1.6) | 0.7973 |
| HRT taken(ref=not taken) | 0.9327 | (0.331, 2.6) | 0.8951 | 0.2899 | (0.047, 1.8) | 0.1805 |
| Duration of breast feeding | 1.0041 | (0.984, 1) | 0.6845 | 1.0025 | (0.972, 1) | 0.8708 |
| Family history (1st degree) (ref=absent) | 1.1482 | (0.811, 3.2) | 0.792 | 0.7333 | (0.618, 3.6) | 0.7036 |
| Family history (2nd) (ref=absent) | 2.8368 | (0.411, 17.6) | 0.2622 | 0.2165 | (0.148, 5.4) | 0.3512 |
| Number of births | 1.1175 | (0.458, 1.5) | 0.4955 | 1.0321 | (0.008, 1.7) | 0.9037 |
| Age at first birth | 1.0105 | (0.967, 1.1) | 0.6358 | 0.9683 | (0.90, 1) | 0.3579 |
| Mammography (ref=no) | 0.8862 | (0.400, 2) | 0.7657 | 0.6822 | (0.187, 2.5) | 0.5619 |
| Education | 1.0516 | (0.734, 1.5) | 0.7834 | 1.3074 | (0.751, 2.3) | 0.3426 |
| Age at menopause | 0.9972 | (0.967, 1) | 0.8567 | 0.973 | (0.925, 1) | 0.2803 |
| BMI (pre-menopause) | 1.0784 | (0.972, 1.2) | 0.151 | 1.0814 | (0.942, 1.2) | 0.2645 |
| BMI (post menopause) | 1.0023 | (0.92, 1.08) | 0.9579 | 1.0904 | (0.95, 1.22) | 0.1987 |
| Central Anatolia (ref=Other) | 1.8892 | (0.595, 6) | 0.2799 | 1.4457 | 0.247, 8.4) | 0.6822 |
| East and South-EastAnatolia (ref=Other) | 1.0509 | (0.23, 4.7) | 0.9481 | 4.2747 | (0.482, 37.9) | 0.1918 |
| Black Sea (ref=Other) | 2.1504 | (0.518, 8.9 | 0.2916 | 2.8848 | (0.334, 24.9) | 0.3353 |
| Births status (ref=no birth) | 0.2358 | (0.040, 1.4) | 0.1081 | 1.1764 | (0.085, 16.1) | 0.9033 |
| Menopause status (ref=No) | 23.5486 | (0.458,1210.4) | 0.116 | 2.5773 | (0.00, 837.7) | 0.7484 |

Table 4.4: OR estimates, CIs, and p-values for two stage polyt. logistic regression for grade

| | Response: Grade | | | | | |
|---|---|---|---|---|---|---|
| | Grade 2 (ref= Grade 1) | | | Grade 3 (ref= Grade 1) | | |
| | OR | 95% CI | p-val | OR | 95% CI | p-val |
| Age | 1.0175 | (0.954, 1.1) | 0.5952 | 1.0421 | (0.968, 1.1) | 0.268 |
| Age at first menstruation | 0.8789 | (0.626, 1.2) | 0.4541 | 0.8823 | (0.596, 1.3) | 0.531 |
| HRT taken (ref=not taken) | 1.1211 | (0.339, 3.7) | 0.8514 | 1.2196 | (0.304, 4.9) | 0.7793 |
| Duration of breast feeding | 0.9942 | (0.968, 1) | 0.6583 | 0.9905 | (0.962, 1) | 0.5229 |
| Family history (1st degree) (ref=absent) | 1.0616 | (0.760, 3.6) | 0.9228 | 0.906 | (0.879, 3.8) | 0.8924 |
| Family history (2nd) (ref=absent) | 0.6559 | (0.316, 4.7) | 0.6735 | 1.2179 | (0.21, 10.5) | 0.8576 |
| Number of births | 1.1869 | (0.092, 1.9) | 0.4506 | 1.4524 | (0.141, 2.4) | 0.145 |

| | | | | | | |
|---|---|---|---|---|---|---|
| Age at first birth | 1.0468 | (0.993, 1.1) | 0.0839 | 1.0803 | (1.01, 1.2) | 0.0168 |
| Mammography (ref=no) | 0.2826 | (0.10, 0.7) | 0.01 | 0.2081 | (0.067, 0.6) | 0.006 |
| Education | 0.9764 | (0.631, 1.5) | 0.9146 | 0.9335 | (0.560, 1.6) | 0.7914 |
| Age of menopause | 1.012 | (0.97, 1) | 0.5074 | 1.0091 | (0.964, 1.1) | 0.6962 |
| BMI (pre-menopause) | 1.0252 | (0.901, 1.2) | 0.7041 | 1.0548 | (0.920, 1.2) | 0.4442 |
| BMI (post menopause) | 1.0801 | (0.97, 1.18) | 0.1418 | 1.0552 | (0.93, 1.17) | 0.3888 |
| Central Anatolia (ref=Other) | 0.5335 | (0.105, 2.7) | 0.4478 | 0.3125 | (0.049, 2) | 0.2154 |
| East and South-East Anatolia (ref=Other) | 0.8802 | (0.118, 6.6) | 0.9009 | 0.7086 | (0.074, 6.8) | 0.7649 |
| Black Sea (ref=Other) | 0.7409 | (0.104, 5.3) | 0.7642 | 0.2763 | (0.03, 2.5) | 0.256 |
| Births status (ref=no birth) | 0.8762 | (0.127, 6) | 0.8931 | 0.3036 | (0.030, 3.1) | 0.3124 |
| Menopause status (ref=No) | 0.1519 | (0.001, 18.6) | 0.4422 | 0.1989 | (0.00, 47.8) | 0.5638 |

Table 4.5: OR estimates, CIs, and p-values for two stage polyt. logistic regression for tumor type and NA

| | Response: Tumor type | | | Response: NA | | |
|---|---|---|---|---|---|---|
| | Tumortype: ILC/Tubular (ref=tumor type IDC) | | | NA: enlarged lymph nodes exist (ref= no enlarged lymph nodes) | | |
| | OR | 95% CI | p-val | OR | 95% CI | p-val |
| Age | 1.0442 | (0.981, 1.1) | 0.1741 | 0.945 | (0.902, 1) | 0.0163 |
| Age at first menstruation | 0.8164 | (0.566, 1.2) | 0.2758 | 1.2124 | (0.93, 1.6) | 0.143 |
| HRT taken (ref=not taken) | 0.617 | (0.161, 2.4) | 0.4802 | 1.1856 | (0.460, 3.1) | 0.724 |
| Duration of breast feeding | 1.0171 | (0.991, 1) | 0.1845 | 1.0075 | (0.989, 1) | 0.4147 |
| Family history (1st degr.) (ref=absent) | 1.413 | (0.614, 4.5) | 0.5592 | 1.3687 | (0.530, 3.6) | 0.5211 |
| Family history (2nd degr.) (ref=absent) | 0.635 | (0.442, 8.9) | 0.7356 | 1.1784 | (0.524, 5.8) | 0.8393 |
| Number of births | 0.9398 | (0.045, 1.4) | 0.7743 | 0.7176 | (0.241, 1) | 0.0311 |
| Age at first birth | 0.9555 | (0.905, 1) | 0.0975 | 1.0028 | (0.960, 1) | 0.898 |
| Mammography (ref=no) | 0.7513 | (0.260, 2.2) | 0.5967 | 1.2997 | (0.617, 2.7) | 0.4903 |
| Education | 1.5116 | (0.936, 2.4) | 0.0907 | 0.5699 | (0.401, 0.8) | 0.0017 |
| Age at menopause | 1.0017 | (0.963, 1) | 0.9327 | 1.0223 | (0.99, 1.19) | 0.1487 |
| BMI (pre-menopause) | 1.0592 | (0.939, 1.2) | 0.3491 | 0.9161 | (0.837, 1) | 0.055 |
| BMI (post menopause) | 0.9449 | (0.83, 1.053) | 0.3068 | 0.9271 | (0.85, 1.00) | 0.0434 |
| Central Anatolia (ref=Other) | 4.1114 | (0.418, 40.4) | 0.2251 | 0.9533 | (0.298, 3) | 0.9357 |
| East and South-East Anatolia (ref=Other) | 11.7268 | (0.979, 140.4) | 0.0519 | 0.577 | (0.133, 2.5) | 0.4624 |
| Black Sea (ref=Other) | 13.6948 | (1.20, 156.2) | 0.0351 | 0.7735 | (0.20, 3) | 0.7097 |
| Births status (ref=no birth) | 1.2014 | (0.164, 8.8) | 0.8566 | 1.9011 | (0.37, 9.7) | 0.4391 |
| Menopause status (ref=No) | 43.5664 | (0.33, 5597) | 0.1277 | 0.2583 | (0.007, 9.4) | 0.46 |

Table 4.6: OR estimates, CIs, and p-values for two stage polyt. logistic regression for ER and PR

| | Response: ER | | | Response: PR | | |
|---|---|---|---|---|---|---|
| | ER: (+) (ref= ER: (-)) | | | PR: (+) (ref= PR: (-)) | | |
| | OR | 95% CI | p-val | OR | 95% CI | p-val |
| Age | 1.0056 | (0.959, 1.1) | 0.8181 | 1.0037 | (0.962, 1) | 0.8615 |
| Age at first menstruation | 1.0739 | (0.818, 1.4) | 0.6073 | 0.8265 | (0.647, 1.1) | 0.1263 |
| HRT taken(ref=not taken) | 0.8395 | (0.316, 2.2) | 0.7255 | 0.5912 | (0.250, 1.4) | 0.2311 |
| Duration of breast feeding | 0.9982 | (0.979, 1) | 0.85 | 1.0159 | (0.99, 1) | 0.0643 |
| Family history (1st degree) (ref=absent) | 0.6823 | (0.861, 1.8) | 0.4336 | 0.4574 | (0.534, 1.1) | 0.0799 |
| Family history (2nd degree) (ref=absent) | 1.4134 | (0.262, 8) | 0.696 | 1.3285 | (0.19, 5.9) | 0.7094 |
| Number of births | 1.1842 | (0.249, 1.69 | 0.2982 | 0.7073 | (0.298, 0.9) | 0.0152 |
| Age at first birth | 1.016 | (0.973, 1.1) | 0.4666 | 1.0204 | (0.981, 1.1) | 0.3042 |
| Mammography (ref=no) | 1.2323 | (0.551, 2.8) | 0.6107 | 1.5311 | (0.761, 3.1) | 0.2319 |
| Education | 1.088 | (0.759, 1.6) | 0.6457 | 0.7978 | (0.582, 1.1) | 0.1601 |
| Age at menopause | 1.0037 | (0.974, 1) | 0.8079 | 1.0506 | (1.021, 1.1) | 0.0005 |
| (BMI (pre-menopause) | 0.9846 | (0.90, 1.1) | 0.7338 | 0.9885 | (0.91, 1.1) | 0.7761 |
| BMI (post menopause) | 0.9772 | (0.89, 1.05) | 0.5595 | 0.9446 | (0.87, 1.01) | 0.1071 |
| Central Anatolia (ref=Other) | 1.0554 | (0.328, 3.4) | 0.9278 | 1.3336 | (0.472, 3.8) | 0.5867 |
| East and South-East Anatolia (ref=Other) | 0.8861 | (0.201, 3.9) | 0.8731 | 0.8315 | (0.21, 3.2) | 0.7878 |
| Black Sea (ref=Other) | 0.9384 | (0.233, 3.8) | 0.9287 | 2.0501 | (0.588, 7.1) | 0.2598 |
| Births status (ref=no birth) | 1.0856 | (0.213, 5.5) | 0.9213 | 0.5341 | (0.122, 2.3) | 0.4037 |
| Menopause status (ref=No) | 0.5448 | (0.01, 20.9) | 0.7441 | 0.2921 | (0.011, 7.2) | 0.4516 |

Table 4.7: OR estimates, CIs, and p-values for two stage polyt. logistic regression for C-ERB

| | Response c-erb | | |
|---|---|---|---|
| | C-erb: (+) (ref=c-erb: (-)) | | |
| | OR | 95% CI | p-value |
| Age | 0.9658 | (0.918, 1) | 0.1764 |
| Age at first menstruation | 1.0452 | (0.792, 1.4) | 0.7543 |
| HRT taken (ref=not taken) | 2.3123 | (0.888, 6) | 0.0858 |
| Duration of breast feeding | 1.0154 | (0.997, 1) | 0.0968 |
| Family history (1st degree) (ref=absent) | 1.1965 | (0.636, 3.3) | 0.7318 |
| Family history (2nd degree) (ref=absent) | 0.774 | (0.428, 4.4) | 0.772 |
| Number of births | 0.897 | (0.136, 1.3) | 0.5347 |
| Age at first birth | 0.9803 | (0.936, 1) | 0.3914 |
| Mammography (ref=no) | 0.6864 | (0.289, 1.6) | 0.393 |
| Education | 1.0224 | (0.699, 1.5) | 0.9089 |
| Age at menopause | 1.0232 | (0.985, 1.1) | 0.2322 |
| BMI (pre-menopause) | 0.9833 | (0.90, 1.1) | 0.7085 |
| BMI (post menopause) | 0.9996 | (0.91, 1.08) | 0.9931 |
| Central Anatolia (ref=Other) | 1.4326 | (0.41, 4.9) | 0.5684 |
| East and South-East Anatolia (ref=Other) | 0.7388 | (0.146, 3.7) | 0.7136 |
| Black Sea (ref=Other) | 1.4685 | (0.336, 6.4) | 0.6095 |
| Births status (ref=no birth) | 1.3841 | (0.253, 7.6) | 0.7075 |
| Menopause status (ref=No) | 0.5243 | (0.011, 24.6) | 0.7423 |

## 5. CONCLUSION

This study focused on modeling diseases with multiple characteristics using a two-stage polytomous logistic regression model. Both simulation experiments and real-world breast cancer data analysis were conducted to evaluate the performance of this approach in capturing the complex relationships between risk factors and disease subtypes. The results demonstrate that the two-stage model is an effective and efficient method for handling high-dimensional epidemiological data, where traditional approaches often struggle due to the large number of parameters and the potential for covariation among disease characteristics.

In the simulation study, we examined the performance of three estimation methods—Maximum Likelihood Estimation (MLE), Bayesian Estimation, and Pseudo-Conditional Likelihood (PCL) Estimation—across different sample sizes and disease subtype configurations. In the M=2×2×2 scenario, where three disease characteristics were cross-classified to create eight disease subtypes, the PCL method consistently outperformed MLE and Bayesian estimation for small and moderate sample sizes. PCL provided lower bias and mean squared error (MSE), especially when the number of disease subtypes was large relative to the sample size, and it converged to its asymptotic properties more quickly. MLE, on the other hand, showed improved performance as the sample size increased, becoming more competitive at larger sample sizes. Bayesian estimation, while flexible and theoretically attractive, was more computationally intensive and less efficient in this particular setting, particularly under the non-informative priors used in the study. These results indicate that for studies with small to moderate sample sizes and complex disease subtype structures, the PCL method offers a clear advantage by effectively reducing dimensionality and providing more stable estimates.

In the data analysis, the two-stage polytomous logistic regression model was applied to a dataset of Turkish female breast cancer patients, which included detailed information on tumor characteristics—such as size, NA status, and grade—along with several established breast cancer risk factors. The application of the two-stage model allowed us to investigate the interaction between these tumor characteristics and the risk factors in a comprehensive

manner. By utilizing the two-stage approach, the model efficiently handled the high-dimensional parameter space created by cross-classifying the disease characteristics into subtypes, while preserving the covariation between these characteristics.

The results of the data analysis demonstrated that specific risk factors, such as family history and reproductive history, had varying impacts on the different breast cancer subtypes. The second-stage parameters provided insights into how these risk factors influence the tumor characteristics simultaneously, offering a more nuanced understanding of the heterogeneity in breast cancer etiology. The two-stage model thus enabled a deeper exploration of the interaction effects that would be difficult to capture with traditional, single-stage models. Moreover, the model's ability to focus on covariate effects while reducing the complexity of intercept estimation proved valuable in the analysis of this real-world dataset, providing interpretable and reliable results.

The advantages of the two-stage polytomous logistic regression model were evident throughout both the simulation study and the data analysis. First, it effectively addresses the dimensionality problem associated with cross-classifying multiple disease characteristics into subtypes, which can quickly lead to a large number of parameters. By focusing on the second-stage parameters, the model reduces the number of regression coefficients that need to be estimated, thus avoiding potential overfitting and instability in the estimates. Second, the model is flexible, allowing researchers to capture the multivariate nature of disease characteristics and investigate potential interactions between these characteristics and risk factors. This is particularly useful in epidemiological studies, where the relationships between risk factors and disease subtypes are often complex and difficult to model using traditional approaches.

Additionally, the two-stage model provides a clear framework for hypothesis testing in epidemiological research. By framing the hypotheses in terms of second-stage parameters, researchers can test for the presence of interactions between disease characteristics and risk factors without needing to explicitly estimate the full set of first-stage parameters. This makes the model not only efficient in terms of estimation but also more convenient for drawing inferences about the underlying associations in the data.

In conclusion, the two-stage polytomous logistic regression model proves to be a powerful tool for analyzing disease data with multiple characteristics, especially when dealing with complex, cross-classified subtypes. It offers a methodologically sound and computationally efficient solution to the challenges posed by high-dimensional parameter spaces, while preserving important covariation between disease characteristics. The model is particularly suited for small to moderate sample sizes, where traditional methods like MLE and Bayesian estimation may fail to provide stable and accurate results. The successful application of the model to both simulated and real-world breast cancer data underscores its practical value in epidemiological studies, where understanding the heterogeneity of disease subtypes is crucial for advancing both scientific knowledge and public health interventions.

Looking forward, the two-stage model offers significant potential for further development and application. Future research could explore its use in more complex scenarios, such as diseases with even more characteristics or levels, or in studies with missing data and censored observations. Additionally, integrating informative priors into the Bayesian framework of the two-stage model could enhance its performance in cases where prior knowledge about disease subtypes is available. Overall, this study highlights the two-stage polytomous logistic regression model as a key tool for future epidemiological research.

## REFERENCES

Agresti, A. (2002). *Categorical data analysis*. John Wiley & Sons Inc.

Brooks, S. A., & Harris, A. (2006). *Breast cancer research protocols*. Humana Press Inc.

Chatterjee, N. (2004). A two-stage regression model for epidemiological studies with multivariate disease classification data. *Journal of the American Statistical Association*, 99(465), 127-138. https://doi.org/10.1198/016214504000000116

Erdem, T. (2011). *Modelling diseases with multiple disease characteristics: Comparison of models and estimation methods* [Master's thesis, Middle East Technical University]. METU.

García-Closas, M., Brinton, L. A., Lissowska, J., Chatterjee, N., Peplonska, B., Anderson, W. F., Szeszenia-Dabrowska, N., Bardin-Mikolajczak, A., Zatonski, W., Blair, A., Kalaylioglu, Z., Rymkiewicz, G., Mazepa-Sikora, D., Kordek, R., Lukaszek, S., & Sherman, M. E. (2006). Established breast cancer risk factors by clinically important tumour characteristics. *British Journal of Cancer*, 95(1), 123-129. https://doi.org/10.1038/sj.bjc.6603216

Harris, J. R., Lippman, M. E., Morrow, M., & Osborne, C. K. (2010). *Diseases of the breast*. Lippincott Williams & Wilkins.

Kleinbaum, D. G., & Klein, M. (2010). *Logistic regression: A self-learning text*. Springer. https://doi.org/10.1007/978-1-4419-1742-3

McFadden, D. (1974). Conditional logit analysis of qualitative choice behavior. In P. Zarembka (Ed.), *Frontiers in econometrics* (pp. 105-142). Academic Press.

Ntzoufras, I. (2009). *Bayesian inference via WinBUGS*. John Wiley & Sons Inc.

Sherman, M. E., Rimm, D. L., Yang, X. R., Chatterjee, N., Brinton, L. A., Lissowska, J., Peplonska, B., Szeszenia-Dabrowska, N., Zatonski, W., Cartun, R., Mandich, D., Rymkiewicz, G., Ligaj, M., Lukaszek, S., Kordek, R., Kalaylioglu, Z., Harigopal, M., Charrette, L., Falk, R. T., Richesson, D., Anderson, W. F., Hewitt, S. M., & García-Closas, M. (2007). Variation in breast cancer hormone receptor and HER2 levels by etiologic factors: A population-based analysis. *International Journal of Cancer*, 121(5), 1079-1085. https://doi.org/10.1002/ijc.22807

Sotiriou, C., & Pusztai, L. (2009). Gene-expression signatures in breast cancer. *The New England Journal of Medicine*, 360, 790-800. https://doi.org/10.1056/NEJMra0801289

# CHAPTER 7

## THE EFFECT OF CRITERIA TYPES ON THE DECISION-MAKING PROCESS IN THE PROMETHEE METHOD

*Feride TUĞRUL*[1]

1 Assist. Prof. Dr., Munzur University, Faculty of Engineering, Department of Computer Engineering, Tunceli, Türkiye.
ORCID: 0000-0001-7690-8080
Corresponding author: feridetugrul@munzur.edu.tr

## 1.Introduction

Fuzzy Sets were established by Lotfi A. Zadeh to address the limitations of crisp set theory in handling uncertainty and vagueness (Zadeh, 1965). In classical sets, an element either belongs to the set (membership = 1) or does not belong (membership = 0). However, many real-world scenarios involve imprecise concepts. For example, the notion of "tall people" can't be precisely defined, as people's perceptions of height vary. Fuzzy sets offer a more flexible approach by allowing partial membership, where an element's membership degree can be any value between 0 and 1. This membership degree represents how strongly an element belongs to the set.

While fuzzy sets capture degrees of membership, they don't account for uncertainty or hesitation in assigning these values. This limitation led to the development of Intuitionistic Fuzzy Sets (IFS) by K. Atanassov (Atanassov, 1983, 1989). An intuitionistic fuzzy set extends the concept of fuzzy sets by developing a degree of non-membership and a degree of hesitation.

Fuzzy sets are effective for modeling imprecise scenarios where partial membership suffices, while intuitionistic fuzzy sets are more powerful in situations where uncertainty or hesitation needs to be explicitly represented. Both concepts have found applications in areas such as decision-making, control systems, pattern recognition, and artificial intelligence.

Decision-making(DM) involves evaluating and selecting the best alternative(s) based on multiple, often conflicting criteria. In reality, decisions are rarely made by considering just one factor. For example, choosing a new car may involve criteria such as cost, fuel efficiency, safety, and design. DM provides structured methods to make such decisions rational and systematic. One of the most used DM methods is the PROMETHEE.

PROMETHEE improved by Jean-Pierre Brans in 1982 (Brans, 1982). Principle of PROMETHEE method is ranks alternatives by comparing preference functions for each criterion. Application areas of PROMETHEE are engineering design, financial decision-making, supplier selection, education, personnel selection, environmental management, logistics, production planning etc. (Brans and Vincke, 1985; Liao and Xu, 2014).

In this study, a MCDM system was created for a company that attaches importance to personnel selection. The issue of personnel selection is a popular topic among decision-making practices (Afshari et al., 2011; Akın, 2016; Asemi and Asemi, 2014; Boran et al., 2011; Değermenci and Ayvaz, 2016). In this decision-making process, the aim was to make the most objective decision in personnel selection by taking into account the opinions of decision makers. IFSs were used to eliminate the uncertainty in the opinions of decision makers. In addition, decision makers determined the criteria weights with linguistic values. In this study, while the application was being made, the effects of different criteria types on the result were researched. Two different criteria evaluation type functions, V shape and Gaussian type functions, were considered and their results were compared and suggestions were presented to researchers.

## 2. Preliminaries

**Definition 2.1:** Let $X \neq \emptyset$. An intuitionistic fuzzy set $A$ in $X$;

$A = \{\langle x, \mu_A(x), \nu_A(x)\rangle | \; x \in X\}$,

$$\mu_A(x), \nu_A(x), \pi_A(x): X \rightarrow [0,1]$$

$$\mu_A(x) + \nu_A(x) + \pi_A(x) = 1$$

defined membership, nonmembership and hesitation degree of the element $x \in X$ respectively (Atanassov, 1983, 1986).

Intuitionistic fuzzy value (IFV) is displayed (Xu, 2007):

$\tilde{a} = (\mu_{\tilde{a}}, \nu_{\tilde{a}}, \pi_{\tilde{a}})$ in which $\mu_{\tilde{a}}, \nu_{\tilde{a}}, \pi_{\tilde{a}} \in [0,1]$.

**Definition 2.2:** For IFVs $\tilde{a} = (\mu_{\tilde{a}}, \nu_{\tilde{a}})$ and $\tilde{b} = (\mu_{\tilde{b}}, \nu_{\tilde{b}})$ operations specified (Xu and Yager, 2006; Xu, 2007):

$$(1)\tilde{a} \oplus \tilde{b} = (\mu_{\tilde{a}} + \mu_{\tilde{b}} - \mu_{\tilde{a}}\mu_{\tilde{b}}, \nu_{\tilde{a}}\nu_{\tilde{b}})$$

$$(2)\tilde{a} \otimes \tilde{b} = (\mu_{\tilde{a}}\mu_{\tilde{b}}, \nu_{\tilde{a}} + \nu_{\tilde{b}} - \nu_{\tilde{a}}\nu_{\tilde{b}})$$

$$(3) \bigoplus_{j=1}^{m} \tilde{a}_j = \left(1 - \prod_{j=1}^{m}(1-\mu_j), \prod_{j=1}^{m}\nu_j\right)$$

$$(4) \bigotimes_{j=1}^{m} \tilde{a}_j = \left(\prod_{j=1}^{m}\mu_j, \prod_{j=1}^{m}(1-\nu_j)\right)$$

As the value of the following function used to rank IFVs decreases, the preferability of that alternative increases (Szmidt and Kacprzyk, 2009):

$$\rho(\alpha) = 0.5(1+\pi_\alpha)(1-\mu_\alpha)$$

In this study, comparisons were made on the same data using different criteria types.
Firstly, V shape criterion type was used:

$$P(d) = \begin{cases} 0, & d \le q \\ \dfrac{d-q}{p-q}, & q < d \le p \\ 1, & d > p \end{cases}$$

Secondly, the Gaussian criterion type was used:

$$P(d) = \begin{cases} 0, & d \leq 0 \\ 1 - e^{-\frac{x^2}{2\sigma^2}}, & d \geq 0 \end{cases}$$

Assess the alternatives with respect to the criteria and calculate the deviations based on pairwise comparisons:

$$d_j(x, y) = c_j(x) - c_j(y)$$

### 2.1 Intuitionistic Fuzzy PROMETHEE

**Definition 2.1.1:** An IF preference relation $R$ on the set $X = \{x_1, x_2, \dots, x_n\}$ is represented by a matrix $R = (r_{ik})_{n\times n}$ where $r_{ik} = \langle (x_i, x_k), \mu(x_i, x_k), \nu(x_i, x_k) \rangle$ for all $i, k = 1,2, \dots, n$. For convenience, we let $r_{ik} = (\mu_{ik}, \nu_{ik})$ where $\mu_{ik}$ denotes the degree to which the object $x_i$ is preferred to the object $x_k$, $\nu_{ik}$ indicates the degree to which the object $x_i$ is not preferred to the object $x_k$, and $\pi(x_i, x_k) = 1 - \mu(x_i, x_k) - \nu(x_i, x_k)$ interpreted as an indeterminacy degree with the condition (Xu, 2007):

$$\mu_{ik}, \nu_{ik} \in [0,1],\ \mu_{ik} + \nu_{ik} \leq 1, \qquad \mu_{ik} = \nu_{ki},\ \mu_{ki} = \nu_{ik}$$

$$\pi_{ik} = 1 - \mu_{ik} - \nu_{ik},$$

for $\forall\ i, k = 1,2, \dots, n$ .

The preference matrix is identified like this (Liao and Xu, 2014):

$$U^{(j)} = (\mu_{ik}^{(j)})_{n\times n} = \begin{bmatrix} - & \mu_{12}^{(j)} & \dots & \mu_{1n}^{(j)} \\ \mu_{21}^{(j)} & - & \dots & \mu_{2n}^{(j)} \\ \vdots & \vdots & - & \vdots \\ \mu_{n1}^{(j)} & \mu_{n2}^{(j)} & \dots & - \end{bmatrix}$$

The IF preference relation matrix is like this:

$$R^{(j)} = (r_{ik}^{(j)})_{n\times n} = \begin{bmatrix} - & \left(\mu_{12}^{(j)}, \nu_{12}^{(j)}\right) & \dots & \left(\mu_{1n}^{(j)}, \nu_{1n}^{(j)}\right) \\ \left(\mu_{21}^{(j)}, \nu_{21}^{(j)}\right) & - & \dots & \left(\mu_{2n}^{(j)}, \nu_{2n}^{(j)}\right) \\ \vdots & \vdots & - & \vdots \\ \left(\mu_{n1}^{(j)}, \nu_{n1}^{(j)}\right) & \left(\mu_{n2}^{(j)}, \nu_{n2}^{(j)}\right) & \dots & - \end{bmatrix}$$

For this study, the IFWA operator was considered among many aggregation operators defined for IFSs. The all IF preference index of the alternative $x_i$ to $x_k$ on all criteria can be obtained as:

$$r(x_i, x_k) = r_{ik} = \bigoplus_{j=1}^{m} \left(\tilde{w}_j \otimes r_{ik}^{(j)}\right)$$

Overall IF preference matrix is determined like this:

$$R = (r_{ik})_{n\times n} = \begin{bmatrix} - & (\mu_{12}, \nu_{12}) & \dots & (\mu_{1n}, \nu_{1n}) \\ (\mu_{21}, \nu_{21}) & - & \dots & (\mu_{2n}, \nu_{2n}) \\ \vdots & \vdots & - & \vdots \\ (\mu_{n1}, \nu_{n1}) & (\mu_{n2}, \nu_{n2}) & \dots & - \end{bmatrix}$$

The IF positive outranking flow:

$$\tilde{\phi}^{+}(x_i) = \frac{1}{n-1} \bigoplus_{k=1,k\neq i}^{n} r(x_i, x_k) = \frac{1}{n-1} \bigoplus_{k=1,k\neq i}^{n} r_{ik}$$

The IF negative outranking flow:

$$\tilde{\phi}^{-}(x_i) = \frac{1}{n-1} \bigoplus_{k=1,k\neq i}^{n} r(x_k, x_i) = \frac{1}{n-1} \bigoplus_{k=1,k\neq i}^{n} r_{ki}$$

The relation between the IF outranking flows can be determined utilizing (Szmidt and Kacprzyk, 2009):

$$\rho(\phi(x_i)) = \rho(\tilde{\phi}^{+}(x_i)) - \rho(\tilde{\phi}^{-}(x_i))$$

## 3. Numerical Experiments

The alternatives of the study include 4 alternatives. In this study, candidates are represented by alternatives. Furthermore the criteria of the study include 4 criteria, namely and respectively; Practical experience, communication, team management, aptitude for technology. There are many methods defined so far when determining the criteria weights. In this study, linguistic threshold was used as the method of determining the criteria weights. Decision makers evaluated each criterion according to the values in the table below.

Criteria weights are determined in linguistic terms so that decision makers can express their thoughts objectively. In this paper, linguistic expressions in the form of IF values of decision makers and controlled sets were utilized. Decision-makers may benefit from using certain methods to determine IF weights. (Çuvalcıoğlu, 2013, 2014; Liao and Xu, 2014; Wang, 2013). $W$ is decided in linguistic terms based on the opinions of the DMs:

| Linguistic Terms | IFNs |
|---|---|
| Very Important | (0.9,0.1) |
| Important | (0.75,0.2) |
| Medium | (0.5,0.45) |
| Unimportant | (0.35,0.6) |
| Very Unimportant | (0.1,0.9) |

**Table 1** Linguistic Terms for Rating the Criterion

Values of alternatives as to criteria are determined as follows Table 2:

| | $B_1$ | $B_2$ | $B_3$ | $B_4$ |
|---|---|---|---|---|
| $A_1$ | 80 | 60 | 85 | 65 |
| $A_2$ | 85 | 80 | 70 | 70 |
| $A_3$ | 75 | 85 | 60 | 80 |
| $A_4$ | 60 | 80 | 75 | 65 |

**Table 2** Values of Alternatives

Using linguistic terms, each decision-maker evaluated the criteria weights. According to linguistic terms, the criteria weights are Very Important, Important, Very Important, Important respectively. $W$ obtained based the decision makers' opinion are given in Table 3:

| Criteria | Weights of Criteria |
|---|---|
| $B_1$ | (0.90, 0.10) |
| $B_2$ | (0.75, 0.20) |
| $B_3$ | (0.90, 0.10) |
| $B_4$ | 0.75, 0.20) |

**Table 3** Weights of Criteria

Firstly, according to the calculations made utilizing the V shape criterion type. Then completing all the steps of the PROMETHEE method, the IF positive and negative outranking flows are given in Table 4 below:

| Positive Outranking Values | | | Negative Outranking Values | | |
|---|---|---|---|---|---|
| $\rho(\tilde{\varphi}^+(A$ | = | 0,72129 | $\rho(\tilde{\varphi}^-(A_1))$ | = | 0,72716 |
| $\rho(\tilde{\varphi}^+(A$ | = | 0,73228 | $\rho(\tilde{\varphi}^-(A_2))$ | = | 0,84742 |
| $\rho(\tilde{\varphi}^+(A$ | = | 0,72673 | $\rho(\tilde{\varphi}^-(A_3))$ | = | 0,74328 |
| $\rho(\tilde{\varphi}^+(A$ | = | 0,99999 | $\rho(\tilde{\varphi}^-(A_4))$ | = | 0,70225 |

**Table 4** IF Positive and Negative Outranking Flows

Net outranking values are given in Table 5 as follows:

| | | |
|---|---|---|
| $\rho(\tilde{\varphi}(A_1))$ | = | -0,00586 |
| $\rho(\tilde{\varphi}(A_2))$ | = | -0,11514 |
| $\rho(\tilde{\varphi}(A_3))$ | = | -0,01655 |
| $\rho(\tilde{\varphi}(A_4))$ | = | 0, 29775 |

**Table 5** IF Net Outranking Flows

The graph showing the ranking of alternatives according to the first criterion type is given below:

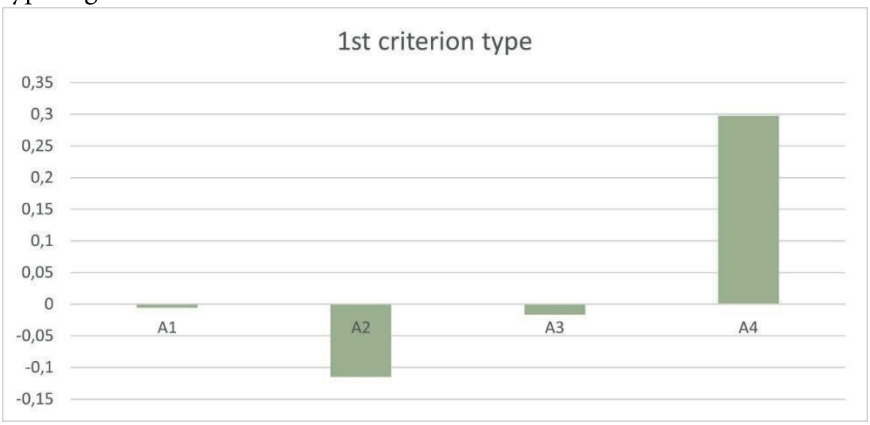


**Fig.1.** Alternative values according to 1st criterion type

According to the values obtained, the best candidate among these 4 candidates is the 2nd candidate, then the 3rd, 4th and 1st candidates, respectively.

Secondly, positive, negative and net outranking flows were calculated based on the results gathered using the Gaussian criterion type:

| Positive Outranking Values | | | Negative Outranking Values | | |
|---|---|---|---|---|---|
| $\rho(\tilde{\varphi}^{+}(A_1$ | = | 0,74124 | $\rho(\tilde{\varphi}^{-}(A_1))$ | = | 0,71492 |
| $\rho(\tilde{\varphi}^{+}(A_2$ | = | 0,72795 | $\rho(\tilde{\varphi}^{-}(A_2))$ | = | 0,82517 |
| $\rho(\tilde{\varphi}^{+}(A_3$ | = | 0,67888 | $\rho(\tilde{\varphi}^{-}(A_3))$ | = | 0,76228 |
| $\rho(\tilde{\varphi}^{+}(A_4$ | = | 0,84815 | $\rho(\tilde{\varphi}^{-}(A_4))$ | = | 0,68532 |

**Table 6** IF Positive and Negative Outranking Flows

| | | |
|---|---|---|
| $\rho(\tilde{\varphi}(A_1))$ | = | 0,02632 |
| $\rho(\tilde{\varphi}(A_2))$ | = | -0,09722 |
| $\rho(\tilde{\varphi}(A_3))$ | = | -0,08339 |
| $\rho(\tilde{\varphi}(A_4))$ | = | 0, 16282 |

**Table 7** IF Net Outranking Flows

The graph showing the ranking of alternatives according to the second criterion type is given below:

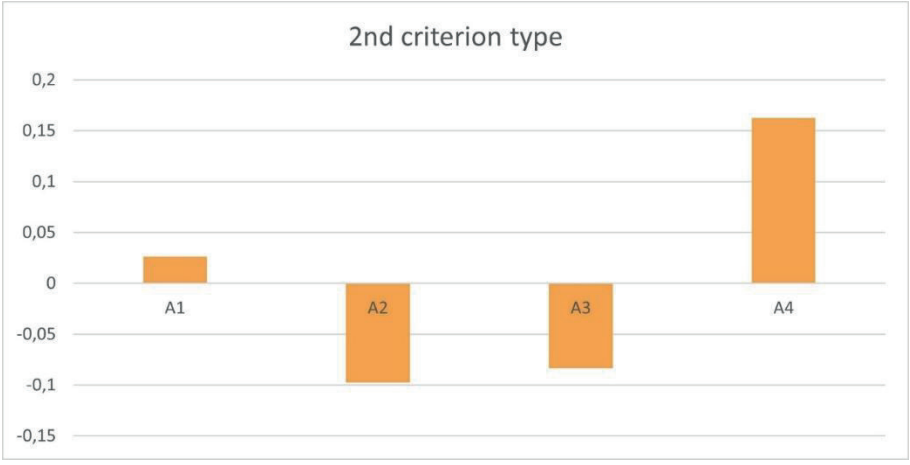


**Fig.2.** Alternative values according to 2nd criterion type

According to the values obtained, the best candidate among these 4 candidates is the 2nd candidate, then the 3rd, 1th and 4st candidates, respectively.

## 4. Comparative Analysis

If we want to interpret the rating of the alternatives, that is, the rating of the candidates for this application, the results obtained using two different criterion types are different from each other. The comparison graph is given below to better understand the difference.

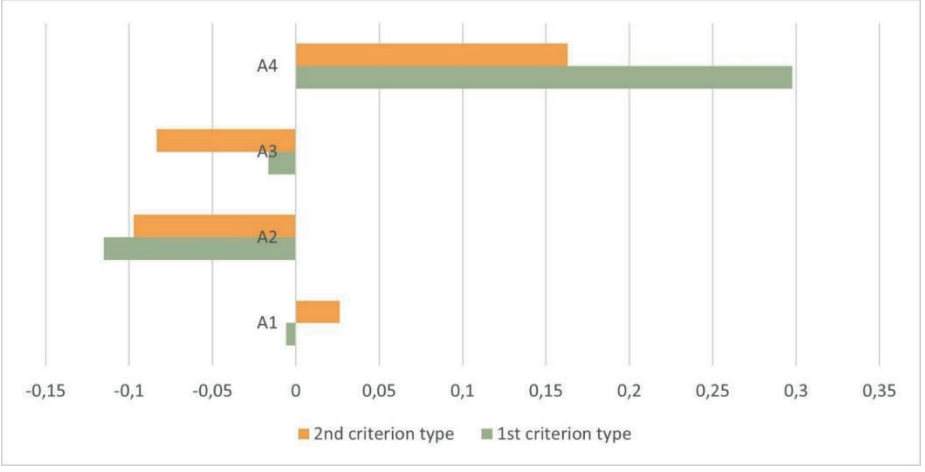


**Fig.3.** Comparison of results of two types of criteria

The rankings of the 1st and 4th candidates have changed. The important factor here is the basic principle on which the criterion types are based. When we compare the two criterion types, the V-shape criterion type emphasizes the threshold values, while the Gaussian criterion type emphasizes the deviation from the mean. As can be seen from this graph, two different results are obtained. This is the reason why consistent results are obtained in 2 candidates and the rankings of the other 2 candidates have changed. Decision makers should determine whether they will consider the threshold values or the

deviation from the mean when evaluating the criteria and alternatives, and choose between the criterion types accordingly.

## 5. Conclusion and Suggestion

An effective application example of intuitionistic fuzzy sets in the DM case with the PROMETHEE method is presented in this study. In this study applied in the field of personnel selection, candidates were first evaluated numerically by decision makers. Afterwards, the values were expressed with intuitionistic fuzzy values and the aim was to eliminate uncertainties. In the stage of determining the criterion weights, decision makers were asked to assess each criterion using lingual expressions. The main point that distinguishes this study from other studies is that decision-making processes were compared using two different criterion types. As a result of the comparison, a difference was observed in the ranking of candidates. The reason for this difference is that in the Gaussian criterion type, decision makers base their evaluations on deviation from the mean. In the V-shaped criterion type, threshold values are the main point for decision makers. Therefore, after determining what they want to consider in terms of evaluation criteria, decision makers should select the criterion types according to their features.

## References

Afshari, R., Yusuff, R.M., Hong, T.S. and Ismail, Y.B. (2011). A review of the applications of multi criteria decision making for personnel selection problem. *Afr. J. Bus. Manag*, 5(28).

Akın, N.G. (2016). Multi-criteria approach to personnel selection: fuzzy Topsis applications. *J Bus Res Turk*, 8(2), 224-254.

Asemi, A. and Asemi, A. (2014). Intelligent MCDM method for supplier selection under fuzzy environment. *International Journal of Information Science and Management (IJISM)*, 33-40.

Atanassov, K.T. (2016). Intuitionistic fuzzy sets, VII ITKR Session, Sofia, 20-23 June 1983. (Deposed in Centr. Sci.-Techn. Library of the Bulg. Acad. of Sci., 1697/84) (in Bulgarian), Reprinted: *Int. J. Bioautomation* 20(S1).

Atanassov, K.T. (1989). More on intuitionistic fuzzy sets. *Fuzzy Sets and Systems*, 33(1), 1989, 37-45.

Boran, F.E., Genç, S. and Akay, D. (2011). personnel selection based on intuitionistic fuzzy sets. *Human Factors and Ergonomics in Manufacturing & Service Industries*, 21(5), 493-503.

Brans, J.P. (1982). *Lingenierie de la decision; Elaboration dinstruments daidealadecision. Lamethode PROMETHEE.* in: R. Nadeau, M. Landry, ed., Laidea la decision: Nature, Instruments et Perspectives d Avenir, Quebec, Canada.Presses de Universite Laval 183-213.

Brans, J.P. and Vincke, P. (1985). A preference ranking organisation method (the PROMETHEE method for multiple criteria decision making). *Management Science*, 31(6), 647-656.

Çuvalcıoğlu, G. (2013). Controlled set theory. *Bogolyubov Readings DIF-2013* Ukraine.

Çuvalcıoğlu, G. (2014). Some properties of controlled set theory. *Notes on Intuitionistic Fuzzy Set*, 20(2), 37-42.

Değermenci, A. and Ayvaz, B. (2016). Fuzzy environment multi criteria decision making techniques personnel selection: Participation in an application in banking sector. *Istanb Commer Univ J Sci*, (15), 77-93.

Liao, H.C. and Xu, Z.S. (2014). Multi-criteria decision making with intuitionistic fuzzy PROMETHEE. *Journal of Intelligent Fuzzy Systems*, 27, 1703-1717.

Liao, H.C. and Xu, Z.S. (2014). Some algorithms for group decision making with intuitionistic fuzzy preference information, *International Journal of Uncertainty Fuzziness and Knowledge-Based Systems*, 22(4), 505-529.

Szmidt, E. and Kacprzyk, J. (2009). Amount of information and its reliability in the ranking of Atanassov's intuitionistic fuzzy alternatives. *in: E. Rakus-Andersson, R.R. Yager, N. Ichalkaranje, L. Jain, ed. Recent advances in decision making (Studies in Computational Intelligence),* Berlin, Germany: Springer, 7-19.

Wang, Z.J. (2013). Derivation of intuitionistic fuzzy weights based on intuitionistic fuzzy preference relations. Applied Mathematical Modelling, 37, 6377-6388.

Xu, Z.S. and Yager, R.R. (2006). Some geometric aggregation operators based on intuitionistic fuzzy set. *International Journal of General Systems*, 35, 417-433.

Xu, Z.S. (2007). Intuitionistic fuzzy aggregation operators. *IEEE Transactions on Fuzzy Systems*, 15, 1179-1187.

Zadeh, L.A. (1965). Fuzzy sets. *Information and Control*, 8, 338-353.

# CHAPTER 8

## 3-PARAMETER GENERALIZED QUATERNIONS WHOSE COEFFICIENTS ARE CERTAIN GENERALIZED FIBONACCI NUMBERS

*Göksal BİLGİCİ* [1]

1 Prof. Dr., Kastamonu University, Faculty OF Education, Department of Elementary Mathematics Education
E-mail: gbilgici@kastamonu.edu.tr, ORCID: 0000-0001-9964-5578

## 1. INTRODUCTION

Fibonacci and Lucas sequences are both important integer sequences. These sequences satisfy the following recurrence relation

$$X_n = X_{n-1} + X_{n-2} \quad (n > 1)$$

except for initial conditions. Fibonacci and Lucas sequences are shown with $\{F_n\}$ and $\{L_n\}$. The initial conditions of the Fibonacci sequence are $F_0 = 0$ and $F_1 = 1$, while the initial conditions of the Lucas sequence are $L_0 = 2$ and $L_1 = 1$.

There are a lot of generalizations of these two sequences defined by some authors. Generally, three well-known methods have been used to generalize these sequences. The first method is to change the initial conditions only whereas the second method is to change the recurrence relation. The last one is to change or generalize both the initial conditions and the recurrence relation.

Bilgici (2014) defined generalized Fibonacci and Lucas sequences by changing the recurrence relation. This certain generalized Fibonacci and Lucas sequences satisfy the recurrence relations

$$X_r = 2mX_{r-1} + (n - m^2)X_{r-2} \quad (X_0 = 0, X_1 = 1)$$

and

$$Y_r = 2mY_{r-1} + (n - m^2)Y_{r-2} \quad (Y_0 = 2, Y_1 = 2m)$$

respectively. These sequences generalize some well-known sequences. For example, $(m, n) = (1/2, 5/4)$ gives Fibonacci and Lucas numbers while $(m, n) = (1/2, 9/4)$ gives Pell and Pell-Lucas numbers, and $(m, n) = (1, 2)$ gives Jacobsthal and Jacobsthal-Lucas numbers.

Generating functions for the sequences $\{X_r\}$ and $\{Y_r\}$ are

$$\sum_{r=0}^{\infty} X_r q^r = \frac{q}{1 - 2mq - (n - m^2)q^2}$$

and

$$\sum_{r=0}^{\infty} Y_r q^r = \frac{2-2mq}{1-2mq-(n-m^2)q^2}$$

respectively. Binet formulas for the generalized Fibonacci and Lucas numbers are

$$X_n = \frac{\sigma^n - \tau^n}{\sigma - \tau} \text{ and } Y_n = \sigma^n + \tau^n. \tag{1.1}$$

Quaternions were introduced by Sir Hamilton to extend complex numbers. There have been some generalizations of these hyper-complex numbers and one of them was given by Senturk and Unal (2022), 3-parameter generalized quaternions. The set of 3-parameter generalized quaternions is $\mathrm{K} = \{c_0 + c_1 e_1 + c_2 e_2 + c_3 e_3\}$ and the versors $\{e_1, e_2, e_3\}$ satisfy the following multiplication rules where $\lambda_1, \lambda_2, \lambda_3$ are arbitrary real numbers.

| | $e_1$ | $e_2$ | $e_3$ |
|---|---|---|---|
| $e_1$ | $-\lambda_1\lambda_2$ | $\lambda_1 e_3$ | $-\lambda_2 e_2$ |
| $e_2$ | $-\lambda_1 e_3$ | $-\lambda_1\lambda_3$ | $\lambda_3 e_1$ |
| $e_3$ | $\lambda_2 e_2$ | $-\lambda_3 e_1$ | $-\lambda_2\lambda_3$ |

Table 1 Multiplication rules of $\{e_1, e_2, e_3\}$

Let $q_1 = s_0 + e_1 s_1 + e_2 s_2 + e_3 s_3$ and $q_2 = t_0 + e_1 t_1 + e_2 t_2 + e_3 t_3$ be two any 3-parameter generalized quaternions. Product of $q_1$ and $q_2$ is

$$\begin{aligned} q_1 q_2 = {} & s_0 t_0 - s_1 t_1 \lambda_1 \lambda_2 - s_2 t_2 \lambda_1 \lambda_3 - s_3 t_3 \lambda_2 \lambda_3 \\ & + e_1 (s_0 t_1 + s_1 t_0 + s_2 t_3 \lambda_3 - s_3 t_2 \lambda_3) \\ & + e_2 (s_0 t_2 + s_2 t_0 - s_1 t_3 \lambda_2 + s_3 t_1 \lambda_2) \\ & + e_3 (s_0 t_3 + s_3 t_0 + s_1 t_2 \lambda_1 - s_2 t_1 \lambda_1). \end{aligned}$$

Horadam (1963) introduced Fibonacci quaternions. After him, some authors studied Fibonacci quaternions (Iyer, 1969; Swamy, 1973; Halici 2012; Akyigit, Kosal and Tosun, 2013; Nukan and Guven, 2015; Yuce and Aydin, 2016; Polatli, Kizilates and Kesim, 2016Ipek, 2017; Bilgici, Tokeser and Unal, 2017; Aydin, 2018; Kizilates and Kone, 2021; Gul, 2022; Dasdemir and Bilgici, 2021). Bilgici (2022) studied 3-parameter generalized quaternions whose coefficients

are Fibonacci numbers. Some authors studied Pell and Pell-Lucas quaternions (Cimen and Ipek, 2016; Catarino, 2016; Tokeser, Unal and Bilgici, 2017; Bilgici and Catarino, 2021; Aydin, 2022) whereas some studied Jacobsthal and Jacobsthal-Lucas quaternions (Szynal-Liana and Wloch, 2016; Torunbalci-Aydin and Yuce, 2017; Torunbalci-Aydin, 2020; Tokeser and Unal, 2022).

**Definition 1.1.** For any non-negative integer $r$, the $r$th generalized Fibonacci 3-parameter quaternion (GF3PQ) and the $r$th generalized Lucas 3-parameter quaternion (GL3PQ) are

$$\varpi_r = X_r + e_1 X_{r+1} + e_2 X_{r+2} + e_3 X_{r+3}$$

and

$$\rho_r = Y_r + e_1 Y_{r+1} + e_2 Y_{r+2} + e_3 Y_{r+3}$$

respectively.

Recurrence relations for the generalized Fibonacci and Lucas numbers with Definition 1.1 give

$$\varpi_r = 2m\varpi_{r-1} + (n - m^2)\varpi_{r-2} \tag{1.2}$$

and

$$\rho_r = 2m\rho_{r-1} + (n - m^2)\rho_{r-2}. \tag{1.3}$$

## 2. GENERATING FUNCTIONS

A generating function for a sequence is a formal power series that encodes the sequence's terms as the coefficients of its terms. It serves as a powerful tool in combinatorics, algebra, and other areas of mathematics for analyzing and working with sequences.

**Theorem 2.1.** Generating functions for the sequences $\{\varpi_r\}$ and $\{\rho_r\}$ are

$$\sum_{r=0}^{\infty} \varpi_r q^r = \frac{e_1 + 2me_2 + (3m^2 + n)e_3 + q(1 + (n - m^2)e_2 + 2(mn - m^3)e_3)}{1 - 2mq - (n - m^2)q^2} \tag{2.1}$$

and

$$\sum_{r=0}^{\infty} \rho_r q^r = \frac{2\left[\begin{matrix}1 + me_1 + (m^2 + n)e_2 + (m^3 + 3mn)e_3 + q(-m + (-m^2 + n)e_1 \\ +(-m^3 + mn)e_2 + (-m^4 + n^2)e_3\end{matrix}\right]}{1 - 2mq - (n - m^2)q^2} \tag{2.2}$$

respectively.

**Proof.** We define $\varpi(q) = \sum_{r=0}^{\infty} \varpi_r q^r$. Then, we obtain

$$\varpi(q) = \varpi_0 + \varpi_1 q + \sum_{r=2}^{\infty} \varpi_r q^r . \tag{2.3}$$

If we multiply Eq.(1.3) by $-2mq$, we get

$$-2mq\varpi(q) = -2m\varpi_0 q - 2m \sum_{r=2}^{\infty} \varpi_{r-1} q^r . \tag{2.4}$$

If we multiply Eq.(1.3) by $-(n-m^2)q^2$, we hev

$$-(n-m^2)q^2\varpi(q) = -(n-m^2) \sum_{r=2}^{\infty} \varpi_{r-2} q^r . \tag{2.5}$$

Summation Eqs. (2.3), (2.4) and (2.5) gives Eq. (2.1). Similarly, Eq. (2.2) can be proved. ■

## 3. BINET – LIKE FORMULAS

Binet's formula is a closed-form expression for the terms of the Fibonacci sequence. It allows direct computation of the n-th Fibonacci number without needing to compute the preceding terms in the sequence.

**Theorem 3.1.** For any non-negative integer $r$, The $r$th GF3PQ and GL3PQ are, respectively

$$\varpi_r = \frac{\sigma^*\sigma^r - \tau^*\tau^r}{\sigma - \tau} \tag{3.1}$$

and

$$\rho_r = \sigma^*\sigma^r + \tau^*\tau^r \tag{3.2}$$

where $\sigma$ and $\tau$ are as defined above and, $\sigma^* = 1 + e_1\sigma + e_2\sigma^2 + e_3\sigma^3$ and $\tau^* = 1 + e_1\tau + e_2\tau^2 + e_3\tau^3$.

**Proof.** Definition 1.1 and Eq. (1.1) gives

$$\begin{aligned}\varpi_r &= X_r + e_1X_{r+1} + e_2X_{r+2} + e_3X_{r+3} \\ &= \frac{1}{\sigma - \tau}[\sigma^r - \tau^r + e_1(\sigma^{r+1} - \tau^{r+1}) + e_2(\sigma^{r+2} - \tau^{r+2}) \\ &\qquad + e_3(\sigma^{r+3} - \tau^{r+3})]\end{aligned}$$

$$= \frac{1}{\sigma - \tau}[\sigma^r(1 + e_1\sigma + e_2\sigma^2 + e_3\sigma^3) - \tau^r(1 + e_1\tau + e_2\tau^2 + e_3\tau^3)].$$

The last equation gives Eq. (3.1). Eq.(3.2) can be proved similarly. ■

We need the following results for proofs of the next theorems.

**Corollary 3.2.** We have

$$\sigma^*\tau^* = \Psi + 2\sqrt{n}\Omega \tag{3.3}$$

and

$$\tau^*\sigma^* = \Psi - 2\sqrt{n}\Omega \tag{3.4}$$

where

$$\Psi = \rho_0 - 1 + (n - m^2)\lambda_1\lambda_2 - (n - m^2)^4\lambda_1\lambda_3 + (n - m^2)^3\lambda_2\lambda_3$$

and

$$\Omega = (n - m^2)[-(n - m^2)\lambda_3 e_1 - 2m\lambda_2 e_2 + \lambda_1 e_3].$$

It should be noted that

$$\sigma^*\tau^* + \tau^*\sigma^* = 2\Psi \quad \text{and} \quad \sigma^*\tau^* - \tau^*\sigma^* = 4\sqrt{n}\Omega. \tag{3.5}$$

## 4. RESULTS

Bilgici (2014) gave the identities $X_{-r} = (-1)^{r+1}(n - m^2)^{-r}X_r$ and $Y_{-r} = (-1)^r(n - m^2)^{-r}Y_r$. These identities give

$$\varpi_{-r} = (-1)^r(n - m^2)^{-r}[X_r - (n - m^2)X_{r+1}e_1 + (n - m^2)^2X_{r+2}e_2 - (n - m^2)^3X_{r+3}e_3]$$

and

$$\rho_{-r} = (-1)^{r+1}(n - m^2)^{-r}[Y_r - (n - m^2)Y_{r+1}e_1 + (n - m^2)^2Y_{r+2}e_2 - (n - m^2)^3Y_{r+3}e_3].$$

**Theorem 4.1.** [Vajda's identities]

For any integers $r, s$ and $t$, the following equations hold

$$\varpi_{r+s}\varpi_{r+t} - \varpi_r\varpi_{r+s+t} = (m^2 - n)^r X_s[\Psi X_t - \Omega Y_t] \tag{4.1}$$

and

$$\rho_{r+s}\rho_{r+t} - \rho_r\rho_{r+s+t} = -(m^2 - n)^r 4nX_s[\Psi X_t - \Omega Y_t]. \tag{4.2}$$

**Proof.** Binet-like formula (3.1) gives

$$\begin{aligned}
&\varpi_{r+s}\varpi_{r+t} - \varpi_r\varpi_{r+s+t} \\
&= \frac{1}{(\sigma-\tau)^2}[(\sigma^*\sigma^{r+s} - \tau^*\tau^{r+s})(\sigma^*\sigma^{r+t} - \tau^*\tau^{r+t}) \\
&\qquad - (\sigma^*\sigma^r - \tau^*\tau^r)(\sigma^*\sigma^{r+s+t} - \tau^*\tau^{r+s+t})] \\
&= \frac{1}{4n}[\sigma^*\tau^*(-\sigma^{r+s}\tau^{r+t} + \sigma^r\tau^{r+s+t}) + \tau^*\sigma^*(-\sigma^{r+t}\tau^{r+s} + \sigma^{r+s+t}\tau^r)] \\
&= \frac{(\sigma\tau)^r}{4n}[\sigma^*\tau^*(-\sigma^s\tau^t + \tau^{s+t}) + \tau^*\sigma^*(-\sigma^t\tau^s + \sigma^{s+t})] \\
&= \frac{(m^2-n)^r}{4n}[-\sigma^*\tau^*\tau^t(\sigma^s - \tau^s) + \tau^*\sigma^*\sigma^t(\sigma^s - \tau^s)] \\
&= \frac{(m^2-n)^r X_s}{2\sqrt{n}}[-\sigma^*\tau^*\tau^t + \tau^*\sigma^*\sigma^t] \\
&= \frac{(m^2-n)^r X_s}{2\sqrt{n}}\left[-\left(\Psi + 2\sqrt{n}\Omega\right)\tau^t + \left(\Psi - 2\sqrt{n}\Omega\right)\sigma^t\right] \\
&= \frac{(m^2-n)^r X_s}{2\sqrt{n}}\left[\Psi(\sigma^t - \tau^t) - 2\sqrt{n}\Omega(\sigma^t - \tau^t)\right].
\end{aligned}$$

The last equation proves Eq. (4.1). Similarly Binet-like formula (3.2) gives

$$\begin{aligned}
&\rho_{r+s}\rho_{r+t} - \rho_r\rho_{r+s+t} \\
&= (\sigma^*\sigma^{r+s} + \tau^*\tau^{r+s})(\sigma^*\sigma^{r+t} + \tau^*\tau^{r+t}) \\
&\qquad - (\sigma^*\sigma^r + \tau^*\tau^r)(\sigma^*\sigma^{r+s+t} + \tau^*\tau^{r+s+t}) \\
&= \sigma^*\tau^*(\sigma^{r+s}\tau^{r+t} - \sigma^r\tau^{r+s+t}) + \tau^*\sigma^*(\sigma^{r+t}\tau^{r+s} - \sigma^{r+s+t}\tau^r) \\
&= (\sigma\tau)^r[\sigma^*\tau^*(\sigma^s\tau^t - \tau^{s+t}) + \tau^*\sigma^*(\sigma^t\tau^s - \sigma^{s+t})] \\
&= (m^2-n)^r[\sigma^*\tau^*\tau^t(\sigma^s - \tau^s) - \tau^*\sigma^*\sigma^t(\sigma^s - \tau^s)] \\
&= (m^2-n)^r 2\sqrt{n}X_s\left[\tau^t\left(\Psi + 2\sqrt{n}\Omega\right) - \sigma^t\left(\Psi - 2\sqrt{n}\Omega\right)\right] \\
&= -(m^2-n)^r 2\sqrt{n}X_s\left[-\Psi(\sigma^t - \tau^t) + 2\sqrt{n}\Omega(\sigma^t - \tau^t)\right].
\end{aligned}$$

This equation proves Eq. (4.2). ■

The Vajda's identities give Catalan's identities for $s = -t$ which are given in the following.

**Theorem 4.2.** [Catalan's identities]

For any integers $r$ and $s$, the following equations hold

$$\varpi_{r-t}\varpi_{r+t} - \varpi_r^2 = -(m^2-n)^{r-t}[\Psi X_t^2 - \Omega X_{2t}] \tag{4.3}$$

and

$$\rho_{r-t}\rho_{r+t} - \rho_r^2 = 4n(m^2-n)^{r-t}[\Psi X_t^2 - \Omega X_{2t}]. \tag{4.4}$$

The Catalan's identities give Cassini's identities for $t = 1$ which are given in the following.

**Theorem 4.3.** [Cassini's identities]

For any integers $r$, the following equations hold

$$\varpi_{r-1}\varpi_{r+1} - \varpi_r^2 = -(m^2-n)^{r-1}[\Psi - 2m\Omega] \tag{4.5}$$

and

$$\rho_{r-1}\rho_{r+1} - \rho_r^2 = 4n(m^2-n)^{r-1}[\Psi - 2m\Omega]. \tag{4.6}$$

Another important identity is d'Ocagne's identity. This identity is significant in the context of Fibonacci numbers because it provides a mathematical tool to relate Fibonacci numbers and trigonometric functions in a concise way. d'Ocagne's identities for GF3PQ and GL3PQ are in the following theorem.

**Theorem 4.4.** [d'Ocagne's identities]

For any integers $r$ and $s$, the following equations hold

$$\varpi_r\varpi_{s+1} - \varpi_{r+1}\varpi_s = (m^2-n)^s[\Psi X_{r-s} + \Omega Y_{r-s}] \tag{4.7}$$

and

$$\rho_r\rho_{s+1} - \rho_{r+1}\rho_s = -4n(m^2-n)^s[\Psi X_{r-s} + \Omega Y_{r-s}]. \tag{4.8}$$

**Proof.** Binet-like formula (3.1) gives

$$\begin{aligned}
&\varpi_r\varpi_{s+1} - \varpi_{r+1}\varpi_s \\
&= \frac{1}{(\sigma-\tau)^2}[(\sigma^*\sigma^r - \tau^*\tau^r)(\sigma^*\sigma^{s+1} - \tau^*\tau^{s+1}) \\
&\qquad - (\sigma^*\sigma^{r+1} - \tau^*\tau^{r+1})(\sigma^*\sigma^s - \tau^*\tau^s)] \\
&= \frac{1}{4n}[\sigma^*\tau^*(-\sigma^r\tau^{s+1} + \sigma^{r+1}\tau^s) + \tau^*\sigma^*(\sigma^s\tau^{r+1} - \sigma^{s+1}\tau^r)] \\
&= \frac{(\sigma\tau)^s}{4n}[\sigma^*\tau^*(-\sigma^{r-s}\tau + \sigma^{r-s+1}) - \tau^*\sigma^*(-\tau^{r-s+1} + \sigma\tau^{r-s})]
\end{aligned}$$

$$= \frac{(m^2-n)^s}{4n}[\sigma^*\tau^*\sigma^{r-s}(\sigma-\tau) - \tau^*\sigma^*\tau^{r-s}(\sigma-\tau)]$$

$$= \frac{(m^2-n)^s X_1}{2\sqrt{n}}\left[\left(\Psi + 2\sqrt{n}\Omega\right)\sigma^{r-s} - \left(\Psi - 2\sqrt{n}\Omega\right)\tau^{r-s}\right]$$

$$= (m^2-n)^s\left[\Psi\left(\frac{\sigma^{r-s}-\tau^{r-s}}{2\sqrt{n}}\right) + \Omega(\sigma^{r-s}+\tau^{r-s})\right].$$

The last equation proves Eq. (4.7). Eq. (4.8) can be proved similarly. ■

3-parameter generalized quaternions are not commutative. The following theorem explains this situation.

**Theorem 4.5.**

For any integers $r$ and $s$, the following equations hold

$$\varpi_r\varpi_s - \varpi_s\varpi_r = -2\Omega(m^2-n)^s X_{r-s} \tag{4.9}$$

and

$$\rho_r\rho_s - \rho_s\rho_r = -8\Omega n(m^2-n)^s X_{r-s}. \tag{4.10}$$

**Proof.** Binet-like formula (3.1) gives

$$\varpi_r\varpi_s - \varpi_s\varpi_r$$

$$= \frac{1}{(\sigma-\tau)^2}[(\sigma^*\sigma^r - \tau^*\tau^r)(\sigma^*\sigma^s - \tau^*\tau^s) - (\sigma^*\sigma^s - \tau^*\tau^s)(\sigma^*\sigma^r - \tau^*\tau^r)]$$

$$= \frac{1}{4n}[\sigma^r\tau^s(-\sigma^*\tau^* + \tau^*\sigma^*) + \sigma^s\tau^r(\sigma^*\tau^* - \tau^*\sigma^*)]$$

$$= -\frac{\Omega}{\sqrt{n}}[\sigma^r\tau^s - \sigma^s\tau^r]$$

$$= -\frac{\Omega(\sigma\tau)^s}{\sqrt{n}}[\sigma^{r-s} - \tau^{r-s}]$$

$$= -2\Omega(m^2-n)^s\left[\frac{\sigma^{r-s}-\tau^{r-s}}{2\sqrt{n}}\right].$$

The final equations proves Eq. (4.9). Eq. (4.10) can be proved similarly. ■

## REFERENCES

Akyigit, M., Kosal, H. H., & Tosun, M. (2013). Split Fibonacci quaternions. *Advances in Applied Clifford Algebras*, *23*, 535-545.

Akyigit, M., Kosal, H. H., & Tosun, M. (2014). Fibonacci generalized quaternions. *Advances in Applied Clifford Algebras*, *24*, 631-641.

Aydin, F. T. (2018). Bicomplex Fibonacci quaternions. *Chaos, Solitons & Fractals*, *106*, 147-153.

Aydin, F. T. (2022). Dual-hyperbolic Pell quaternions. *Journal of Discrete Mathematical Sciences and Cryptography*, 25(5), 1321-1334.

Bilgici, G. (2014). New generalizations of Fibonacci and Lucas sequences. *Applied Mathematical Sciences*, 8(29), 1429-1437.

Bilgici, G. (2022). Fibonacci 3-Parameter Generalized Quaternions. *European Journal of Science and Technology*, *41*, 357-361.

Bilgici, G., & Catarino, P. (2021). Unrestricted Pell and Pell-Lucas quaternions. *International Journal of Mathematics and Systems Science*, 4(1).

Bilgici, G., Tokeser, U. & Unal, Z. (2017). k-Fibonacci and k-Lucas generalized quaternıons. *Konuralp Journal of Mathematics, 5*(2), 102-113

Catarino, P. (2016). The modified Pell and the modified k-Pell quaternions and octonions. *Advances in Applied Clifford Algebras*, 26, 577-590.

Cimen, C. B., & Ipek, A. (2016). On pell quaternions and Pell-Lucas quaternions. *Advances in Applied Clifford Algebras*, 26, 39-51.

Dasdemir, A., & Bilgici, G. (2021). Unrestricted Fibonacci and Lucas quaternions. *Fundamental Journal of Mathematics and Applications, 4*(1), 1-9.

Falcon, S. (2011). On the k-Lucas numbers. *International Journal of Contemporary Mathematical Sciences, 6*(21), 1039-1050.

Falcon, S., & Plaza, A. (2007). On the Fibonacci k-numbers. *Chaos, Solitons & Fractals, 32*(5), 1615-1624.

Gul, K. (2022). Generalized k-order Fibonacci hybrid quaternions. *Erzincan University Journal of Science and Technology, 15*(2), 670-683.

Halici, S. (2012). On Fibonacci quaternions. *Advances in Applied Clifford Algebras, 22*(2), 321-327.

Horadam, A. F. (1963). Complex Fibonacci numbers and Fibonacci quaternions. *The American Mathematical Monthly, 70*(3), 289-291.

Ipek, A. (2017). On (p, q)-Fibonacci quaternions and their Binet formulas, generating functions and certain binomial sums. *Advances in Applied Clifford Algebras, 27*, 1343-1351.

Kizilates, C., & Kone, T. (2021). On higher order Fibonacci quaternions. *The Journal of Analysis*, 1-12.

Nurkan, S. K., & Guven, I. A. (2015). Dual Fibonacci quaternions. *Advances in Applied Clifford Algebras, 25*, 403-414.

Sentürk, T. D., & Unal, Z. (2022). 3-parameter generalized quaternions. *Computational Methods and Function Theory, 22*(3), 575-608.

Swamy, M. N. S. (1973). On generalized Fibonacci quarternions. *The Fibonacci Quarterly, 11*(5), 547-549.

Szynal-Liana, A., & Wloch, I. (2016). A note on Jacobsthal quaternions. Advances in Applied Clifford Algebras, 26, 441-447.

Tokeser, U., & Unal, Z. (2022). Split dual Jacobsthal and Jacobsthal-Lucas quaternions. Asian Journal of Mathematics and Computer Research, 29(3), 1-9.

Tokeser, U., Unal, Z., & Bilgici, G. (2017). Split Pell and Pell–Lucas Quaternions. *Advances in Applied Clifford Algebras*, 27, 1881-1893.

Torunbalci-Aydin, F.(2020). Dual jacobsthal quaternions. Communications in Advanced Mathematical Sciences, 3(3), 130-142.

Torunbalci-Aydin, F., & Yuce, S. (2017). A new approach to Jacobsthal quaternions. Filomat, 31(18), 5567-5579.

Yuce, S., & Aydin, F. T. (2016). A new aspect of dual Fibonacci quaternions. Advances in Applied Clifford Algebras, 26, 873-884.

# CHAPTER 9

# MARKOV CHAIN METHOD FOR ANALYZING THE RELATIONSHIP BETWEEN UNEMPLOYMENT AND INFLATION IN TÜRKİYE

*Özge ELMASTAŞ GÜLTEKİN*[1]
*Aslı KILIÇ*[2]

1 Assoc.Prof., Ege University, Faculty of Science, Department of Statistics, Izmir, TÜRKİYE. ozge.elmastas@ege.edu.tr, Orcid ID: 0000-0001-7452-3240.
2 Assist.Prof., Ege University, Faculty of Science, Department of Statistics, Izmir, TÜRKİYE. asli.kilic@ege.edu.tr, Orcid ID: 0000-0002-3926-8608.

## INTRODUCTION

The relationship between unemployment and inflation in Türkiye is complex and influenced by multiple factors, such as economic structure, policy decisions, and external shocks. The Phillips Curve may explain short-term dynamics in certain periods, but long-term trends in Türkiye often deviate from traditional theory. Studying the relationship between unemployment and inflation is vital for formulating effective policies, ensuring economic stability, addressing regional inequalities, and promoting sustainable growth. It also offers insights into how external and internal factors shape macroeconomic outcomes, enabling policymakers to better address challenges and improve public welfare.

Analyzing inflation and unemployment with the Markov Chain allows researchers and policymakers to better understand the dynamics of these variables, predict their future trends, and design targeted economic policies that will increase stability and growth. Markov chains analyze systems in which the probability of moving to a future state depends only on the current state. This method is especially useful for studying variables such as the unemployment rate and inflation, which change dynamically over time.

In this study, data on inflation and unemployment rate were taken monthly and cover the period of 01.2014-10.2024. Changes in inflation and unemployment rate compared to the previous month were evaluated together for both variables: decrease (-1), constant (0) and increase (+1). Thus, the state space consists of the states (-1,-1), (-1,0), (-1,+1), (+1,-1), (+1,0) and (+1,+1) in two dimensions. A matrix of transition probabilities between states was created and the equilibrium states to be reached in the long term were obtained by the Markov chain method. According to the values obtained, interpretations were made according to the changes in inflation and unemployment rate.

## 1. LITERATURE REVIEW

In the literature, some of the studies in which the Markov chain and Markov models are applied in the economic field are summarized as follows:

Samuel (2020) proposes a Markov chain model that addresses irregularity and randomness in market fluctuations to predict stock market trends in Nigeria. Although Markov models are often used to predict stock market indices, their application to individual stocks is limited. The research focuses on modeling and predicting the trend of Dangote Cement shares on the Nigerian Stock Exchange using daily closing price data from January 1, 2018 to December 31, 2019 (464 trading days). Based on a probability transition matrix and an initial state vector, the model predicts that in the long term, Dangote Cement shares will show depreciation, stability, and appreciation trends regardless of their current state.

Yenisu (2020) applied the method of Markov chains, a stochastic process approach in which the future state depends only on the present, to financial markets. The analysis focuses on the 10 stocks with the highest trading volume among BIST 100 companies using the daily closing prices between 31.12.2018 and 31.12.2019. Unlike previous studies, this research method applies to leading stocks with relatively low volatility. The findings highlight differences in the long-term expected returns of these stocks.

Buthelezi (2023) examined the impact of inflation on different unemployment situations in South Africa using the Phillips curve framework. Using Markov-switching dynamic regression with data from 2008 to 2022, the study identifies two unemployment states with average unemployment rate of 25.55% and 33.59%, lasting 67 and 7 quarters respectively. The probabilities of staying in the same situation are 98.51% and 86.99%. In Situation 1, a 1% increase in inflation leads to a 2.61% increase in unemployment, while in case 2 it leads to a decrease of 0.06%. The findings show that the Phillips curve rationale is not always valid, highlighting the need for policies to increase employment opportunities and reconsider the trade-offs between inflation and unemployment.

Ersen et al. (2023) applied Markov chains to predict the stock prices of companies in the paper and paper products industry traded on the BIST. Analysis using the closing prices of seven companies for the period 01.06.2022 - 31.05.2023 concluded that six stocks are likely to decline in the long term, while TEZOL stock is expected to increase. Among the

companies, VIKING was found to have the highest expected stock return, while KARTN had the lowest return.

Karaca & Alp (2017) investigated the long-run relationship between gold prices and stock prices using the Markov Chain method. Markov Chains are characterized by the principle that the probability distribution of a future event depends only on the current situation and not on the previous sequence of events. Focusing on the period between 27/07/1995 and 27/07/2015, the analysis predicts the steady-state relationship between gold prices and the closing prices of the BIST 100 Index in the long run using the Markov Chain method.

Saraç & Yıldırım (2016) aimed to evaluate the validity of the relationship between inflation and unemployment in the Turkish economy by using the Markov Exchange Technique. The findings show that unemployment rates affected inflation rates during the recession period in Türkiye between January 2015 and February 2016.

Some of the studies on inflation and unemployment in the literature are summarized as follows.

Uysal & Erdoğan (2004) analyzed the relationship between price levels and unemployment rates in the Turkish economy from 1980 to 2002 using the Phillips Curve framework. After compiling data on the relevant variables, they conducted a regression analysis following a nonlinear inverse model. In the study, they also examined the causality relationships between the variables.

Bozkurt & Gökmenoğlu (2023) examined 2,382 studies from the Web of Science core collection covering the years 1980-2022 and conducted certain analyzes. Common research themes such as "unemployment", "inflation" and "Phillips Curve" have been frequently used. Notably, the most influential studies were published after 2000. The analysis provides a comprehensive overview of the evolution of the literature over time, helping researchers identify gaps and add important insights to the field.

Çolak & Durgun (2023) empirically examined the relationship between unemployment and inflation during Türkiye's inflation targeting period. According to the results of the cointegration test, there was no long-term relationship or causality between unemployment and inflation in the period under consideration.

Kızılkaya (2017) aimed to predict Türkiye's inflation and unemployment rate by using Artificial Neural Networks (ANN) and ARIMA models, which are widely used in forecast modeling. Annual unemployment rate data (1923-2014) and inflation rate data (1969-2014) were analyzed, and estimates for the period 2015-2020 were obtained using Multilayer Perceptron (MLP), a common ANN model, and Box-Jenkins methods for ARIMA processes. The findings showed higher accuracy compared to official estimates.

Balkaya & Bozma (2023) discussed the increase in the minimum wage, which is one of the causes of inflation and unemployment, and examined the relationship between the minimum wage and inflation and unemployment with its theoretical foundations.

Karacan (2018) investigated the relationship between inflation and unemployment in Türkiye and discussed the study in three main sections. The introduction section is a literature review summarizing local and international studies from different periods, and an empirical analysis section. In the empirical analysis conducted using monthly data between 2005-2018, econometric methods such as "Granger Causality Analysis", "Cointegration Test" and "Error Correction Model" were used using the Eviews-9 program. The data were taken from the Turkish Statistical Institute (TurkStat). As a result, a relationship between inflation and unemployment has not been demonstrated, and as a result, unemployment and inflation cannot be considered as directly equivalent.

Konya (2023) examined the relationship between inflation, unemployment and economic growth at the regional level in Türkiye. Using data from 26 NUTS-2 regions between 2005 and 2021, he applied methods that account for cross-sectional dependency and used the Pooled Mean Group (PMG) estimator for coefficient estimation. The analysis revealed a negative and

significant error correction parameter, indicating that deviations of about 42% were corrected in the next period, and the system was oriented towards long-term equilibrium. It shows that inflation and unemployment have negative and meaningful long-term effects on economic growth, reducing growth over time. These findings highlight the critical role of inflation and unemployment in economic growth.

Sarica (2018) investigated the existence and direction of the long-run relationship between labor productivity, unemployment rate and inflation using quarterly data from Turkish industry for the period 2007:1 to 2017:3. He used ARDL (Bounds Test Approach) and Granger Causality Test. Empirical findings revealed a long-term relationship between productivity, unemployment and inflation. The Granger Causality Test shows that there is a strong one-way causality from unemployment to productivity in both the short and long run, while a one-way causality from inflation to productivity is observed only in the short term.

## 2. STOCHASTIC MODEL BASED ON MARKOV CHAIN

### 2.1 Markov Chain

A stochastic process is a collection of random variables which change over time and it is represented by $\{X(t), t \in T\}$. Index or parameter $t$ generally represents time and the set $T$ is the index set of the stochastic process. The random variable $X(t)$ is the state of the process at time $t$. Time can be discrete or continuous. If the set $T$ is a countable set which is $T = \{0, 1, 2, \dots\}$ then it is discrete and the stochastic process having countable index set is called $T$ discrete-time or discrete-parameter stochastic process and represented by $\{X_n, n = 0, 1, 2, \dots\}$. On the other hand, if the set $T$ is an interval of time which is in the form of $T = [0, \infty)$, then the index set $T$ is continuous. The stochastic process with continuous index set is called continuous-time or continuous-parameter stochastic process and represented by $\{X(t), t \geq 0\}$. Similarly, the state space $S$ of a stochastic process may be discrete or continuous and it includes the values $X_n$ or $X(t)$ variables can assume, respectively. For this reason, according to the type of

$T$ parameter space and $S$ state space, a stochastic process may be divided into the following four classes:

- Discrete-time and discrete state space
- Discrete-time and continuous state space
- Continuous-time and discrete state space
- Continuous-time and continuous state space

Suppose that state space $S$ is discrete and the sequence of random variables $X_0, X_1, X_2, \ldots$ take values in this state space. A stochastic process $\{X_n, n = 0, 1, 2, \ldots\}$ is called Markov chain if the following property is hold for every $x_i \in S$:

$$P\{X_n = j | X_{n-1} = i, X_{n-2} = x_{n-2}, \ldots, X_1 = x_1, X_0 = x_0\} = P\{X_n = j | X_{n-1} = i\}$$

This means that given the present state and past states of the system, the future state of the system is independent of the past and only depends on the present state $X_{n-1}$. $P\{X_n = j | X_{n-1} = i\} = p_{ij}$ conditional probability is called one step transition probability from state *i* to state *j*. The $p_{ij}$ is the probability that when the process is in state *i*, it will make a transition to state *j* one step later (Medhi, 1994).

## 2.2 Transition Probability Matrix

Let $\boldsymbol{P}$ the one step transition probability matrix whose *ij*th entry in the matrix is represented by $p_{ij}$, $i, j \in S$ and it is given as follows:

$$\boldsymbol{P} = \begin{bmatrix} p_{11} & p_{12} & p_{13} & \cdots \\ p_{21} & p_{22} & p_{23} & \cdots \\ p_{31} & p_{32} & p_{33} & \cdots \\ \cdots & \cdots & \cdots & \cdots \\ \cdots & \cdots & \cdots & \cdots \end{bmatrix}$$

$\boldsymbol{P}$ is a stochastic square matrix having the following properties:

**i.** $p_{ij} \geq 0$ for all *i, j*.

**ii.** $\sum_j p_{ij} = 1$ for all *i*.

Let ${p_{ij}}^{(n)} = P\{X_n = j | X_0 = i\}$ be the $n$-th step transition probability and it satisfies the following relation for $n > 1$ (Karlin, 1966):

$$ {p_{ij}}^{(n)} = \sum_{k=1}^{n} {p_{ik}}^{(n-1)} p_{kj} $$

### 2.3 Limiting Distribution

The limiting distribution of a Markov chain over the state space $S$ is represented by $\boldsymbol{\pi} = [\pi_1, \pi_2, \dots, \pi_m]$. The limiting distribution or long-run behaviour of a Markov chain means that the system settles down to a state after a sufficiently long period of time passed regardless of the initial state of the chain.

$$ \lim_{n\to\infty} {p_{ij}}^{(n)} = \pi_j $$

In short $\pi_j$ represent the long-run probability that the chain reaches state *j*. The limiting probabilities $\pi_j$ can be determined as follows:

$$ \pi_j = \textstyle\sum_i \pi_i \, p_{ij}, \;\; \forall j \in S \;\; \text{and} \;\; \sum_j \pi_j = 1 $$

In matrix terminology, it can be written as follows:

$$ \boldsymbol{\pi} = \boldsymbol{\pi P} $$

$$ \boldsymbol{\pi}(\boldsymbol{I} - \boldsymbol{P}) = \boldsymbol{0} $$

If a limiting distribution exist, then the distribution is unique. In addition to the computation method given above, it is also possible to determine limiting distribution by taking high matrix powers until obtaining a probability matrix having identical rows. In this situation, each common row is called limiting distribution of the chain (Stewart, 2009).

## 3. MARKOV CHAIN METHOD FOR ANALYZING THE RELATIONSHIP BETWEEN UNEMPLOYMENT AND INFLATION IN TÜRKİYE

In this study, the relationship between inflation and unemployment rate in Türkiye was analyzed with the Markov chain. For this purpose, between 01.2014 and 10.2024, unemployment rate (%) and inflation (CPI) values were handled monthly and the data were taken from the Electronic Data Distribution System (EVDS) of the Central Bank of the Republic of Türkiye.

In order to apply the Markov chain analysis, the changes of inflation and unemployment rate values compared to the previous month were examined. Changes are considered as three states: decrease, remain constant and increase. Accordingly, the two-dimensional states that arise for both variables and their explanations are shown in Table 1.

**Table 1:** Changes in Inflation and Unemployment Rate and Their Explanations

| **States** | **Description of States** |
|---|---|
| -1, -1 | Decrease in inflation; decrease in the unemployment rate |
| -1, 0 | Decrease in inflation; constant unemployment rate |
| -1, +1 | Decrease in inflation; increase in the unemployment rate |
| +1, -1 | Increase in inflation; decrease in the unemployment rate |
| +1, 0 | Increase in inflation; constant unemployment rate |
| +1, +1 | Increase in inflation; increase in the unemployment rate |

First of all, the changes in inflation and unemployment rate compared to the previous month are formed according to the decrease, constant and increase states. Then, according to these changes, the changes in inflation and unemployment rate are considered together according to the decrease, constant and increase states in the same way, and a matrix of transition probabilities is created and shown in Table 2. Here, the rows in the matrix

show the changes in inflation and unemployment that occur at time *t*, and the columns show the changes that occur at time *t+1*.

**Table 2:** Matrix of Transition Probabilities for Changes in Inflation and Unemployment Rate

| t \ t+1 | | Inflation, Unemployment Rate | | | | | |
|---|---|---|---|---|---|---|---|
| | | **-1, -1** | **-1, 0** | **-1, +1** | **+1, -1** | **+1, 0** | **+1, +1** |
| **Inflation, Unemployment Rate** | **-1, -1** | 0 | 0 | 0,3333 | 0,3333 | 0 | 0,3334 |
| | **-1, 0** | 0 | 0 | 0 | 0,5 | 0 | 0,5 |
| | **-1, +1** | 0 | 0 | 0,3333 | 0,3333 | 0 | 0,3334 |
| | **+1, -1** | 0,0392 | 0,0196 | 0 | 0,3725 | 0,1765 | 0,3922 |
| | **+1, 0** | 0 | 0 | 0 | 0,5789 | 0,1053 | 0,3158 |
| | **+1, +1** | 0,02 | 0,02 | 0,02 | 0,34 | 0,16 | 0,44 |

The matrix of transition probabilities given in Table 2 can also be expressed as follows:

$$P = \begin{bmatrix} 0 & 0 & 0{,}3333 & 0{,}3333 & 0 & 0{,}3334 \\ 0 & 0 & 0 & 0{,}5 & 0 & 0{,}5 \\ 0 & 0 & 0{,}3333 & 0{,}3333 & 0 & 0{,}3334 \\ 0{,}0392 & 0{,}0196 & 0 & 0{,}3725 & 0{,}1765 & 0{,}3922 \\ 0 & 0 & 0 & 0{,}5789 & 0{,}1053 & 0{,}3158 \\ 0{,}02 & 0{,}02 & 0{,}02 & 0{,}34 & 0{,}16 & 0{,}44 \end{bmatrix}$$

According to the changes in inflation and unemployment rate, the initial probabilities for the 6 different states given in Table 1 are as follows:

**Table 3:** Initial Probabilities

| **Inflation change, unemployment rate change** | | | | | |
|---|---|---|---|---|---|
| **-1, -1** | **-1, 0** | **-1, +1** | **+1, -1** | **+1, 0** | **+1, +1** |
| 0,0235 | 0,0156 | 0,0235 | 0,3984 | 0,1484 | 0,3906 |

Using the initial probabilities given in Table 3, the stationary probabilities of inflation and unemployment rate are calculated by months and are given in the table below:

**Table 4:** Stationary State Analysis Results

| | **Inflation change, unemployment rate change** | | | | | |
|---|---|---|---|---|---|---|
| | **-1, -1** | **-1, 0** | **-1, +1** | **+1, -1** | **+1, 0** | **+1, +1** |
| **11,2024** | 0,023429 | 0,015621 | 0,023477 | 0,390582 | 0,14844 | 0,398451 |
| **12,2024** | 0,02328 | 0,015624 | 0,023603 | 0,390341 | 0,148321 | 0,398831 |
| **01,2025** | 0,023278 | 0,015627 | 0,023603 | 0,390306 | 0,148326 | 0,39886 |
| **02,2025** | 0,023277 | 0,015627 | 0,023603 | 0,390306 | 0,148325 | 0,398861 |
| **03.2025*** | 0,023277 | 0,015627 | 0,023602 | 0,390306 | 0,148326 | 0,398862 |
| **04,2025** | 0,023277 | 0,015627 | 0,023602 | 0,390306 | 0,148326 | 0,398862 |
| **05,2025** | 0,023277 | 0,015627 | 0,023602 | 0,390306 | 0,148326 | 0,398862 |

*: Month of stationary

According to Table 4, according to the stationary state analysis regarding the changes in inflation and unemployment rate in the coming months, stationary is achieved at the end of the next 5th month. Accordingly, with a probability of 39.89%, both an increase in inflation and an increase in the unemployment rate will be the highest.

Without considering the initial time when the process goes to a stationary state, long-run equilibrium state probabilities can also be obtained by equations to be created according to the transition probability matrix.

$$[\pi_{-1,-1} \quad \pi_{-1,0} \quad \pi_{-1,+1} \quad \pi_{+1,-1} \quad \pi_{+1,0} \quad \pi_{+1,+1}] =$$
$$= [\pi_{-1,-1} \quad \pi_{-1,0} \quad \pi_{-1,+1} \quad \pi_{+1,-1} \quad \pi_{+1,0} \quad \pi_{+1,+1}] \times$$
$$\times \begin{bmatrix} 0 & 0 & 0{,}3333 & 0{,}3333 & 0 & 0{,}3334 \\ 0 & 0 & 0 & 0{,}5 & 0 & 0{,}5 \\ 0 & 0 & 0{,}3333 & 0{,}3333 & 0 & 0{,}3334 \\ 0{,}0392 & 0{,}0196 & 0 & 0{,}3725 & 0{,}1765 & 0{,}3922 \\ 0 & 0 & 0 & 0{,}5789 & 0{,}1053 & 0{,}3158 \\ 0{,}02 & 0{,}02 & 0{,}02 & 0{,}34 & 0{,}16 & 0{,}44 \end{bmatrix}$$

After the procedures, the limiting probabilities were obtained in a similar way as in Table 4 and shown in Table 5.

**Table 5:** Limiting Probabilities

| | **States** | **Limiting Probabilities** |
|---|---|---|
| **Inflation, Unemployment Rate** | -1, -1 | 0,023277 |
| | -1, 0 | 0,015627 |
| | -1, +1 | 0,023602 |
| | +1, -1 | 0,390306 |
| | +1, 0 | 0,148326 |
| | +1, +1 | 0,398862 |

When the limiting probabilities are analyzed, it is concluded that at the end of the long run, both inflation and unemployment rate will decrease in 2.33% of the cases; inflation will decrease and unemployment rate will remain constant in 1.56% of the cases; inflation will decrease and unemployment rate will increase in 2.36% of the cases; inflation will increase and unemployment rate will decrease in 39.03% of the cases; inflation will increase and unemployment rate will remain constant in 14.83% of the cases; and inflation will increase and unemployment rate will increase in 39.89% of the cases.

In addition, when the results are considered in terms of states where inflation decreases, the unemployment rate decreases in 37.2% (0.023277/0.062506), the unemployment rate remains constant in 25%

(0.015627/0.062506) and the unemployment rate decreases in 37.8% (0.023602/0.062506).

Similarly, when the results are considered in terms of states where inflation increases, unemployment decreases in 41.6% (0.390306/0.937494), unemployment remains constant in 15.8% (0.148326/0.937494) and unemployment increases in 42.6% (0.398862/0.937494).

## 4. CONCLUSION

In the economic literature, the issue of inflation and unemployment has become very popular since the 1960s. In addition, the fight against inflation and unemployment has long been an important issue among economic problems and is of interest to both politicians and economists. These issues not only affect individual well-being, but also have political significance. Low inflation and unemployment rate are expected to have a positive effect on individual happiness, as well as positive political consequences.

The aim of this study is to analyze the relationship between inflation and unemployment rate and their changes compared to the previous month over a long period with the Markov chain method. The changes in inflation and unemployment rate, which are handled monthly between the periods of 01.2014-10.2024, are expressed in 3 states as decrease, constant and increase when considered separately for each variable. On the other hand, when the co-change of both variables is considered, 6 states emerge.

Long-run equilibrium state probabilities for the transition probability matrices obtained for the co-change of inflation and unemployment rate were obtained. Accordingly, when the inflation and unemployment rate move in the same or opposite direction, 41.4% of them moved in the opposite direction, while 42.2% of them moved in the same direction. At 16.4%, inflation increased or decreased, while the unemployment rate remained constant.

## REFERENCES

Agbam, A. S., & Udo, E. O. (2020). Application of Markov chain (MC) model to the stochastic forecasting of stocks prices in Nigeria: The case study of Dangote Cement. *International journal of applied science and Mathematical theory*, *6*(1), 14-33.

Balkaya, E., & Bozma, K. (2023). Enflasyon ve İşsizlik Çıkmazında Asgari Ücret Üzerine Bir Değerlendirme. *Türkiye Ekonomisinin Dört Çıkmazı*, Detay Yayıncılık, Ankara, 49-69.

Bozkurt, A. A., & Gökmenoğlu, M. (2023). Enflasyon ve İşsizlik Arasındaki İlişkiyi Konu Alan Çalışmaların Bibliyometrik Ağ Analizi. *Anadolu Üniversitesi İktisadi ve İdari Bilimler Fakültesi Dergisi*, *24*(2), 78-110.

Buthelezi, E. M. (2023). Impact of Inflation in Different States of Unemployment: Evidence with the Phillips Curve in South Africa from 2008 to 2022. *Economies*, *11*(1), 29.

Çolak, H. M., & Durgun, A. (2023). Türkiye'de Enflasyon Hedeflemesi Döneminde Enflasyon ve İşsizlik İlişkisi. *Ekonomi Bilimleri Dergisi*, *15*(2), 125-139.

Ersen, N., Akyüz, İ., & Akyüz, K. C. (2023). Markov Chain Model for Predicting the Stock Price of Paper and Paper Products Industry. *Turkish Journal of Forest Science*, *7*(2), 178-188.

Karaca, M. E., & Alp, S. (2017). Markov Zincirleri Yöntemi Kullanılarak Altın Fiyatları ile BIST 100 Endeksi Arasındaki İlişkinin Analizi. *Sosyal ve Beşerî Bilimler Araştırmaları Dergisi*, *18*(40), 1-12.

Karacan, R. (2018). Phillips Eğrisi Yaklaşımı ile Türkiye'de Enflasyon ve İşsizlik Arasındaki Nedensellik İlişkisi. *Social Mentality and Researcher Thinkers Journal*, *4*(10), 242-249.

Karlin, S. (1966) A First Course in Stochastic Processes, Academic Press, 498pp.

Kızılkaya, O. (2017). Türkiye'nin Enflasyon ve İşsizlik Oranının Yapay Sinir Ağları ve Box-Jenkins Yöntemiyle Tahmini. *Social Sciences Studies Journal*, *3*(12), 2197-2207.

Konya, S. (2023). Enflasyon, İşsizlik ve Ekonomik Büyüme: Türkiye İçin Bölgesel Bir Araştırma. *Nişantaşı Üniversitesi Sosyal Bilimler Dergisi*, *11*(Özel Sayı), 87-111.

Medhi, J. (1994). Stochastic processes. J. Wiley, Hindistan, 598pp.

Saraç, T. B., & Yıldırım, A. E. (2016). Enflasyon ile İşsizlik Arasındaki İlişki: Türkiye Örneği. *Turan: Stratejik Araştırmalar Merkezi*, *8*(32), 363.

Sarıca, S. (2018). İşgücü Verimliliği Üzerine Enflasyon ve İşsizlik Oranının Etkisi: Türkiye Ekonomisi Üzerine Bir Ampirik Analiz. *The Journal of Academic Social Sciences*, *72*(72), 276-292.

Stewart, W. J. (2009). Probability, Markov Chains, Queues, and Simulation: The Mathematical Basis of Performance Modeling. Birleşik Krallık: Princeton University Press, 758 pp.

Uysal, D., & Erdoğan, S. (2004). Enflasyon ile İşsizlik Oranı Arasındaki İlişki ve Türkiye Örneği (1980-2002). *Sosyal Ekonomik Araştırmalar Dergisi*, *3*(6), 35-47.

YenīSu, E. (2020). Hisse Senedi Fiyatlarının Markov Zincirleri ile Analizi: BIST 100 Şirketleri Üzerine Bir Uygulama. *Giresun Üniversitesi İktisadi ve İdari Bilimler Dergisi*, *6*(2), 261-277.

# CHAPTER 10

# THE INVOLUTE CURVES OF TIMELIKE SALKOWSKI CURVES IN MINKOWSKI 3-SPACE

*Sümeyye GÜR MAZLUM*[1]
*Mehmet BEKTAŞ*[2]

1 Gümüşhane University, Kelkit Aydın Doğan Vocational School, Department of Computer Technology, Gümüşhane, Türkiye,
E-mail: sumeyyegur@gumushane.edu.tr, ORCID: https://orcid.org/0000-0003-2471-1627
2 Fırat University, Faculty of Science, Department of Mathematics, Elazığ, Türkiye
E-mail: mbektas@firat.edu.tr, ORCID: https://orcid.org/0000-0002-5797-4944

## 1. Introduction

Differential geometry is an important discipline that forms the basis for many areas of physics, engineering and mathematics by examining the geometric properties of surfaces and curves. In particular, Minkowski space, as the geometric framework of the theory of special relativity, has a four-dimensional structure in which temporal and spatial dimensions are considered together. In this context, curves defined in Minkowski space provide a useful tool for modelling concepts such as motion, energy and momentum in the physical world. In addition, curves and surfaces have been studied by many authors in Minkowski space (Akutagava and Nishikawa, 1990; Altın and Kazan, 2024; Beem, Paul and Kevin, 2017; Birman and Nomizu, 1984; Kazan and Altın, 2018; Lopez, 2014; O'Neill, 1983; Ratcliffe, 1994; Uğurlu, 1997; Uğurlu and Çalışkan, 2012; Woestijne, 1990). In Minkowski 3-space, curves are divided into three causal characters: timelike, spacelike and lightlike. Some studies on timelike and spacelike curves are (Aksan and Gür Mazlum, 2023; Bilici and Çalışkan, 2011; Bilici and Çalışkan, 2019; Bükcü and Karacan, 2007; Gür Mazlum, 2024).

Salkowski curves, introduced by E. Salkowski in 1909, are a class of special curves with variable torsion and constant curvature (Salkowski, 1909). Some differential properties of these curves were put forward by (Monterde, 2009). These curves have been studied in many theoretical and applied problems and have been enriched with various generalizations in different spaces. In Minkowski 3-space, the timelike properties of such curves have a special importance in terms of modelling timelike motions. The expression of the timelike Salkowski curves in Minkowski space was presented by (Ali, 2009). Geodesic curvatures and Frenet vectors of timelike Salkowski curves have also been studied (Şenyurt, Gür and Ozyılmaz, 2015).

In mathematics, an involute is a new class of curves derived from the another curve and generally deepens the physical interpretation of motion or curvature. The involute of a curve is the geometric shape obtained by stretching a string from a point on that curve. The involute traces the path of points that are always perpendicular to the curve when the rope is wrapped or unwound around the curve. This corresponds to the perpendicularity of the tangent vectors to the two curves along the curve. For example, the involute of a circle would be the path followed by a string stretched around the circle and its end point. Some studies on the involute of a curve in three dimensional

Minkowski space are (Abdel-Aziz, Saad and Abdel-Salam, 2019; Bilici and Çalışkan, 2011; Bilici and Çalışkan, 2019; Gür Mazlum, 2024). The study of involute curves of timelike Salkowski curves both contributes to the theory of differential geometry and expands the physical interpretations of these curves. In this study, involute curves of timelike Salkowski curves defined in Minkowski 3-space are examined in detail, and the geometric properties and differential relations of such curves are examined.

## 2. Preliminaries

Let $\vec{\mathbb{R}}=(\mathfrak{r}_1,\ \mathfrak{r}_2,\ \mathfrak{r}_3)$ and $\vec{\mathbb{Q}}=(\mathfrak{q}_1,\ \mathfrak{q}_2,\ \mathfrak{q}_3)\in\mathbb{E}_1^3$ be two vectors. For these vectors, the Lorentzian inner product function and Lorentzian vector product function are defined as follows:

$$\langle,\rangle_{\mathbb{L}}:\mathbb{E}_1^3\times\mathbb{E}_1^3\to\mathbb{E}_1^3,\qquad \left\langle\vec{\mathbb{R}},\vec{\mathbb{Q}}\right\rangle_{\mathbb{L}}=\mathfrak{r}_1\mathfrak{q}_1+\mathfrak{r}_2\mathfrak{q}_2-\mathfrak{r}_3\mathfrak{q}_3 \tag{1}$$

and

$$\wedge_{\mathbb{L}}:\mathbb{E}_1^3\times\mathbb{E}_1^3\to\mathbb{E}_1^3,\quad \vec{\mathbb{R}}\wedge_{\mathbb{L}}\vec{\mathbb{Q}}=(\mathfrak{r}_3\mathfrak{q}_2-\mathfrak{r}_2\mathfrak{q}_3,\mathfrak{r}_1\mathfrak{q}_3-\mathfrak{r}_3\mathfrak{q}_1,\mathfrak{r}_1\mathfrak{q}_2-\mathfrak{r}_2\mathfrak{q}_1).$$

Here, the space $\mathbb{E}_1^3$ is called the Minkowski 3-space. In Minkowski 3-space, the causal character of any vector $\vec{\mathbb{R}}=(\mathfrak{r}_1,\mathfrak{r}_2,\mathfrak{r}_3)$, if $\left\langle\vec{\mathbb{R}},\vec{\mathbb{R}}\right\rangle_{\mathbb{L}}>0$ or $\vec{\mathbb{R}}=\vec{0}$, then $\vec{\mathbb{R}}$ is spacelike, if $\left\langle\vec{\mathbb{R}},\vec{\mathbb{R}}\right\rangle_{\mathbb{L}}<0$, then $\vec{\mathbb{R}}$ is timelike, or if $\left\langle\vec{\mathbb{R}},\vec{\mathbb{R}}\right\rangle_{\mathbb{L}}=0$ and $\vec{\mathbb{R}}\neq\vec{0}$, then $\vec{\mathbb{R}}$ is null (or lightlike). The Lorentzian norm of $\vec{\mathbb{R}}$ is $\left\|\vec{\mathbb{R}}\right\|_{\mathbb{L}}=\sqrt{\left|\left\langle\vec{\mathbb{R}},\vec{\mathbb{R}}\right\rangle_{\mathbb{L}}\right|}$ and if $\left\|\vec{\mathbb{R}}\right\|_{\mathbb{L}}=1$, $\vec{\mathbb{R}}$ is a unit vector. For $\vec{\mathbb{R}},\ \vec{\mathbb{Q}}\in\mathbb{E}_1^3$, if $\left\langle\vec{\mathbb{R}},\vec{\mathbb{Q}}\right\rangle_{\mathbb{L}}=0$, $\vec{\mathbb{R}}$ and $\vec{\mathbb{Q}}$ are Lorentzian orthogonal vectors. Let $\vec{\mathbb{R}}$ and $\vec{\mathbb{Q}}$ be nonzero Lorentzian orthogonal vectors in $\mathbb{E}_1^3$, in this case if $\vec{\mathbb{R}}$ is timelike, then $\vec{\mathbb{Q}}$ is spacelike, (Ratcliffe, 1994). An differentiable curve $\left(\vec{\mathbb{J}}\right)$ in $\mathbb{E}_1^3$ is called the spacelike, timelike or lightlike curve, if the tangent vector at every point $\vec{\mathbb{J}}(t)$ of the curve is spacelike, timelike or lightlike, respectively. Let $\left\{\vec{\mathbb{T}},\vec{\mathbb{N}},\vec{\mathbb{B}}\right\}$ be Frenet frame, $\mathbb{K}$ and $\mathbb{P}$ be the curvature and torsion $\left(\vec{\mathbb{J}}\right)$.

Based on the causal character of $\left(\vec{\mathbb{J}}\right)$, these elements are described by the following equations: (Uğurlu and Çalışkan, 2012):

- if $\left(\vec{\mathbb{J}}\right)$ is a timelike curve, $\vec{\mathbb{T}}$ is timelike, $\vec{\mathbb{N}}$ and $\vec{\mathbb{B}}$ are spacelike vectors, then

$$\vec{\mathbb{T}}=\frac{\vec{\mathbb{J}}'}{\left\|\vec{\mathbb{J}}'\right\|_{\mathbb{L}}},\quad \vec{\mathbb{N}}=-\vec{\mathbb{B}}\wedge_{\mathbb{L}}\vec{\mathbb{T}},\quad \vec{\mathbb{B}}=-\frac{\vec{\mathbb{J}}'\wedge_{\mathbb{L}}\vec{\mathbb{J}}''}{\left\|\vec{\mathbb{J}}'\wedge_{\mathbb{L}}\vec{\mathbb{J}}''\right\|_{\mathbb{L}}}, \tag{2}$$

$$\vec{\mathbb{T}}\wedge_{\mathbb{L}}\vec{\mathbb{N}}=-\vec{\mathbb{B}},\qquad \vec{\mathbb{N}}\wedge_{\mathbb{L}}\vec{\mathbb{B}}=\vec{\mathbb{T}},\qquad \vec{\mathbb{B}}\wedge_{\mathbb{L}}\vec{\mathbb{T}}=-\vec{\mathbb{N}}$$

and

$$\overrightarrow{\mathbb{T}'}=\left\|\vec{\mathbb{J}}'\right\|_{\mathbb{L}}\mathbb{K}\vec{\mathbb{N}},\quad \overrightarrow{\mathbb{N}'}=\left\|\vec{\mathbb{J}}'\right\|_{\mathbb{L}}\left(\mathbb{K}\vec{\mathbb{T}}-\mathbb{P}\vec{\mathbb{B}}\right),\quad \overrightarrow{\mathbb{B}'}=\left\|\vec{\mathbb{J}}'\right\|_{\mathbb{L}}\mathbb{P}\vec{\mathbb{N}}, \tag{3}$$

- if $\left(\vec{\mathbb{J}}\right)$ is a spacelike curve, $\vec{\mathbb{T}}$ and $\vec{\mathbb{N}}$ are spacelike, $\vec{\mathbb{B}}$ is timelike vectors, then

$$\vec{\mathbb{T}}=\frac{\vec{\mathbb{J}}'}{\left\|\vec{\mathbb{J}}'\right\|_{\mathbb{L}}},\quad \vec{\mathbb{N}}=-\vec{\mathbb{B}}\wedge_{\mathbb{L}}\vec{\mathbb{T}},\quad \vec{\mathbb{B}}=\frac{\vec{\mathbb{J}}'\wedge_{\mathbb{L}}\vec{\mathbb{J}}'}{\left\|\vec{\mathbb{J}}'\wedge_{\mathbb{L}}\vec{\mathbb{J}}'\right\|_{\mathbb{L}}}, \tag{4}$$

$$\vec{\mathbb{T}}\wedge_{\mathbb{L}}\vec{\mathbb{N}}=\vec{\mathbb{B}},\qquad \vec{\mathbb{N}}\wedge_{\mathbb{L}}\vec{\mathbb{B}}=-\vec{\mathbb{T}},\qquad \vec{\mathbb{B}}\wedge_{\mathbb{L}}\vec{\mathbb{T}}=-\vec{\mathbb{N}}$$

and

$$\overrightarrow{\mathbb{V}_1'}=\left\|\vec{\mathbb{J}}'\right\|_{\mathbb{L}}\mathbb{K}\vec{\mathbb{N}},\quad \overrightarrow{\mathbb{N}'}=\left\|\vec{\mathbb{J}}'\right\|_{\mathbb{L}}\left(-\mathbb{K}\vec{\mathbb{T}}+\mathbb{P}\vec{\mathbb{B}}\right),\quad \overrightarrow{\mathbb{B}'}=\left\|\vec{\mathbb{J}}'\right\|_{\mathbb{L}}\mathbb{P}\vec{\mathbb{N}}. \tag{5}$$

For two cases, the curvature and torsion of $\left(\vec{\mathbb{J}}\right)$ are

$$\mathbb{K}=\frac{\left\|\vec{\mathbb{J}}'\wedge_{\mathbb{L}}\vec{\mathbb{J}}''\right\|_{\mathbb{L}}}{\left\|\vec{\mathbb{J}}'\right\|_{\mathbb{L}}^{3}},\quad \mathbb{P}=\frac{\left\langle\vec{\mathbb{J}}'\wedge_{\mathbb{L}}\vec{\mathbb{J}}'',\vec{\mathbb{J}}'''\right\rangle_{\mathbb{L}}}{\left\|\vec{\mathbb{J}}'\wedge_{\mathbb{L}}\vec{\mathbb{J}}''\right\|_{\mathbb{L}}^{2}}. \tag{6}$$

Also, the Darboux vector $\vec{\mathbb{D}}$ and pole vector $\vec{\mathbb{C}}$ are as follows:

- if $\left(\vec{\mathbb{J}}\right)$ is a timelike curve, then

$$\vec{\mathbb{D}}=\left\|\vec{\mathbb{J}}'\right\|_{\mathbb{L}}\left(\mathbb{P}\vec{\mathbb{T}}-\mathbb{K}\vec{\mathbb{B}}\right) \tag{7}$$

and in this case,

if $\vec{\mathbb{D}}$ is spacelike, then

$$\vec{\mathbb{C}} = \sinh(\Omega)\vec{\mathbb{T}} - \cosh(\Omega)\vec{\mathbb{B}}$$

or if $\vec{\mathbb{D}}$ is timelike, then

$$\vec{\mathbb{C}} = \cosh(\Omega)\vec{\mathbb{T}} - \sinh(\Omega)\vec{\mathbb{B}}, \tag{8}$$

 if $\vec{\mathbb{J}}(t)$ is a spacelike curve with timelike binormal, then

$$\vec{\mathbb{D}} = \left\|\vec{\mathbb{J}}'\right\|_{\mathbb{L}} \left(\mathbb{P}\vec{\mathbb{T}} - \mathbb{K}\vec{\mathbb{B}}\right) \tag{9}$$

and in this case,

- if $\vec{\mathbb{D}}$ is spacelike, then

$$\vec{\mathbb{C}} = \cosh(\Omega)\vec{\mathbb{T}} - \sinh(\Omega)\vec{\mathbb{B}}, \tag{10}$$

- or if $\vec{\mathbb{D}}$ is timelike, then

$$\vec{\mathbb{C}} = \sinh(\Omega)\vec{\mathbb{T}} - \cosh(\Omega)\vec{\mathbb{B}},$$

where, for two cases, $\Omega$ is the Lorentzian timelike angle between the vectors $\vec{\mathbb{B}}$ and $\vec{\mathbb{D}}$.

The Lorentzian timelike angle between the vectors $\vec{\mathbb{B}}$ (spacelike) and $\vec{\mathbb{D}}$ (timelike) a timelike curve or the vectors $\vec{\mathbb{B}}$ (timelike) and $\vec{\mathbb{D}}$ (spacelike) a spacelike curve is as Figure 1. And so,

$$\begin{cases} \cosh(\Omega) = \dfrac{\left\|\vec{\mathbb{J}}'\right\|_{\mathbb{L}}\ \mathbb{P}}{\left\|\vec{\mathbb{D}}\right\|}, \\ \sinh(\Omega) = \dfrac{\left\|\vec{\mathbb{J}}'\right\|_{\mathbb{L}}\ \mathbb{K}}{\left\|\vec{\mathbb{D}}\right\|}. \end{cases} \tag{11}$$

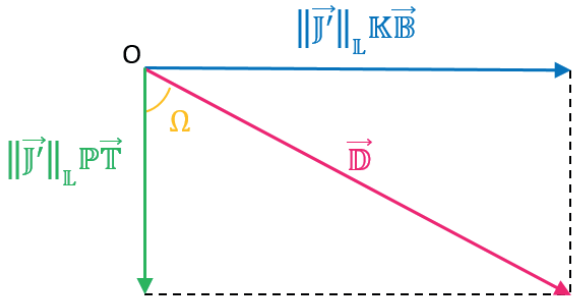


**Figure 1.** Timelike Darboux vector of a timelike curve

**Definition 2.1.** For any $m>1\in\mathbb{R}$ and $n=\dfrac{m}{\sqrt{m^2-1}}$, timelike Salkowski curves in $\mathbb{E}_1^3$ are given by

$$\vec{\mathbb{J}}(t)=\frac{n}{4m}\left(\frac{1}{m}\cosh(2nt),\ \frac{n-1}{1+2n}\sinh((1+2n)t)-\frac{n+1}{1-2n}\sinh((1-2n)t)+2\sinh(t),\right.$$
$$\left.\frac{n-1}{1+2n}\cosh((1+2n)t)-\frac{n+1}{1-2n}\cosh((1-2n)t)+2\cosh(t)\right), \tag{12}$$

(Ali, 2009), Figure 2. Here, according to the Lorentzian inner product in (1), the timelike Salkowski curves's parametric equation is obtained again as in (12). For this curve,

$$\mathfrak{y}(t)=\left\|\frac{\vec{\mathbb{J}}(t)}{dt}\right\|_{\mathbb{L}}=\left\|\vec{\mathbb{J}}'(t)\right\|_{\mathbb{L}}=\frac{n}{m}\left|\sinh(nt)\right|. \tag{13}$$

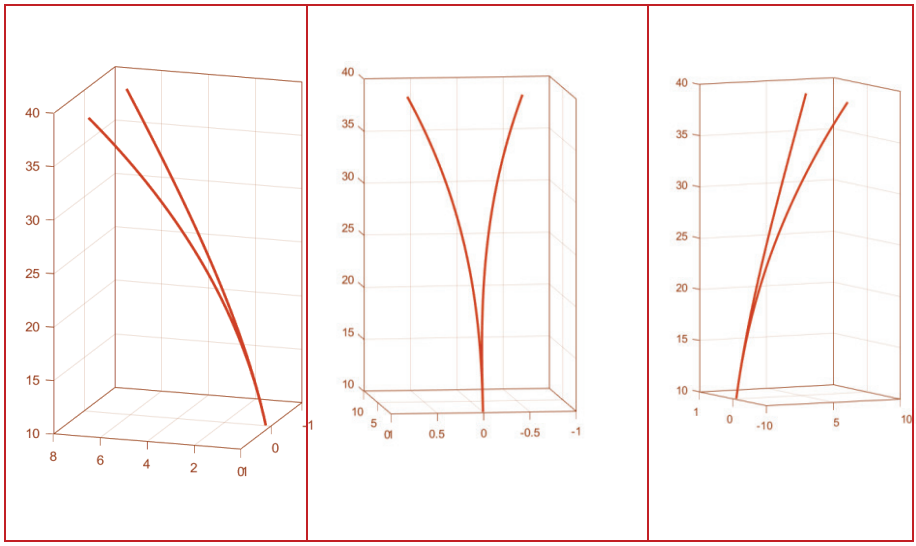

**Figure 2.** Timelike Salkowski curve in $\mathbb{E}_1^3$ for $m=10$.

Thus, using (2) and (6), the curvature $\mathbb{K}(t)$, torsion $\mathbb{P}(t)$ and Frenet frame $\left\{\vec{\mathbb{T}}(t),\vec{\mathbb{N}}(t),\vec{\mathbb{B}}(t)\right\}$ for (12) are obtained as follows:

$$\begin{cases}\mathbb{K}(t)=1,\\ \mathbb{P}(t)=-\coth(nt)\end{cases} \tag{14}$$

and

$$\begin{cases}\vec{\mathbb{T}}(t)=\left(\dfrac{n}{m}\cosh(nt),\mathbb{A}(t),\mathbb{C}(t)\right) & \text{timelike},\\ \vec{\mathbb{N}}(t)=\left(n,\dfrac{n}{m}\sinh(t),\dfrac{n}{m}\cosh(t)\right) & \text{spacelike},\\ \vec{\mathbb{B}}(t)=-\left(\dfrac{n}{m}\sinh(nt),\mathbb{D}(t),\mathbb{E}(t)\right) & \text{spacelike},\end{cases} \tag{15}$$

where

$$\begin{cases} \mathbb{A}(t) = n\sinh(t)\cosh(nt) - \cosh(t)\sinh(nt), \\ \mathbb{C}(t) = n\cosh(t)\cosh(nt) - \sinh(t)\sinh(nt), \\ \mathbb{D}(t) = n\sinh(t)\sinh(nt) - \cosh(t)\cosh(nt), \\ \mathbb{E}(t) = n\cosh(t)\sinh(nt) - \sinh(t)\cosh(nt). \end{cases}$$

Besides, considering (7), the Darboux and pole vectors for (12) is obtained as

$$\vec{\mathbb{D}}(t) = -\frac{n^2}{m}\left(\frac{1}{m}, \sinh(t), \cosh(t)\right) \qquad \text{timelike} \qquad (16)$$

and

$$\vec{\mathbb{C}}(t) = \frac{\vec{\mathbb{D}}(t)}{\left\|\vec{\mathbb{D}}(t)\right\|} = -n\left(\frac{1}{m}, \sinh(t), \cosh(t)\right) \qquad \text{timelike}. \qquad (17)$$

Here, addition, since $\left\langle \vec{\mathbb{D}}(t), \vec{\mathbb{D}}(t) \right\rangle = -\frac{n^2}{m^2} < 0$ and $\left\langle \vec{\mathbb{C}}(t), \vec{\mathbb{C}}(t) \right\rangle = -1$, $\vec{\mathbb{D}}(t)$ and $\vec{\mathbb{C}}(t)$ are timelike vectors.

If (13), (14) and (16) are substituted in (11), then

$$\begin{cases} \cosh\left(\Omega(t)\right) = \cosh(nt), \\ \sinh\left(\Omega(t)\right) = \sinh(nt) \end{cases} \qquad (18)$$

are obtained. Thus,

$$\Omega(t) = nt$$

is gotten. On the other hand, if (15) and (18) is substituted in (8), then (17) is obtained again.

## 3. The Involute Curves of Timelike Salkowski Curves in Minkowski 3-Space

In this section, we will see that involute curves of timelike Salkowski curves in Minkowski 3-space are spacelike curves with timelike binormal. We will also obtain the Frenet vectors, curvatures and torsions of these curves. Furthermore, we will examine the Darboux and pole vectors of these curves.

**Theorem 3.1.** The involutes of timelike Salkowski curves in $\mathbb{E}_1^3$ are obtained as

$$\begin{aligned}\overrightarrow{\mathbb{J}_{inv}}(t)=&\left(\frac{n}{4m^2}\cosh(2nt)-\frac{n}{m}\left(\frac{1}{m}\cosh(nt)+\mathfrak{c}\right)\cosh(nt),\right.\\&\frac{n}{4m}\left(\frac{n-1}{1+2n}\sinh\left((1+2n)t\right)-\frac{n+1}{1-2n}\sinh\left((1-2n)t\right)+2\sinh(t)\right)\\&-\left(\frac{1}{m}\cosh(nt)+\mathfrak{c}\right)\mathbb{A}(t),\\&\left.\frac{n}{4m}\left(\frac{n-1}{1+2n}\cosh\left((1+2n)t\right)-\frac{n+1}{1-2n}\cosh\left((1-2n)t\right)+2\cosh(t)\right)\right.\\&\left.-\left(\frac{1}{m}\cosh(nt)+\mathfrak{c}\right)\mathbb{C}(t)\right),\end{aligned}\tag{19}$$

where $\mathfrak{c}\in\mathbb{R}$, Figure 3.

**Proof.** The parametric equation of involute curves of $\left(\vec{\mathbb{J}}\right)$ is written with

$$\overrightarrow{\mathbb{J}_{inv}}(t)=\vec{\mathbb{J}}(t)-\left(\int\mathfrak{y}(t)\,dt\right)\vec{\mathbb{T}}(t),\tag{20}$$

(Gür Mazlum, 2024). If (12), (13) and (15) are substituted in (20), (19) is obtained.

**Corollary 3.2.** The Lorentzian distance between the points $\overrightarrow{\mathbb{J}_{inv}}(t)$ of $\left(\overrightarrow{\mathbb{J}_{inv}}\right)$ and $\vec{\mathbb{J}}(t)$ of $\left(\vec{\mathbb{J}}\right)$ is

$$\left\|\overrightarrow{\mathbb{J}_{inv}}(t)-\vec{\mathbb{J}}(t)\right\|_{\mathbb{L}}=\left|\frac{1}{m}\cosh(nt)+\mathfrak{c}\right|,\quad \mathfrak{c}\in\mathbb{R}.$$

**Proof:** From (13) and (20), proof is clear.

**Theorem 3.3.** The Frenet frame of the involute curves of timelike Salkowski curves in $\mathbb{E}_1^3$ is

$$\begin{cases} \overrightarrow{\mathbb{T}_{inv}}(t) = -\left(n, \dfrac{n}{m}\sinh(t), \dfrac{n}{m}\cosh(t)\right) & \text{spacelike,} \\ \overrightarrow{\mathbb{N}_{inv}}(t) = -\left(0, \cosh(t), \sinh(t)\right) & \text{spacelike,} \\ \overrightarrow{\mathbb{B}_{inv}}(t) = \left(\dfrac{n}{m}, n\sinh(t), n\cosh(t)\right) & \text{timelike.} \end{cases}$$

**Proof:** From (19),

$$\overrightarrow{\mathbb{J}_{inv}}'(t) = -\frac{n^2}{m^2}\sinh(nt)\left(\frac{1}{m}\cosh(nt) + \mathfrak{c}\right)\left(m, \sinh(t), \cosh(t)\right) \quad (21)$$

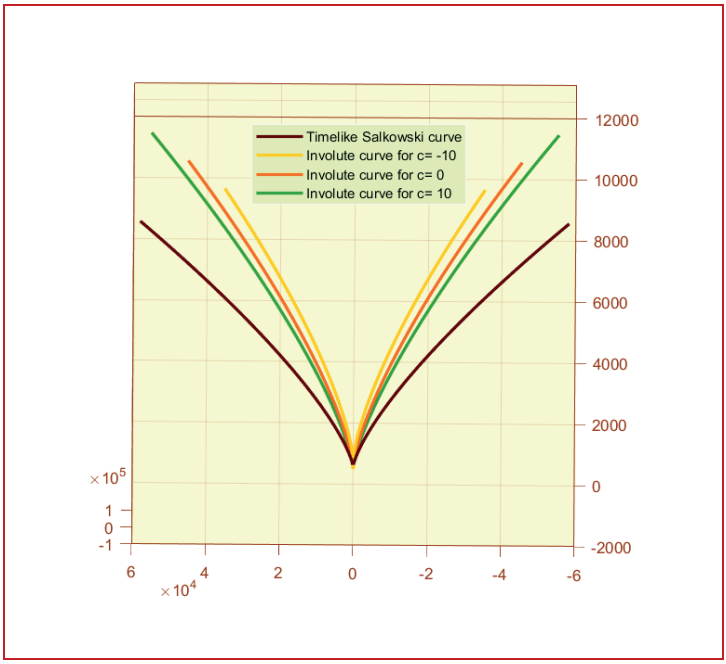

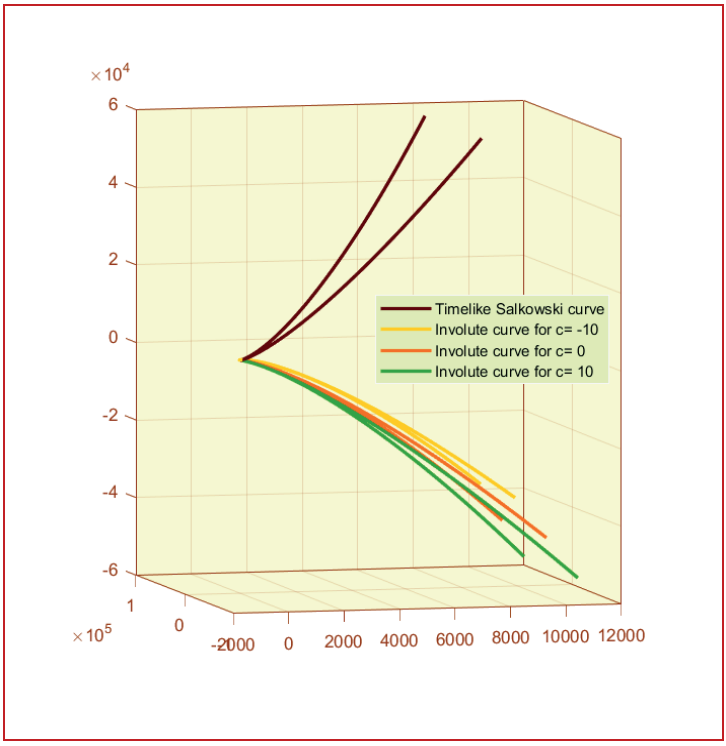


**Figure 3.** Timelike Salkowski curve for $m=\frac{3}{2}$ and its involute curves for $c=-10,0,10$.

and

$$\left\|\overrightarrow{\mathbb{J}_{inv}}'(t)\right\|=\mathfrak{y}_{inv}(t)=\frac{n}{m}\left|\sinh(nt)\left(\frac{1}{m}\cosh(nt)+\mathfrak{c}\right)\right| \tag{22}$$

are gotten. If (21) and (22) are substituted in (4), the unit tangent vector $\overrightarrow{\mathbb{T}_{inv}}(t)$ of $\overrightarrow{\mathbb{J}_{inv}}(t)$ is obtained as follows:

$$\overrightarrow{\mathbb{T}_{inv}}(t)=-\frac{n}{m}\left(m,\sinh(t),\cosh(t)\right). \tag{23}$$

Since $\left\langle\overrightarrow{\mathbb{T}_{inv}}(t),\overrightarrow{\mathbb{T}_{inv}}(t)\right\rangle_{\mathbb{L}}=1$, $\overrightarrow{\mathbb{T}_{inv}}(t)$ is spacelike and so $\overrightarrow{\mathbb{J}_{inv}}(t)$ is a spacelike curve. Also, from (15) and (23), it seen that $\left\langle\vec{\mathbb{T}}(t),\overrightarrow{\mathbb{T}_{inv}}(t)\right\rangle_{\mathbb{L}}=0$.

This is also a consequence of the definition of the involute of a curve. On the other hand, from (21),

$$\begin{aligned}\overrightarrow{\mathbb{J}_{inv}}''(t) = -\frac{n^2}{m^2}\Big( & n\sinh^2(nt) + nm\Big(\frac{1}{m}\cosh(nt) + \mathfrak{c}\Big)\cosh(nt), \\ & \frac{n}{m}\sinh(t)\sinh^2(nt) + \Big(\frac{1}{m}\cosh(nt) + \mathfrak{c}\Big)\big(\cosh(t)\sinh(nt) + n\sinh(t)\cosh(nt)\big) \\ & \frac{n}{m}\cosh(t)\sinh^2(nt) + \Big(\frac{1}{m}\cosh(nt) + \mathfrak{c}\Big)\big(\sinh(t)\sinh(nt) + n\cosh(t)\cosh(nt)\big)\Big),\end{aligned}$$

(24)

is gotten. Considering (21) and (24),

$$\overrightarrow{\mathbb{J}_{inv}}'(t) \wedge \overrightarrow{\mathbb{J}_{inv}}''(t) = \frac{n^4}{m^4}\sinh^2(nt)\Big(\frac{1}{m}\cosh(nt) + \mathfrak{c}\Big)^2\big(1, m\sinh(t), m\cosh(t)\big) \quad (25)$$

and

$$\left\|\overrightarrow{\mathbb{J}_{inv}}'(t) \wedge \overrightarrow{\mathbb{J}_{inv}}''(t)\right\| = \frac{n^3}{m^3}\sinh^2(nt)\Big(\frac{1}{m}\cosh(nt) + \mathfrak{c}\Big)^2 \quad (26)$$

are obtained. If (25) and (26) are substituted in (4),

$$\overrightarrow{\mathbb{B}_{inv}}(t) = \Big(\frac{n}{m}, n\sinh(t), n\cosh(t)\Big) \quad (27)$$

is gotten. Since $\left\langle \overrightarrow{\mathbb{B}_{inv}}(t), \overrightarrow{\mathbb{B}_{inv}}(t)\right\rangle_{\mathbb{L}} = -1$, $\overrightarrow{\mathbb{B}_{inv}}(t)$ is timelike. That means, the involute curves of timelike Salkowski curves are spacelike curves with timelike binormal.

Last, if (23) and (27) are substituted in (4), the principal normal vector of $\overrightarrow{\mathbb{J}_{inv}}(t)$ is

$$\overrightarrow{\mathbb{N}_{inv}}(t) = -\big(0, \cosh(t), \sinh(t)\big). \quad (28)$$

Since $\left\langle \overrightarrow{\mathbb{N}_{inv}}(t), \overrightarrow{\mathbb{N}_{inv}}(t)\right\rangle_{\mathbb{L}} = 1$, $\overrightarrow{\mathbb{N}_{inv}}(t)$ is spacelike. Thus, the proof is completed.

**Corollary 3.4.** The Frenet frames of their involute curves and timelike Salkowski curves in $\mathbb{E}_1^3$ have the following matrix relationship:

$$\begin{bmatrix} \overrightarrow{\mathbb{T}_{inv}}(t) \\ \overrightarrow{\mathbb{N}_{inv}}(t) \\ \overrightarrow{\mathbb{B}_{inv}}(t) \end{bmatrix} = \begin{bmatrix} 0 & -1 & 0 \\ \sinh(nt) & 0 & \cosh(nt) \\ \cosh(nt) & 0 & \sinh(nt) \end{bmatrix} \begin{bmatrix} \vec{\mathbb{T}}(t) \\ \vec{\mathbb{N}}(t) \\ \vec{\mathbb{B}}(t) \end{bmatrix}.$$

**Proof:** Considering (15), (23), (27) and (28), the proof is completed.

**Theorem 3.5.** The curvature of involute curves of timelike Salkowski curves in $\mathbb{E}_1^3$ is as follows:

$$\mathbb{K}_{inv}(t) = \frac{\left|\operatorname{cosech}(nt)\right|}{\left|\frac{1}{m}\cosh(nt) + \mathfrak{c}\right|}. \tag{29}$$

**Proof:** If (22) and (26) are substituted in (6), (29) is obtained.

**Corollary 3.6.** The curvatures of their involute curves and timelike Salkowski curves in $\mathbb{E}_1^3$ have the following relationship:

$$\mathbb{K}_{inv}(t) = \frac{\left|\operatorname{cosech}(nt)\right|\mathbb{K}(t)}{\left|\frac{1}{m}\cosh(nt) + \mathfrak{c}\right|}.$$

**Proof:** It can be written from (14) and (29).

**Theorem 3.7.** The torsion of involute curves of timelike Salkowski curves in $\mathbb{E}_1^3$ is as follows:

$$\mathbb{P}_{inv}(t) = \frac{m\operatorname{cosech}(nt)}{\frac{1}{m}\cosh(nt) + \mathfrak{c}}. \tag{30}$$

**Proof:** From (24),

$$\begin{aligned}\overrightarrow{\mathbb{J}_{inv}}'''(t) = -\frac{n^2}{m^2}\Big(&3n^2\cosh(nt)\sinh(nt)+n^2m\Big(\frac{1}{m}\cosh(nt)+\mathfrak{c}\Big)\sinh(nt),\\ &\frac{2n}{m}\cosh(t)\sinh^2(nt)+\frac{3n^2}{m}\sinh(t)\cosh(nt)\sinh(nt)\\ &+\Big(\frac{1}{m}\cosh(nt)+\mathfrak{c}\Big)\Big(\big(n^2+1\big)\sinh(t)\sinh(nt)+2n\cosh(t)\cosh(nt)\Big),\\ &\frac{2n}{m}\sinh(t)\sinh^2(nt)+\frac{3n^2}{m}\cosh(t)\cosh(nt)\sinh(nt)\\ &+\Big(\frac{1}{m}\cosh(nt)+\mathfrak{c}\Big)\Big(\big(n^2+1\big)\cosh(t)\sinh(nt)+2n\sinh(t)\cosh(nt)\Big)\end{aligned} \tag{31}$$

and from (21), (24) and (31),

$$\left\langle \overrightarrow{\mathbb{J}_{inv}}'(t)\wedge\overrightarrow{\mathbb{J}_{inv}}''(t),\overrightarrow{\mathbb{J}_{inv}}'''(t)\right\rangle = \frac{n^6}{m^5}\sinh^3(nt)\left(\frac{1}{m}\cosh(nt)+\mathfrak{c}\right)^3 \tag{32}$$

are gotten. If (26) and (32) are substituted in (6), (30) is obtained.

**Corollary 3.8.** The torsions of their involute curves and timelike Salkowski curves in $\mathbb{E}_1^3$ have the following relationship:

$$\mathbb{P}_{inv}(t) = -\frac{m\,\mathrm{sech}(nt)\,\mathbb{P}(t)}{\frac{1}{m}\cosh(nt)+\mathfrak{c}}.$$

**Proof:** It can be written, if considering (14) and (30).

**Theorem 3.9.** The Darboux vector of involute curves of timelike Salkowski curves in $\mathbb{E}_1^3$ is as follows:

$$\overrightarrow{\mathbb{D}_{inv}}(t) = (1,0,0) \qquad \text{spacelike.} \tag{33}$$

**Proof:** If (22), (23), (27), (29) and (30) are substituted in (9), (33) is obtained.

**Corollary 3.10.** The Lorentzian timelike angle between the vectors $\vec{\mathbb{B}}$ (timelike) and $\vec{\mathbb{D}}$ (spacelike) of involute curves of timelike Salkowski curves in $\mathbb{E}_1^3$ is

$$\Omega(t) = -\operatorname{arccoth}(m).$$

**Proof: I**f (22), (29), (30) and (33) are substituted in (11),

$$\begin{cases} \cosh\left(\Omega(t)\right) = \cosh\left(nt\right) = -n, \\ \sinh\left(\Omega(t)\right) = \sinh\left(nt\right) = \dfrac{n}{m} \end{cases} \tag{34}$$

are obtained. And so, proof is completed.

**Corollary 3.11.** The Darboux vectors of their involute curves and timelike Salkowski curves in $\mathbb{E}_1^3$ have the following relationship:

$$\overrightarrow{\mathbb{D}_{inv}}(t) = \vec{\mathbb{D}}(t) + n\vec{\mathbb{N}}(t).$$

**Proof:** From (15), (16) and (33), it is clear.

**Theorem 3.12.** The pole vector of involute curves of timelike Salkowski curves in $\mathbb{E}_1^3$ is as follows:

$$\overrightarrow{\mathbb{C}_{inv}}(t) = (1,0,0) \qquad \text{spacelike.} \tag{35}$$

**Proof:** It is clear from (33), but if (23), (27) and (34) are substituted in (10), (35) is obtained again.

**Corollary 3.13.** The pole vectors of their involute curves and timelike Salkowski curves in $\mathbb{E}_1^3$ have the following relationship:

$$\overrightarrow{\mathbb{C}_{inv}}(t) = \vec{\mathbb{C}}(t) + m\ \vec{\mathbb{N}}(t).$$

**Proof:** From (15), (17) and (35), it is clear.

## 5. Conclusions

In present study, we saw that involute curves of timelike Salkowski curves in Minkowski 3-space are timelike binormal spacelike curves. We also examined the Frenet vectors, curvatures, torsions, Darboux and Pol vectors of these curves and included the relations between these elements. Comparable analyses can be conducted for other variations of Salkowski curves in Minkowski 3-space.

## REFERENCES

Abdel-Aziz, H.S., Saad, M.K., Abdel-Salam, A.A. (2019). On involute-evolute curve couple in the hyperbolic and de Sitter spaces. Journal of the Egyptian Mathematical Society, 27, 1-18.

Aksan, B., Gür Mazlum, S. (2023). On the spherical indicatrix curves of the spacelike Salkowski curve with timelike principal normal in Lorentzian 3-space. Honam Mathematical J., 45(3), 513-541.

Akutagava, K., Nishikawa, S. (1990). The Gauss map and space-like surfaces with prescribed mean curvature in Minkowski 3-space. Tohoku Math. J., 42, 67–82.

Ali, A. T. (2009). Time-like Salkowski and anti-Salkowski curves in Minkowski space $E_1^3$. arXiv:0905.1404.

Altın, M., Kazan, A. (2024). Timelike general rotational surfaces in Minkowski 4-space with density. Journal of Korean Math. Soc., 61(6), 1051-1071.

Beem, J. K., Paul, E. E., Kevin, L. E. (2017). Global lorentzian geometry. Routledge.

Bilici, M., Çalışkan, M. (2011). Some new notes on the involutes of the timelike curves in Minkowski 3-space. Int. J. Math. Sciences, 6(41), 2019–2030.

Bilici, M., Çalışkan, M. (2019). Some new results on the curvatures of the spherical indicatrices of the involutes of a spacelike curve with a spacelike binormal in Minkowski 3-space, MathLAB Journal, 2(1), 110–119.

Birman, G. S., Nomizu, K. (1984). Trigonometry in Lorentzian geometry. Ann. Math. Mont. 91, 534–549.

Bükcü, B., Karacan, M. K. (2007). On the involute and evolute curves of the timelike curve in Minkowski 3-space. Demonstratio Mathematica, 40(3), 721–732.

Gür Mazlum, S. (2024). The involute curves of any non-unit speed timelike curve in Minkowski 3-space. Dayangaç, A., Akgül, H., Öztürk, G. (Ed.) In: International Studies and Evaluations in the Field of Science and Mathematics, pp. 91-113, Serüven Publishing, Ankara.

Kazan, A., Altın, M. (2023). Loxodromes on twisted surfaces in Lorentz–Minkowski 3-space. Asian-European Journal of Mathematics, 16(4), 2350058.

Lopez, R. (2014). Differential geometry of curves and surfaces in Lorentz-Minkowski space. International Electronic Journal of Geometry, 7, 44–107.

O'Neill, B. (1983). Semi-Riemannian geometry with applications to relativity. Academic Press: London, England.

Monterde, J. (2009). Salkowski curves revisited: A family of curves with constant curvature and non-constant torsion. Computer Aided Geometric Design, 26(3), 271-278.

Ratcliffe, J. G. (1994). Foundations of hyperbolic manifolds. Springer-Verlag: Tokyo, Japanese.

Salkowski, E. (1909). Zur transformation von raumkurven. Mathematische Annalen, 66(4), 517-557.

Şenyurt, S., Gür, S., Ozyılmaz, E. (2015). The Frenet vectors and the geodesic curvatures of spherical indicatrix of the timelike Salkowski curve in Minkowski 3-space. Journal of Advanced Research in Dynamical and Control Systems, 7(4), 20-42.

Uğurlu, H. H. (1997). On the geometry of time-like surfaces, Communications Faculty of Sciences, University of Ankara, A1 Series, 46, 211-223.

Uğurlu, H. H., Çalışkan, A. (2012). Darboux ani dönme vektörleri ile spacelike ve timelike yüzeyler geometrisi. Celal Bayar University Press: Manisa, Turkiye.

Woestijne, I. V. (1990). Minimal surfaces of the 3-dimensional Minkowski space, Geometry and Topology of Submanifolds: II, Word Scientific, Singapore, 344–369.

# CHAPTER 11

## TRUNCATION AND FUNCTORIALITY IN SIMPLICIAL LIE ALGEBRAS

*İbrahim İlker AKÇA*[1]

*Ummahan EGE ARSLAN*[2]

1 Prof. Dr.; Eskişehir Osmangazi University, Department of Mathematics and Computer Sciences, Faculty of Science, iakca@ogu.edu.tr,ORCID No:0000-0003-4269-498X

2 Prof. Dr.; Eskişehir Osmangazi University, Department of Mathematics and Computer Sciences, Faculty of Science, uege@ogu.edu.tr ORCID No:0000-0002-2995-0718

## Introduction

Simplicial Lie algebras, which emerge within the framework of simplicial homotopical algebra ([9], [18]), have garnered significant attention due to their intriguing homotopy theory. The study of these algebras provides valuable insights into the interplay between simplicial structures and homotopical properties, making them a subject of considerable interest in modern algebraic research.

Kassel and Loday [14] (see also [15], [17]) introduced the concept of crossed modules of Lie algebras as algebraic structures that are computationally equivalent to simplicial Lie algebras with an associated Moore complex of length 1. This formulation provides a framework for simplifying the study and analysis of simplicial Lie algebras by translating their homotopical properties into the language of crossed modules. In this context, crossed modules serve as a powerful tool for understanding the internal structure and homotopy-theoretic relationships of Lie algebras, offering significant insights into simplicial homotopy theory and its algebraic applications.

Building on Conduché's work in the context of group theory, Ellis [12] formalized the algebraic structure of a Moore complex of length 2 through his definition of a 2-crossed module of Lie algebras. In the homotopy theory of simplicial Lie algebras, analogues of Samelson and Whitehead products are represented as sums over shuffle $(a;b)$ of Lie brackets of the form $[s_b x, s_a y]$. This development provides a deeper understanding of the homotopical and algebraic interactions within simplicial Lie algebras.

In [1], the connection between these shuffles and crossed modules, as well as crossed 2-modules, was explored. This work provides an explanation of how the shuffle operations in the homotopy theory of simplicial Lie algebras are related to the algebraic structures of crossed modules and crossed 2-modules, offering deeper insights into their homotopical and algebraic interactions.

It is well known that the category of simplicial Lie algebras is equivalent to both the category of crossed modules of Lie algebras and the

category of 2-crossed modules of Lie algebras. This equivalence establishes a strong connection between these algebraic structures, providing a unified framework for studying their homotopical properties and interactions.

In [12], G. Ellis proved that the category of crossed modules of Lie algebras is equivalent to the category of simplicial Lie algebras with a Moore complex of length 1, and that the category of 2-crossed modules of Lie algebras is equivalent to the category of simplicial Lie algebras with a Moore complex of length 2. This result establishes a direct correspondence between these algebraic structures, offering a powerful tool for exploring their homotopical and algebraic properties.

In this paper, we present an encoding method that shows how crossed modules and 2-crossed modules are equivalent to truncated simplicial Lie algebras. This approach provides a new perspective on the relationship between these algebraic structures, further enhancing the understanding of their homotopical and algebraic properties.

**Review of Simplicial Lie Algebras**

A simplicial Lie algebra is an algebraic structure that arises in the study of algebraic topology and homotopy theory, particularly in the context of simplicial sets. It provides a way to model and investigate the homotopical properties of Lie algebras in the framework of simplicial objects. Simplicial Lie algebras offer a robust framework for bridging algebraic structures with topological concepts. Their homotopy theory is of significant interest, and their connections with crossed modules and higher-dimensional algebraic structures continue to be a rich area of research in mathematics.

All Lie algebras will be over a fixed commutative ring $k$ in this work. .A simplicial Lie algebra **L** consists of a family of Lie algebras $\{L_n\}$ together with face and degeneracy maps

$$d_i = d_i^n : \quad L_n \to L_{n-1}, \quad 0 \le i \le n \ \ (n \neq 0)$$
$$s_i = s_i^n : \quad L_n \to L_{n+1}, \qquad 0 \le i \le n.$$

satisfying the usual simplicial identities given in Andre [2] or [13], for example. It can be completely described as a functor $\mathbf{L} : \Delta^{op} \to \mathbf{LieAlg}_k$ where $\Delta$ is the category of finite ordinals $[n] = \{0 < 1 < \cdots < n\}$ and increasing maps. Elements $x \in L_n$ are called *n-dimensional simplices.* A

simplex $x$ is called *degenerate* if $x = s_i(y)$ for some $y$.

Simplicial Lie algebras play a crucial role in homotopy theory. They are used to understand the homotopy types of certain algebraic structures, such as loop spaces and higher homotopy groups. The homotopy theory of simplicial Lie algebras involves analyzing the relationships between the Lie algebras $L_n$ and their various face and degeneracy maps, often by studying the Moore complex associated with a simplicial Lie algebra. Simplicial Lie algebras offer a robust framework for bridging algebraic structures with topological concepts. Their homotopy theory is of significant interest, and their connections with crossed modules and higher-dimensional algebraic structures continue to be a rich area of research in mathematics.

A simplicial map is defined as a collection of homomorphisms $f_n : L_n \to L_n'$ that are compatible with the face and degeneracy maps of the simplicial Lie algebras. The category of simplicial Lie algebras is denoted by SLA.

A key resource in this area is Carrasco's thesis [6], which systematically introduced many of the foundational techniques employed in the present work. This thesis also defined the concept of a hypercrossed complex, albeit within a different context.

The following notation and terminology is derived from the analogous group theoretic case treated in [6], [7]. For the ordered set $[n] = \{0 < 1 < \ldots < n\}$, let $\alpha_i^n : [n+1] \to [n]$ be the increasing surjective map given by

$$\alpha_i^n(j) = \begin{cases} j & \text{if} \quad j \le i \\ j-1 & \text{if} \quad j > i. \end{cases}$$

Let $S(n, n-r)$ be the set of all monotone increasing surjective maps from $[n]$ to $[n-r]$. This can be generated from the various $\alpha_i^n$ by composition. The composition of these generating maps is subject to the following rule $\alpha_j \alpha_i = \alpha_{i-1} \alpha_j, \ j < i.$ This implies that every element $\alpha \in S(n, n-r)$ has a unique expression as $\alpha = \alpha_{i_1} \circ \alpha_{i_2} \circ \ldots \circ \alpha_{i_r}$ with

$0 \le i_1 < i_2 < \ldots < i_r \le n-1$ , where the indices $i_k$ are the elements of $[n]$ such that $\{i_1,\ldots,i_r\} = \{i : \alpha(i) = \alpha(i+1)\}$. We thus can identify $S(n,n-r)$ with the set $\{(i_r,\ldots,i_1) : 0 \le i_1 < i_2 < \ldots < i_r \le n-1\}$. In particular, the single element of $S(n,n)$, defined by the identity map on $[n]$ , corresponds to the empty $0$ -tuple $()$ denoted by $\emptyset_n$. Similarly the only element of $S(n,0)$ is $(n-1,n-2,\ldots,0)$. For all $n \ge 0$, let

$$S(n) = \bigcup_{0 \le r \le n} S(n,n-r).$$

We say that $\alpha = (i_r,\ldots,i_1) < \beta = (j_s,\ldots,j_1)$ in $S(n)$

if $i_1 = j_1,\ldots,i_k = j_k$ but $i_{k+1} > j_{k+1}$ $(k \ge 0)$ or

if $i_1 = j_1,\ldots,i_r = j_r$ and $r < s$.

This makes $S(n)$ an ordered set. For instance, the orders in $S(2)$ and in $S(3)$ are respectively:

$S(2) = \{\emptyset_2 < (1) < (0) < (1,0)\}$;

$S(3) = \{\emptyset_3 < (2) < (1) < (2,1) < (0) < (2,0) < (1,0) < (2,1,0)\}$.

We also define $\alpha \cap \beta$ as the set of indices which belong to both $\alpha$ and $\beta$ .

**The Moore Complex of a Simplicial Lie Algebra**

The Moore complex **NL** of a simplicial Lie algebra **L** is the complex

$$\mathbf{NL}: \quad \cdots \to NL_n \xrightarrow{\partial_n} NL_{n-1} \to \cdots \to NL_1 \xrightarrow{\partial_1} NL_0 \xrightarrow{\partial_0} 0$$

where

$$NL_0 = E_0, \quad NL_n = \bigcap_{i=0}^{n-1} \mathrm{Ker} d_i, \quad \partial_n = d_n \text{ (restricted to } NL_n).$$

We say that the Moore complex **NL** of a simplicial Lie algebra is of length $k$ if $NL_n = 0$ for all $n \ge k+1$ so that a Moore complex is of length $r$ for $r \ge k$.

We will need to make use of the semidirect product decomposition several times. The foundational concept underlying this idea was first introduced by Conduché [8]. A comprehensive analysis of this framework within the context of simplicial groups is provided by Carrasco and Cegarra in [7]. The corresponding algebraic formulation of this structure is detailed in Carrasco's doctoral thesis [6]:

Proposition: If **L** is a simplicial Lie algebra, then for any $n \geq 0$

$$L_n \cong (\ldots(NL_n \rtimes s_{n-1}NL_{n-1}) \rtimes \ldots \rtimes s_{n-2}\ldots s_0NL_1) \rtimes (\ldots(s_{n-2}NL_{n-1} \rtimes s_{n-1}s_{n-2}NL_{n-2}) \rtimes \ldots \rtimes s_{n-1}s_{n-2}\ldots s_0NL_0).$$

Proof: This is by repeated use of the following lemma.

Lemma: Let **L** be a simplicial Lie algebra. In this framework, the Lie algebra $L_n$ associated with **L** admits a decomposition as a semidirect product. This decomposition is given by:

$L_n \cong \mathrm{Ker}d_n^n \rtimes s_{n-1}^{n-1}(L_{n-1})$.

Proof: The isomorphism is defined as follows:

$$\theta: \begin{array}{ccc} L_n & \longrightarrow & \mathrm{Ker}d_n^n \rtimes s_{n-1}^{n-1}(L_{n-1}) \\ e & \longmapsto & (e - s_{n-1}d_ne, s_{n-1}d_ne). \end{array}$$

where θ is a map that preserves the Lie algebra structure and respects the semidirect product decomposition. This mapping satisfies the necessary properties of a Lie algebra homomorphism, meaning it preserves the Lie bracket:

$$\theta[e_1, e_2] = [\theta(e_1), \theta(e_2)]$$

for all $e_1, e_2 \in L_n$. The structure of the semidirect product ensures that the action of $s_{n-1}^{n-1}(L_{n-1})$ on $\mathrm{Ker}d_n^n$ is incorporated into the isomorphism, allowing the Lie algebra $L_n$ to be fully described in terms of $\mathrm{Ker}d_n^n$ and $s_{n-1}^{n-1}(L_{n-1})$.

**Truncations**

In the context of simplicial Lie algebras, truncations refer to a process where higher-dimensional terms in a simplicial algebra are "cut off" or reduced, simplifying the structure to a certain degree. This concept is important in both algebraic topology and homotopy theory, particularly when dealing with objects like simplicial Lie algebras or crossed modules.

Truncation provides a way to simplify chain complexes of Lie algebras, focusing only on terms up to a specified level while preserving the differential structure in the truncated portion. This operation is functorial, making it compatible with chain maps and facilitating the study of Lie algebra structures at lower dimensions.

This concept is important in both algebraic topology and homotopy theory, particularly when dealing with objects like simplicial Lie algebras or crossed modules.

In the context of crossed modules and higher Lie algebra structures, truncation allows for focusing on the lower-dimensional components of a complex or algebra, which can significantly simplify calculations and analysis of homotopical properties. For example, truncating a complex at level kkk removes any contributions from higher degrees, making it possible to study the interactions between the first few terms in isolation.

By an ideal chain complex of Lie algebras, we refer to a chain complex X of Lie algebras where each image $\mathrm{Im}d_{i+1}$ of the differential map $d_{i+1}$ is an ideal of the Lie algebra $X_i$. This structure ensures that each successive differential maps into an ideal, providing a strong structural relationship between the elements of the complex.

Given an ideal chain complex X of Lie algebras and an integer n, the truncation $t_{n|}X$ of the complex at level n is defined as follows:

$$(t_{n|}X)_i = \begin{cases} X_i & \text{if} \quad i < n \\ X_i/\mathrm{Im}d_{n+1} & \text{if} \quad i = n \\ 0 & \text{if} \quad i > n. \end{cases}$$

The differential $d$ of $t_{n|}X$ is that of $X$ for $i > n$, $d_n$ is induced from the $n^{th}$ differential of $X$ and all other are zero (for more information see Illusie [13]). Truncation is of course functorial.

Proposition: There is a truncation functor $t_{n|}$ : **SLA** $\rightarrow$ **SLA** such that there is a natural isomorphism

$t_{n|}N \cong Nt_{n|}$,

where $N$ is the Moore complex functor from **SLA** to the category of chain complexes of Lie algebras.

We first note that $d_{n+1}^{n+1}(NL_{n+1})$ is contained in $L_n$ as an ideal and that all face maps of $\mathbf{L}$ vanish on it. We can thus take

$$t_{n|}\mathbf{L} = \begin{cases} L_i & \text{for all } i < n \\ L_n / d_{n+1}^{n+1}(NL_{n+1}) & \text{for } i = n \end{cases}$$

and for $i > n$, we apply the semidirect product decomposition of $L_i$ as stated in above Proposition, removing all instances of $NL_k$ for $k > n$ and substituting any occurrence of $NL_n$ with $NL_n / d_{n+1}^{n+1}(NL_{n+1})$. The definitions of face and degeneracy maps are straightforward, and it is easy to verify that $t_{n|}N$ and $Nt_{n|}$ are equivalent.

This truncation functor has nice properties. (In the chain complex case, these are discussed in Illusie [13]).

Proposition: Let $T_{n|}$ be the full subcategory of **SLA** defined by the simplicial Lie algebras whose Moore complex is trivial in dimensions greater than $n$ and let $i_n : T_{n|} \to$ **SLA** be the inclusion functor.

(a) The functor $t_{n|}$ is left adjoint to $i_n$. (We will usually drop the $i_n$ and so also write $t_{n|}$ for the composite functor. )

(b) The natural transformation $\eta$, the co-unit of the adjunction, is a natural epimorphism which induces an isomorphism on $\pi_i$ for $i \le n$.

(c) For any simplicial Lie algebra **L**, $\pi(t_{n|}\ \mathbf{L}\ ) = 0$ if $i > n$.

(d) To the inclusion $T_{n|} \to T_{n+1|}$, there corresponds a natural epimorphism $\eta_n$ from $t_{n+1|}$ to $t_{n|}$. If **L** is simplicial Lie algebra, the kernel of $\eta_n$ (**L**) is a $K(\pi_{n+1}(\ \mathbf{L}\ ), n+1)$, i.e. has a single non-zero homotopy module in dimension $n+1$, that being $\pi_{n+1}(\ \mathbf{L}\ )$.

The proof will be omitted, as each assertion can be easily validated using the Moore complex and the semidirect product decomposition.

A comparison between these properties and those of the coskeleta functors, as discussed by Artin and Mazur [3], is worth exploring. Recall that, for any integer $k \ge 0$, the coskeleton functor cosk $_n$ is a construction defined on the category of simplicial sets. This functor is formed as the composition of a truncation functor (defined differently from the one in the current context) and its right adjoint. The $n$ -simplicies of cosk $_k \mathbf{X}$ are given by

$$\text{cosk}_k\,(\boldsymbol{X})_n = \text{Hom}(\text{sk}_{\,k}\,\Delta[n], \mathbf{X}\,)$$

where $\text{sk}_{\,k}\Delta[n]$ denotes the k-skeleton of the n-simplex $\Delta[n]$, and $\mathbf{X}$ is the simplicial set under consideration. In other words, $\text{cosk}_k\,(\boldsymbol{X})_n$ is the set of simplicial maps from the truncated k-skeleton of $\Delta[n]$ to **X**.

This construction provides a way to "extend" the information from the lower-dimensional components (up to k) of **X** to higher dimensions, while maintaining compatibility with the simplicial structure. Comparing this approach with truncation methods in other settings highlights both the utility and the limitations of coskeleta in capturing algebraic and topological information.

There is a canonical map from $\mathbf{X}$ to $\text{cosk}_{\,k}\mathbf{X}$ whose homotopy fibre an Eilenberg-Maclane space of type $(\pi_k(\mathbf{X}), k)$. This $k$-skeleton is constructed using finite limits and there is an analogue in any category of simplicial objects in a category $\mathbf{C}$ provided that $\mathbf{C}$ has finite limits, thus in particular in **SLA**. It can be calculated the Moore complex of $\text{cosk}_{\,k}\mathbf{L}$ for a simplicial Lie algebra $\mathbf{L}$ using a construction described in Duskin's Memoir [10]. This gives

$$\begin{aligned} N(\text{cosk}_k\mathbf{L})_l &= 0 \text{ if } l > k+1 \\ N(\text{cosk}_k\mathbf{L})_{k+1} &= Ker(\partial_k : NL_k \to NL_{k-1}) \\ N((\text{cosk}_k\mathbf{L})_l) &= NL_l \text{ if } l \le k. \end{aligned}$$

There is a natural epimorphism from $\text{cos}\,k_{k+1}\mathbf{L}$ to $t_{k|}\mathbf{L}$ which on passing to Moore complexes gives

$$\begin{array}{ccccccccc} 0 & \longrightarrow & Ker\partial_{k+1} & \longrightarrow & NL_{k+1} & \longrightarrow & NL_k & \xrightarrow{\partial_k} & NL_{k-1} \\ \downarrow & & \downarrow & & \downarrow & & \downarrow & & \downarrow \\ 0 & \longrightarrow & 0 & \longrightarrow & 0 & \longrightarrow & NL_k/Im\partial_{k+1} & \longrightarrow & NL_{k-1} \end{array}$$

This epimorphism of chain complexes thus has an acyclic kernel. The epimorphism therefore induces an isomorphism on all homotopy modules and hence is a weak homotopy equivalence. We may thus use either $t_{k|}\mathbf{L}$ or $\text{cos}\,k_{k+1}\mathbf{L}$ as a model for $k$-type of simplicial Lie algebra $\mathbf{L}$.

**Truncated Simplicial Lie Algebras**

It is well known that the category of simplicial Lie algebras is equivalent to the category of crossed modules of Lie algebras and category of 2-crossed modules of Lie algebras. In [12], G. Ellis proved that the category of crossed modules of Lie algebras is equivalent to the category of simplicial Lie algebras with Moore complex of length 1 and that the category of 2-crossed modules of Lie algebras is equivalent to the category of simplicial Lie algebras with Moore complex of length 2. In this section we will give slight reformulations of this results by means of the truncated simplicial Lie algebras. As a first step to understanding truncated simplicial Lie algebras a bit more, we will give a variant of an argument. We will look at a 1-truncated simplicial Lie algebra.

Proposition: (c.f [1]) Let $I_2$ be the ideal of $L_2$ generated by elements of the form

$M_{(1)(0)}(x,y)=[s_1(x),s_0(y)-s_1(y)].$

The image of $I_2$ by $\partial_2$ is known to be $[\ker d_0,\ker d_1]$ by direct calculation.

The form of this element

$M_{(1)(0)}(x,y)$ , is obtained by taking the two elements, $x$ and $y$ , of degree 1 in the Moore complex of a simplicial Lie algebra, $\mathbf{L}$ , mapping them up to degree 2 by complementary degeneracies, and then looking at the component of the result that is in the Moore complex term, $NL_2$. (It is easy to show that $L_2$ is a semidirect product of $NL_2$ and degenerate copies of lower degree Moore complex terms.) The idea behind this pairing can be extended to higher dimensions. It gives the Peiffer pairings

$M_{\alpha,\beta}\ :\ NL_p\times NL_q\to NL_{p+q}.$

In general, these take $x\in NL_p$ and $y\in NL_q$ and $(\alpha,\beta)$ a complimentary pair of index strings (of suitable lengths), and sends $(x,y)$ to the component in $NL_{p+q}$ of $s_\alpha(x)s_\beta(y)$ ; see the paper [1].

**Crossed Modules of Lie Algebras**

J.H.C. Whitehead (1949) [19] explored crossed modules in multiple contexts, particularly in his study of the algebraic structure of relative

homotopy groups. Kassel and Loday [14] later introduced the concept of crossed modules specifically within the framework of Lie algebras.

A Lie action provides a way for a Lie algebra to act on a vector space or another Lie algebra, preserving the structure of the Lie bracket through the Leibniz rule. This action is fundamental in the study of Lie algebra representations, homotopy theory, and algebraic topology, playing a key role in the development of various mathematical fields.

Let $M$ and $P$ be two Lie algebras. By an *action* of $P$ on $M$ we mean a **k**-bilinear map $P\times M \to M, \quad (p,m)\mapsto p\cdot m$ satisfying

$$[p,p']\cdot m = p\cdot(p'\cdot m)-p'(p\cdot m)$$
$$p\cdot[m,m'] = [p\cdot m,m']+[m,p\cdot m']$$

for all $m,m'\in M, p,p'\in P.$ For instance, if $P$ is a subalgebra of some Lie algebra $^{Q}$ (including possibly the case $P=Q$ ), and if $M$ is an ideal in $Q,$ then Lie multiplication in $Q$ yields an action of $P$ on $M.$

Suppose that $M$ and $N$ are Lie algebras with an action of $M$ on $N$ and action of $N$ on $M.$ For any Lie algebra $Q$ we call a bilinear function $h : M\times N\to Q$ a *Lie pairing* [11] if

$$h([m,m'],n) = h(m,m'\cdot n)-h(m',m\cdot n),$$
$$h(m,[n,n']) = h(n'\cdot m,n)-h(n\cdot m,n'),$$
$$h(n\cdot m,m'\cdot n') = -[h(m,n),h(m',n')],$$

for all $m,m'\in M,n,n'\in N.$ For example if $M$ and $N$ are both ideals of some Lie algebra then the function $M\times N\to M\cap N, \quad (m,n)\mapsto[m,n]$ is a Lie pairing.

Recall from [14] the notion of a crossed module of Lie algebras. *A crossed module of Lie algebras* consists of a Lie homomorphism $\partial : M\to P$ together with an action of $P$ on $M$ such that the following condition holds:

CM1) $\partial(p\cdot m)=[\partial m,p]$ CM2) $\partial m\cdot m'=[m,m']$

for all $m,m'\in M, p\in P.$

The second condition (CM2) is known as the *Peiffer identity.* A standard example of a crossed module is any ideal $I$ in a Lie algebra $P$, which gives an inclusion map $I\to P,$ that forms s a crossed module. Conversely, for any crossed module $\partial : M\to P,$ the image $I=\partial M$ of $M$ is an ideal in

$P$. This illustrates the interaction between crossed modules and ideal structures in Lie algebras.

**1- and 2-Truncated Simplicial Algebras**

Suppose that $\mathbf{L}$ is a simplicial Lie algebra and that $NL_i = 0$ for $i \geq 2$. This leaves us just with

$\partial : NL_1 \to NL_0$.

We make $NL_0 = L_0$ act on $NL_1$ by

$g \cdot c = [c, s_0(g)]$ for $g \in L_0$, $c \in NL_1$,

and

$\partial(g \cdot c) = \partial[c, s_0(g)] = [\partial(c), g]$.

Thus the first crossed module axiom is satisfied. For the other one, we note that $M_{(1)(0)}(c_1 \otimes c_2) \in NL_2$, which is trivial, so

$$\begin{aligned} 0 &= d_2[s_1c_1, s_0c_2 - s_1c_2] \\ &= [d_2s_1c_1, d_2s_0c_2 - d_2s_1c_2] \\ &= [c_1, s_0d_1c_2 - c_2] \\ &= [c_1, s_0d_1c_2] - [c_1, c_2] \\ &= d_1(c_2) \cdot c_1 - [c_1, c_2] \end{aligned}$$

so the Peiffer identity holds as well. Thus $\partial : NL_1 \to NL_0$ is a crossed module. Thus we have the following slight reformulation of results in [12].

Proposition: The category of crossed modules of Lie algebras is equivalent to the subcategory $T_{1]}$ of 1-truncated simplicial Lie algebras.

The primary motivation for restating and proving this result in its current form is that it allows us to extract additional insights from the proof, which will be useful for investigating the next level, namely 2-truncated simplicial Lie algebras. By reworking the proof, we can better understand the structure and properties of these higher-level objects.

If we substitute our 1-truncated simplicial Lie algebra with a general simplicial Lie algebra, we have already defined the concept of a Peiffer commutator between two elements. Additionally, we previously referred to the notion of Peiffer lifting, though we did not elaborate on its specific significance or purpose within the construction.

We recall that here: Given a simplicial Lie algebra, $\mathbf{L}$ , and two elements $c_1, c_2 \in NL_1$ as above, then the Peiffer commutator of $c_1$ and $c_2$ is defined by

$$\langle c_1, c_2 \rangle = \partial(c_2) \cdot c_1 - [c_1, c_2].$$

We met earlier, $M_{(1)(0)}$ , which gives the Peiffer lifting denoted

$$\{-,-\} : NL_1 \times NL_1 \to NL_2$$

where

$$\{c_1, c_2\} = [s_1 c_1, s_0 c_2 - s_1 c_2]$$

and we noted

$$\partial_2 \{c_1, c_2\} = \langle c_1, c_2 \rangle.$$

These structures come into their own for a 2-truncated simplicial Lie algebra. Suppose that $\mathbf{L}$ is now a simplicial Lie algebra, which is 2-truncated, so its Moore complex looks like:

$$\ldots 0 \to NL_2 \xrightarrow{\partial_2} NL_1 \xrightarrow{\partial_1} NL_0.$$

For the moment, we will concentrate our attention on the morphism $\partial_2$.

The Lie algebra $NL_1$ acts on $NL_2$ by

$$g \cdot c = [c, s_1(g)].$$

for $g \in NL_1$ and $c \in NL_2$ . It is clear that $\partial_2(g \cdot c) = \partial_2[c, s_1(g)] = [\partial_2(c), g]$ and as before, we consider for $c_1, c_2 \in NL_2$ this time, the Peiffer pairing given by

$$[s_2 c_1, s_1 c_2 - s_2 c_2]$$

which is in $NL_3$.

However, the latter Lie algebra is trivial, which implies that this element is trivial, and consequently, its image in $NL_2$ . With this $s_1$ -based action of $NL_1$ on $NL_2$ , $(NL_2, NL_1, \partial_2)$ is a crossed modüle, according to the same computation as previously

We also know that there is a Peiffer lifting
$\{-,-\} : NL_1 \times NL_1 \to NL_2$,
which measures the obstruction to $NL_1 \to NL_0$ being a crossed module, since $\partial\{-,-\}$ is the Peiffer commutator, whose vanishing is equivalent to $NL_1 \to NL_0$ being a crossed module.

Our investigation has not yet provided a thorough understanding of how the two structures interact, nor have we identified any other distinguishing properties of them. While we will not provide a detailed derivation here, we can derive the following from it:

Proposition: Let $\mathbf{L}$ be a 2-truncated simplicial Lie algebra. The Peiffer lifting
$\{-,-\} : NL_1 \times NL_1 \to NL_2$,
has the following properties:
(i) it is a map such that if $c_1, c_2 \in NL_1$
$\partial_2\{c_1, c_2\} = \partial(c_2) \cdot c_1 - [c_1, c_2]$,

(ii) if $l_0, l_1 \in NL_2$
$\{\partial_2(l_0), \partial_2(l_1)\} = [l_0, l_1]$,

(iii) if $l \in NL_2$ and $c \in NL_1$
$\{\partial_2(l), c\} = c \cdot l - \partial_1(c) \cdot l$,

(iv) if $l \in NL_2$ and $c \in NL_1$
$\{c, \partial_2(l)\} = c \cdot l$,

(v) if $n \in L_0, c_1, c_2 \in NL_1$
$n \cdot \{c_1, c_2\} = \{n \cdot c_1, c_2\} + \{c_1, n \cdot c_2\}$,

(vi) if $c_1, c_2, c_3 \in NL_1$
$$\{[c_1, c_2], c_3\} = \partial_1(c_2) \cdot \{c_1, c_3\} + \{c_2, [c_1, c_3]\} - \partial_1(c_1) \cdot \{c_2, c_3\} - \{c_1, [c_2, c_3]\},$$

(vii) if $c_1, c_2, c_3 \in NL_1$

$$\{c_1,[c_2,c_3]\} = \partial_1(c_3)\cdot\{c_1,c_2\} - \partial_1(c_2)\cdot\{c_1,c_3\} + \{c_2,[c_1,c_3] - \partial_1(c_3)\cdot c_1\} - \{c_3,[c_1,c_2] - \partial_1(c_2)\cdot c_1\}.$$

The above can be encoded in the definition of a 2-crossed module of Lie algebras.

Definition: A 2-crossed module of Lie algebras consists of a complex of Lie algebras

$$M_2 \overset{\partial_2}{\to} M_1 \overset{\partial_1}{\to} M_0$$

with $\partial_2, \partial_1$ morphisms of Lie algebras, where the algebra $M_0$ acts on $M_1$, $M_2$ and acts on itself by Lie bracket, further there is a $M_0$ -bilinear function giving

$$\{-,-\} : M_1 \times M_1 \to M_2,$$

which satisfies the following axioms: for all $x, x_1, x_2 \in M_2, y, y_0, y_1, y_2 \in M_1$ and $z \in M_0$

1: $\partial_2\{y_0, y_1\} = \partial_1(y_1)\cdot y_0 - [y_0, y_1]$

2: $\{\partial_2(x_1), \partial_2(x_2)\} = [x_1, x_2]$

3: $\{\partial_2(x), y\} = y\cdot x - \partial_1(y)\cdot x$

4: $\{y, \partial_2(x)\} = y\cdot x$

5: $z\cdot\{y_0, y_1\} = \{z\cdot y_0, y_1\} + \{y_0, z\cdot y_1\}$

6:

$$\{[y_0, y_1], y_2\} = \partial_1(y_1)\cdot\{y_0, y_2\} + \{y_1,[y_0, y_2]\} - \partial_1(y_0)\cdot\{y_1, y_2\} - \{y_0,[y_1, y_2]\}$$

7:

$$\{y_0,[y_1, y_2]\} = \partial_1(y_2)\cdot\{y_0, y_1\} - \partial_1(y_1)\cdot\{y_0, y_2\} + \{y_1,[y_0, y_2] - \partial_1(y_2)\cdot y_0\} - \{y_2,[y_0$$

The pairing $\{-,-\} : M_1 \times M_1 \to M_2$ is often called the *Peiffer lifting* of the 2-crossed module. Note that we have not specified that $M_1$ acts on $M_2$. We could done that as follows: if $y \in M_1$ and $x \in M_2$ define

$$y\cdot x = \{y, \partial_2(x)\}.$$

Therefore with this action

$$\partial_2 : M_2 \to M_1$$

is a crossed module of Lie algebras.

We denote such a 2-crossed module by $\{M_2, M_1, M_0, \partial_2, \partial_1\}$ . A morphism of 2-crossed modules is given by a diagram

$$\begin{array}{ccccc} M_2 & \xrightarrow{\partial_2} & M_1 & \xrightarrow{\partial_1} & M_0 \\ \downarrow{\scriptstyle f_2} & & \downarrow{\scriptstyle f_1} & & \downarrow{\scriptstyle f_0} \\ M_2' & \xrightarrow[\partial_2']{} & M_1' & \xrightarrow[\partial_1']{} & M_0' \end{array}$$

where $f_0\partial_1 = \partial_1' f_1, f_1\partial_2 = \partial_2' f_2,$

$f_1(z \cdot y) = f_0(z) \cdot f_1(y), f_2(z \cdot x) = f_0(z) \cdot f_2(x),$

and

$\{-,-\}(f_1 \times f_1) = f_2\{-,-\},$

for all $x \in M_2, y \in M_1, z \in M_0.$

These compose a category which we will denote by $2-LCMod$ . The following should be clear.

Theorem The Moore complex of a 2-truncated simplicial Lie algebra is a 2-crossed module of Lie algebras. The assignment is functorial.

We will denote this functor by $\lambda : T_{2]} \to 2-LCMod.$ It is an equivalence of categories.

## References

[1] Akça, İ., Arvasi Z.: Simplicial and crossed Lie algebras, Homology, Homotopy and Application, vol. 4(1), 43-57, (2002).

[2] Andre, M: Homologie des algebres commutatives, Grundlehren Band. 206, Springer, Verlag, Berlin, 1974.

[3] Artin, M. Mazur, B.: Etale Homotopy. Lecture Notes in Maths. 100, Springer Verlag, 1968.

[4] Arvasi Z., Porter, T. : Freeness conditions of 2-crossed modules of commutative algebras, Applied Categorical Structures. 6: 455-471 (1998).

[5] Arvasi, Z., Porter, Z: Higher dimensional Peiffer elements in simplicial commutative algebras, Theory and Applications of Categories. Vol.3, No. 1 pp. 1-23, (1997).

[6] Carrasco, P.: Complejos Hipercruzados: Cohomología y Extensiones. Ph.D. Thesis, Univ. de Granada, 1987.

[7] Carrasco, P., Cegarra, A. M.: Group-theoretic algebraic models for homotopy types. Journal Pure Appl. Algebra. 75, 195-235, (1991).

[8] Conduche, D.: Modules croise generalises de longueur 2. Journal Pure Appl. Algebra. 34, 155-178, (1984).

[9] Curtis, E., B.: Simplicial homotopy theory. Adv. in. Math. 6, 107-209, (1971).

[10] Duskin, J.: Simplicial methods and the interpretation of triple cohomology. Mem. Amer. Math. Soc. 163, 117-136, (1970).

[11] Ellis, G. J.: Crossed modules and their higher dimensional algebras. Ph.D. Thesis. U.C.N.N., 1984.

[12] Ellis, G., J.: Homotopical aspects of Lie algebras. J.Austral.Math.Soc. (Series A), 54, 393-419, (1993).

[13] Illsue, L.: Complex cotengent et deformations I, II. Springe Lecture Notes in Maths. 239, (1971), II, 283, (1972).

[14] Kassel, C., Loday, J. L.: Extensions centrales d'algebres de Lie., Ann. Inst. Fourier (Grenoble). 33, 119-142, (1982).

[15] Lavendhomme, R., Roisin, J. R.: Cohomologie non abélienne the structures algebriques (French). SL. Algebra, 67, no.2, 385-414, (1980).

[16] Porter, T: Homology of commutative algebras and an invariant of Simis and Vasconceles. J.Algebra, 109, 458-465, (1987).

[16] Porter, T: Extensions, crossed modules and internal categories of groups with operations. Proc. Edinburgh Math. Soc. 2, 30, no.3, 373-381, (1987).

[17] Quillen, D.: Rational homotopy theory. Ann. of Math. vol.90 no:2, 205-295, (1969).

[18] Whitehead, J. H. C.: Combinatorial Homotopy I and II, Bull. Amer. Math. Soc. 55, 231-245 and 453-456 (1949).